SOLAR PILOT PLANT, PHASE I.

Quarterly Report No. 2, January—March 1976

August 20, 1976

Work Performed Under Contract E(04-3)-1109

Energy Resources Center
Honeywell, Incorporated
Minneapolis, Minnesota

ENERGY RESEARCH AND DEVELOPMENT ADMINISTRATION
Division of Solar Energy

MASTER

DISCLAIMER

DISCLAIMER

Portions of this document may be illegible in electronic image products. Images are produced from the best available original document.

SOLAR PILOT PLANT
PHASE I

QUARTERLY REPORT NO. 2
(January - March 1976)

(APPROVED)

20 August 1976

CDRL Item No. 10

ERDA Contract No. E(04-3)-1109

Honeywell, Incorporated
Energy Resources Center
2600 RIDGWAY PARKWAY,
MINNEAPOLIS, MINNESOTA 55413

MASTER

FOREWORD

This is the final submittal of Solar Pilot Plant Quarterly Technical Report No. 2 per Contract Data Requirements List Item 10 of ERDA Contract E(04-3)-1109. The report has been reviewed by ERDA for technical content and patent clearance, and has been released for normal distribution.

ABSTRACT

Honeywell Inc. is investigating the technical and economic feasibility of
generating electricity from solar energy under Energy Research and Develop-
ment Administration (ERDA) contract E(04-3)1109. During the report period
(1 January through 31 March 1976), conceptual designs for the collector and
steam generator subsystem research experiments (SREs) were approved, and
design detailing began. The thermal storage SRE concept was modified
through additional analyses and engineering model experiments and resub-
mitted for evaluation. Detailed designs for all three subsystems will be
submitted during the next quarter. Preparation for SRE testing proceeded
through procurement of long-leadtime items and detailed definition of test
arrangements. Analysis and design of the electrical generation subsystem
and balance of the plant proceeded essentially on schedule.

THIS PAGE

WAS INTENTIONALLY

LEFT BLANK

CONTENTS

ILLUSTRATIONS

TABLES

SECTION I

INTRODUCTION

BACKGROUND

The Energy Research and Development Administration (ERDA) is commis-
sioned to identify and evaluate alternate sources of energy to ensure orderly
and timely development of those offering potential for supplementing and/or
replacing conventional fuels that will be in increasingly short supply. An
alternate source with great potential is solar energy, and one goal of the
overall national energy program is to demonstrate the technical and economic
feasibility of a central receiver solar power plant for generating electricity.
Pursuant to that goal, ERDA, on 1 July 1975, awarded Honeywell Inc. a
2-year contract to develop a preliminary design for a 10-MW(e) proof-of-
concept pilot plant.

PROGRAM SCOPE

The program being conducted by Honeywell under ERDA Contract E(04-3)1109
calls for preparing a solar pilot plant baseline design and carrying out
research experiments on three key subsystems to obtain data for evaluating
the baseline. Since these subsystems (collector, receiver, and thermal stor-
age) and their integration are critical to the success of this portion of the
program and to initiation of the next phase [constructing and operating the
10-MW(e) pilot plant], Honeywell is using a team approach to provide a low-
risk, cost-effective preliminary design. The team and individual responsi-
bilities are shown in Figure 1.
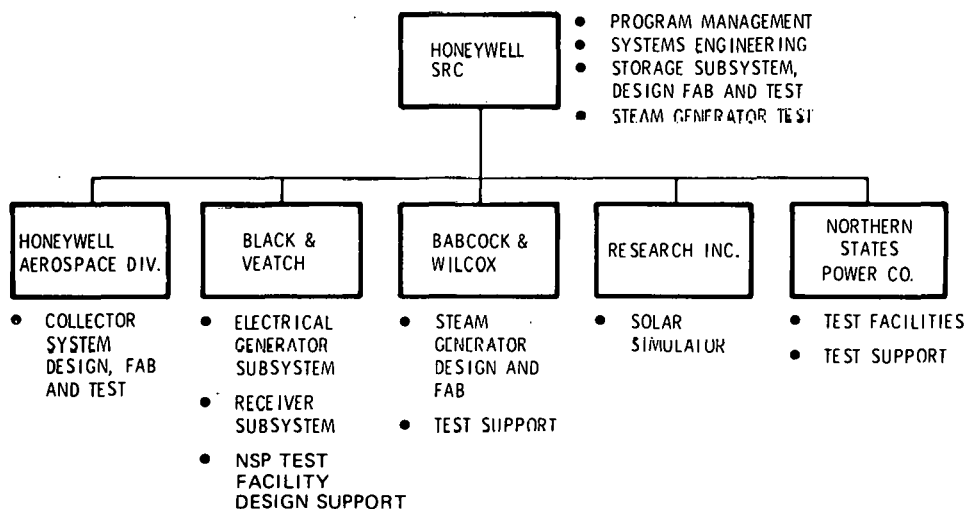
Figure 1. Honeywell Team for Solar Pilot
Plant Program

PROGRAM STATUS

Figure 2 is the program schedule.

TASK	1975						1976								1977						
	J A S O N D J F M	A M J J A S O N D	J F M A M J J A
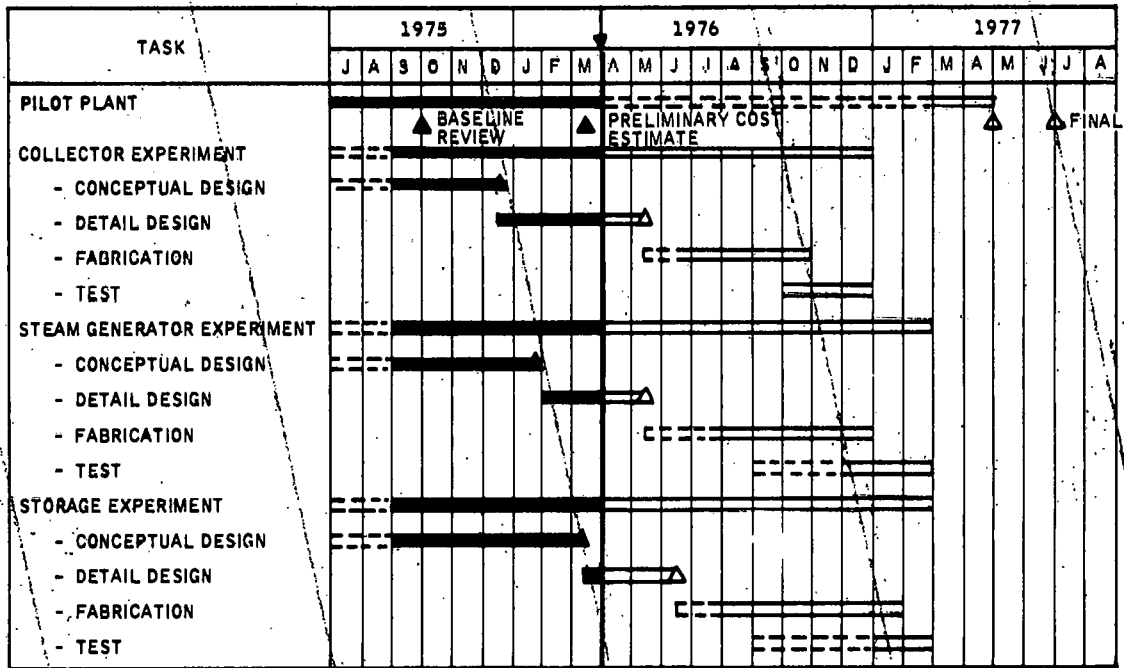
Figure 2. Solar Pilot Plant Phase I Schedule

The figure shows a preliminary cost estimate for the pilot plant was completed during the report period, based on the preliminary baseline design. Also completed were the conceptual designs for the collector and steam generator subsystem research experiments (SREs). The conceptual design for the thermal storage SRE was awaiting approval at the end of the period. Its completion was delayed because certain aspects required further investigation and analysis. The delay is not expected to affect the overall SRE schedule.

During the next quarter, detailed designs for all three SREs will be reviewed. Procurement of hardware will continue preparatory to fabrication and test.

SECTION II
SOLAR PILOT PLANT CHARACTERISTICS

CONCEPT

Description

The pilot plant concept generated for this program and refined during the first 9 months consists of a circular field of heliostats that concentrate solar energy through the annulus aperture of a central receiver, as illustrated in Figure 3.
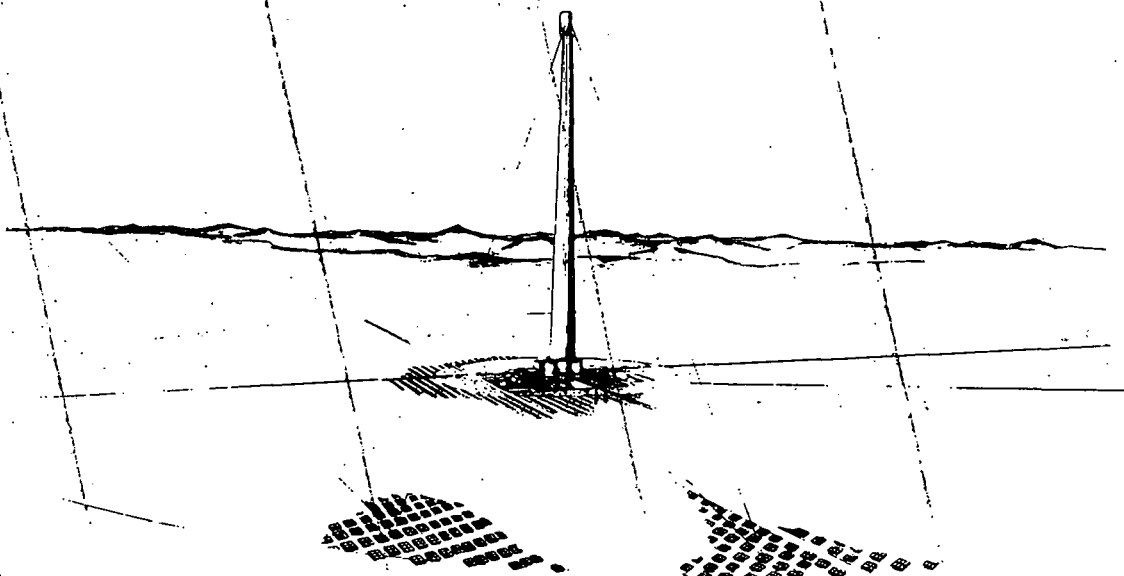
Figure 3. Solar Pilot Plant Concept

The concentrated solar energy is converted to thermal energy by an array of boiler and superheater tubes in the cavity to generate electricity from super-heated steam produced in the receiver, or from thermal energy stored by melting a eutectic salt (Figure 4).
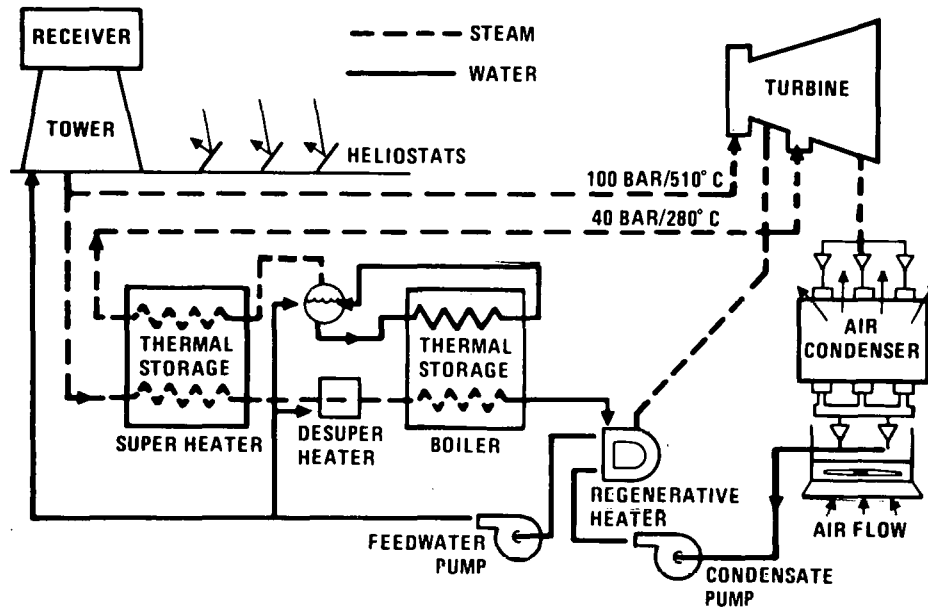
Figure 4. Solar Pilot Plant Baseline Schematic

The 10-MW(e) pilot plant is scaled from a 215-MW(e) nameplate capacity plant, which is considered upper limit commercial size due to the limiting factor of tower height. A preliminary seismic analysis of the pilot plant receiver support tower is presented in Appendix A. The scaling ensures that data obtained from the pilot plant will be applicable to commercial-size operations. A comparison is presented in Figure 5.

	COMMERCIAL	PILOT PLANT	
NAMEPLATE CAPACITY	215 MW(e)	15 MW(e)	
AVERAGE POWER (NET ~4000 HOURS)	172 MW(e)	10 MW(e)	
TOWER HEIGHT	569 m	137 m	
FIELD OD.	2402 m	579 m	
NUMBER OF HELIOSTATS	32,766	1905	
HELIOSTAT SIZE	40 m^2	40 m^2	(A)
TURBINE CYCLE (FROM RCVR)	12.4 MPa/510^{0}C	---	
TURBINE CYCLE (FROM STORAGE)	0.5 MPa/007^{0}C	===	(C)
STORAGE TYPE	PHASE CHANGE	---	
STORAGE CAPACITY	TO BE DETERMINED	315 MWhr(t)	(C)
RECEIVER	CAVITY	---	
COOLING	DRY	---	
LOCATION	INYOKERN	---	

(A) = Added.

(C) = Change from last report.

Figure 5. Comparison of Commercial and Pilot Plant Parameters

Changes to Original Baseline

Major changes in the original baseline, proposed during the report period as results of system tradeoff studies, were:

1) Storage Tank Parameters -- Study showed there were signifi-cant cost benefits to be derived from placing the storage tanks at ground level (as opposed to below ground) and not housing them in a building (Table 1). Round tanks proved to be less expensive than rectangular. Table 2 shows that thinner-than-specified insulation on individual tanks is cost effective com-pared with the specified amount of insulation.

2) Phase-Change Material -- The phase-change material was changed from a ternary eutectic salt mixture of $NaCl$ - $NaNO_3$ - Na_2SO_4 to a mixture of $NaNO_3$ - $NaOH$ to decrease cost, up-grade heat recovery, and increase scraper efficiency. The change was a result of experimentation with an engineering model of the storage tank.

There were, and will continue to be, changes and additions to initial values as findings of the SREs (both in design detailing and experimentation) are applied to the pilot plant. For that reason, tables listing significant features are included in each report. Changes in values from those reported previously are so indicated (C). Values identified and assigned for the first time are indicated (A).

Earlier changes, described in Quarterly Technical Report No. 1, were:

● Change from heliostat azimuth/elevation gimbal order to tilt-tilt.

● Change from primary turbine admission of steam to dual-pressure admission.

● Change from 59 bar (5.9 MPa)/510°C receiver steam to 100 bar (10 MPa)/510°C steam.

MAJOR SUBSYSTEMS

Major subsystems of the pilot plant are listed in Table 3. The first three are of primary interest in this phase of the program, since practical genera-tion of electricity is dependent on how well they function as a system. Fig-ure 6 shows how the subsystems interface.

Table 1. Pilot Plant Scale Design Comparison (At Optimal Insulation Thickness and I/O Rates)

Parameter	No Building, Rectangular 4 x 1 Tanks	No Building, Round Tanks*	With Building, Rectangular 4 x 1 Tanks**	With Building, Round Tanks
Storage cost ($/kWhr)	137 +Δ18	119 0	150 +Δ31	135 +Δ16
Energy cost (mills/kWhr)	85.5 +Δ3.8	83.7 0	87.5 +Δ3.8	85.5 +Δ1.8
Tank cost ($/kWhr)	27 +Δ17	10 0	27 +Δ17	10 0
Insulation cost ($/kWhr)	0.9	7.C	0.0	8.8
Building cost ($/kWhr)	0	0	10.5	11.7
Heat loss (% charge in 100 hours)	45 +Δ5	40 0	24 -Δ16	26 -Δ14
Heat loss (% annual collected)	4.2 +Δ0.4	3.8 0	2.2 -Δ1.6	2.4 -Δ1.4

*Proposed new baseline.
**Old baseline.

Table 2. Tank Comparison

Parameter	Full-Scale, 8 Round Tanks, 4.5 inches of Insulation	Full-Scale, 8 Round Tanks, Meets Insulation Specification	Δ
$/kWhr, total	86.2	94.9	8.7
$/kWhr, insulation	4.8	12.8	8.0
% Loss/100 hours	27.3	10.0	17.3
% Scraping loss	8.7	8.7	0.0
% Annual heat loss	2.5	0.0	1.6
Mills/kWhr	71.4	72.5	1.1
Cycle	940/587	940/587	---
Δ$/kWhr, condenser to spec	+3.0	+3.0	---
ΔMills/kWhr, condenser to spec	+0.5	+0.5	---

Table 3. Solar Pilot Plant Major Subsystems

Parameter	Value	
Collector Subsystem:		
Field outer radius	290 m	
Number of heliostats	1905	
Receiver Subsystem:		
Tower height	137 m	
Cavity diameter	11.4 m	(C)
Cavity height	13.7 m	
Thermal Storage Subsystem:		
Thermal storage capacity	315 MWhr(t)	(C)
Total quantity of phase-change material (NaNO$_3$ - NaOH)	7.33×10^6 kg	(C)
Electrical-Generation Subsystem:		
Turbine name-plate capacity	15,000 kW	
High-pressure steam turbine inlet conditions	10 MPa/510°C	(C)
Low-pressure steam turbine conditions	6.5 MPa/307°C	(C)

(C) indicates change in value from last report.
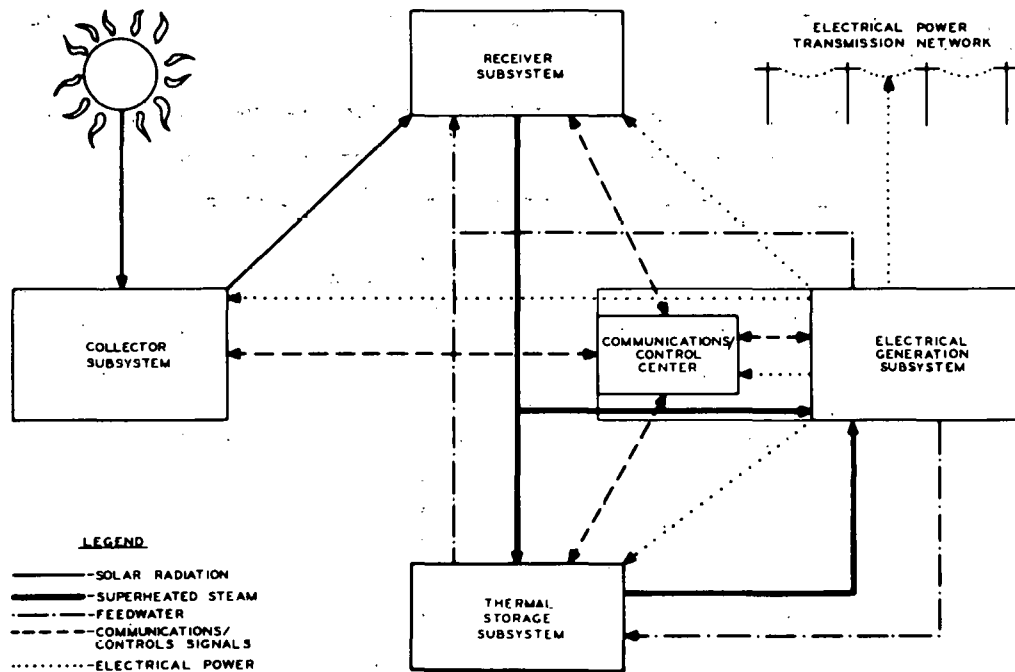
Figure 6. Subsystem Interfaces

8

Collector Subsystem

The collector subsystem is designed to gather and transmit as much solar energy as is economically feasible using prefocused heliostats (Table 4).

Table 4. Collector Subsystem Characteristics

Parameter	Value
Field outer radius	290 m
Field inner radius	55 m
Number of heliostats	1905
Individual heliostat area	40 m^2
Total heliostat area	76,200 m^2
Peak thermal power into aperture	53 MW
Annual thermal energy into cavity aperture	1.58×10^5 MWhr
Net annual thermal energy per unit mirror area	1.95 MWhr/m^2
Net peak power per unit mirror area (thermal)	0.66 kW/m^2

Receiver Subsystem

The receiver subsystem receives the solar energy from the collector subsystem. Feedwater in the receiver boiler tubes is superheated and piped directly to the electrical-generation subsystem and/or to the thermal storage subsystem (Table 5).

Table 5. Receiver Subsystem Characteristics

Parameter	Value	
Tower height	137 m	
Cavity diameter	11.4 m	(C)
Cavity height	13.7 m	
Steam generator housing height	20 m	
Steam generator housing diameter	18.28 m	(C)
Aperture slant height	5.0 m	(C)
Aperture lower diameter	6.1 m	
Annulus aperture area	133 m^2	
Peak absorbed thermal power	49 MW	
Peak wall incident thermal power flux	450 kW/m^2	(C)
Annual thermal energy absorbed by cavity working fluid	1.49×10^5 MWhr	

(C) denotes changes from last report.

Thermal Storage Subsystem

The thermal storage subsystem supplies feedwater to the receiver and receives superheated steam during the charge cycle. During the discharge cycle, it receives feedwater from the electrical-generation subsystem and discharges steam (Table 6).

Table 6. Thermal Storage Subsystem Characteristics

Parameter	Value
Thermal storage capacity	315 MWhr(t) (C)
Total quantity of phase change materials ($NaNO_3$ - NaOH)	7.33×10^6 kg (C)
Maximum thermal power input to storage	31.58 MW (C)
Maximum thermal power output from storage	31.58 MW for (C) 6 hr
Net annual electrical energy produced if storage is charged and discharged daily	4.15×10^4 MWhr
Net annual electrical energy produced if storage is not used	4.4×10^4 MWhr
Outlet stream conditions	6.5 MPa/307°C (C)

(C) denotes changes from last report.

Electrical Generation Subsystem

The electrical generation subsystem receives steam from the receiver boiler tubes and/or thermal storage and pumps back feedwater. It also provides electrical power to the other subsystems and the communication/control center (Table 7).

Table 7. Electrical Generation Subsystem Characteristics

Parameter	Value
Turbine nameplate capacity	15,000 kW
Turbine type	Dual-pressure admission
High-pressure steam turbine inlet conditions	10 MPa/510°C (C)
Low-pressure steam turbine inlet conditions	6.5 MPa/307°C (C)
Peak steam flow rate to turbine inlet	80,150 kg/hr (C)

(C) denotes changes from last report.

Subsystems Control

The plant control scheme (Figure 7) is based on providing centralized coordination and control of the subsystems while maximizing utilization of the solar energy collected. Safety is a primary consideration, and adequate protection against dangerous operating conditions is incorporated in the control scheme.
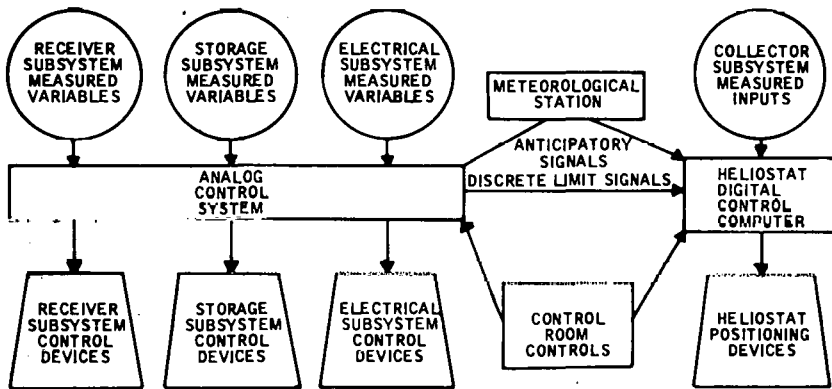
Figure 7. Control Coordination of Plant Subsystems

PLANT LAYOUT

The pilot plant site plan (Figure 8) respects the functional relationships be-
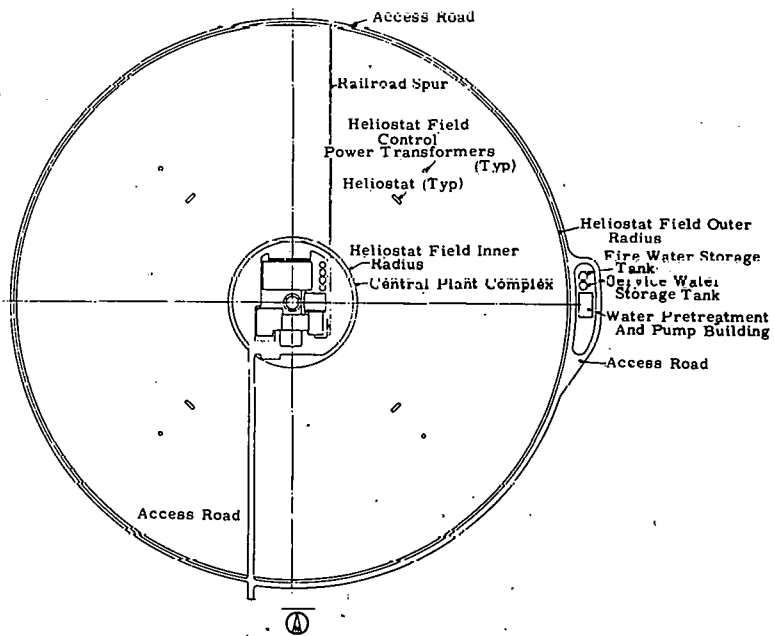
Figure 8. 10-MW Solar Pilot Plant Site Plan

tween plant systems. The site arrangement was developed by giving priorities to those major facilities whose parameters can be manipulated least.

The collector field location is governed by topographical features accommodating the specified outer radius (i. e., the concept of a flat field is maintained).

The central plant complex (Figure 9) is positioned at the center of the collector field in such a manner as to avoid blocking any of the heliostats on the collector field inner radius. The receiver tower, at the center of the complex, and of the collector field, maximizes the amount of solar energy collected annually.
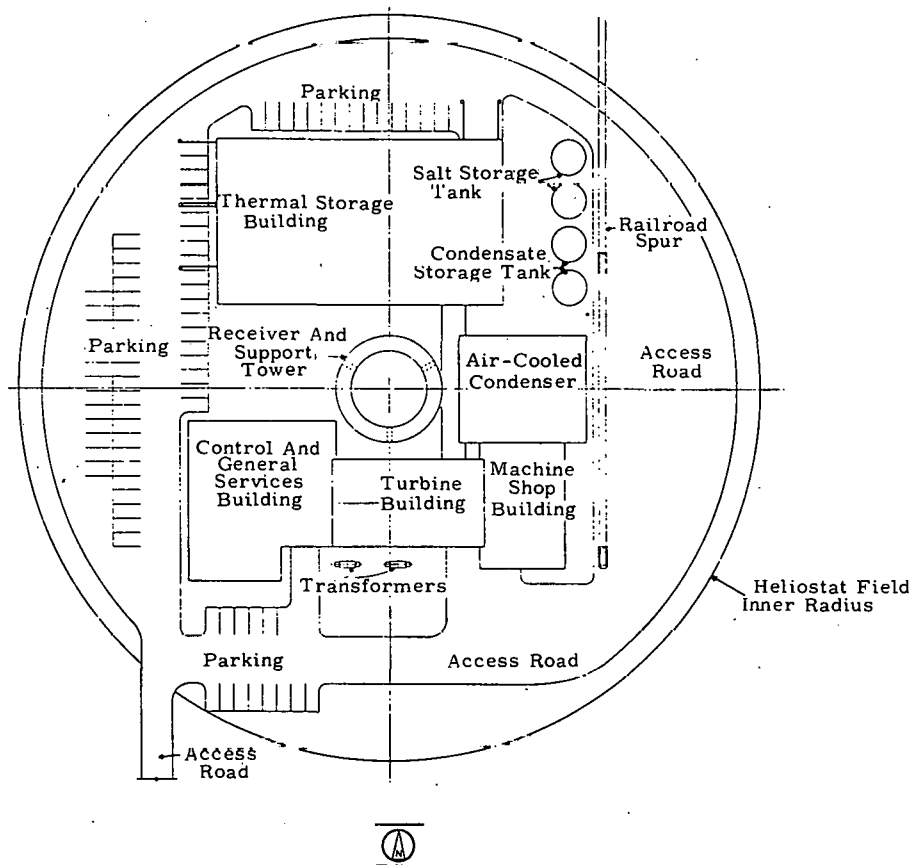
Figure 9. 10-MW Solar Pilot Plant -
Central Plant Complex

An access road and rail line into the plant site are located to facilitate plant operation and maintenance while minimizing energy loss in the collector field.

The electrical transmission lines that integrate the plant output with the existing network are located to minimize interference with other facilities or lines.

SECTION III
COLLECTOR SUBSYSTEM RESEARCH EXPERIMENT

DESCRIPTION OF SUBSYSTEM

The essential elements of the solar collector subsystem are shown in Figure 10. This baseline features:

- Computed sun tracking and calculation of heliostat commands based on line-of-sight vectors to the sun and the tower

- Low-profile, two-axis gimbaled heliostats

- Commands to two motors at each heliostat from the central controller

- Periodic heliostat calibration on a target array on the tower near the receiver

- Continuous central control of heliostats for flexibility of power plant operation. The subsystem control scheme is shown in Figure 11.
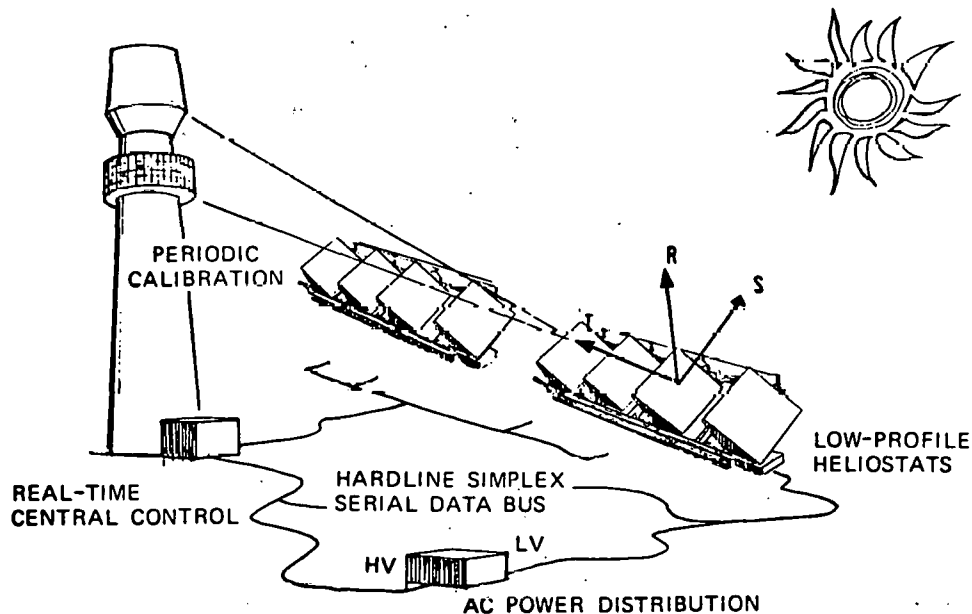
Figure 10. Collector Subsystem Baseline

A FIELD OF 1905 HELIOSTATS
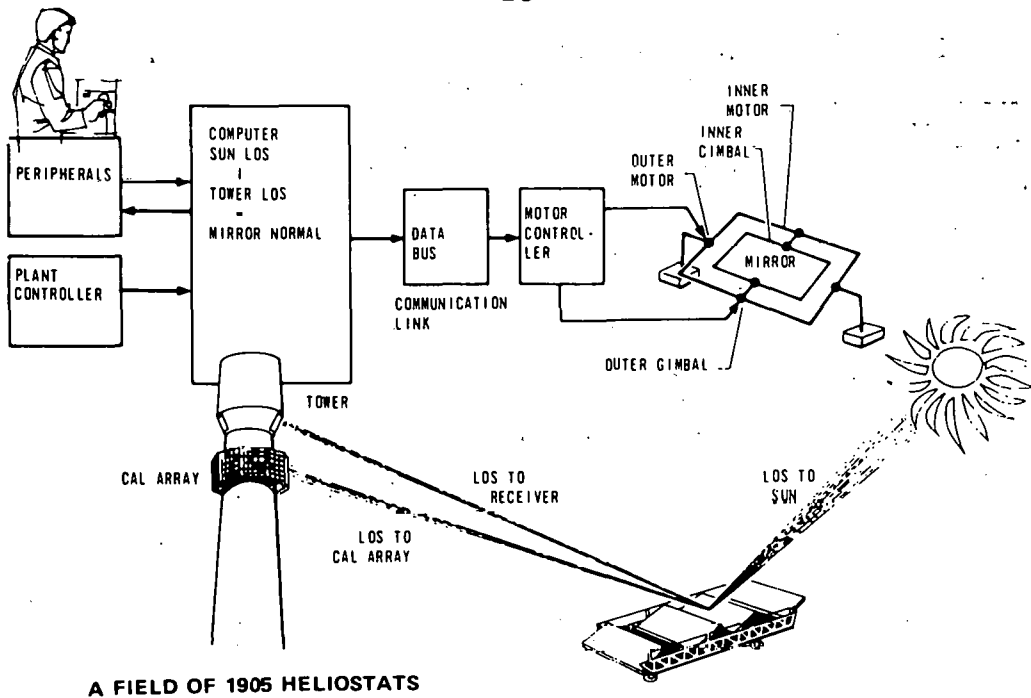
Figure 11. Collector Subsystem Control
Scheme

OBJECTIVE OF THE EXPERIMENT

The collector subsystem research experiment (CSRE) is designed to evaluate
the preliminary baseline by testing:

- Signal distribution to heliostats

- Noise rejection and signal detection at the calibration array

- Tracking and control concepts

- Environmental effects on field operation of the subsystem

The findings of the experiment will be directly applicable to the subsystem
design for the pilot plant. Table 8 compares the current elements of the
experiment with those of the current conceptual pilot plant.

STATUS OF THE EXPERIMENT

The conceptual design for the collector SRE was accepted after review on
17 December 1975. During this report period, good progress was made in
detailing the design for review in early May. Limited fabrication activity was
carried out on the calibration array, special tooling, and test equipment.
Preparation for collector SRE testing is proceeding to the schedule shown in
Figure 12.

14

Table 8. Comparison of Research Experiment Elements
with Pilot Plant Concepts

Element	Research Experiment	Pilot Plant
Heliostat	40-square-meter tilt-tilt heliostat	Same
Power distribution	110V, 60-Hz, plus battery. No high voltage.	High voltage, 110V, 60-Hz, plus battery
Signal distribution	Serial data bus	Same
Tower	Simulated, scaled	Concrete, about 400 ft high
Calibration array	Light detectors on a matrix grid with electronics	Same
Target	Similar to calibration array	Receiver
Processor	One minicomputer with special I/O	Could be same except increased quantity
Control software	Sized for experiment; simulates operator and central controller I/O	Differs in heliostat quantity, geodetic and field layout constants
Test software	As necessary for data collection and correlation for research experiment	As necessary for initialization and maintenance for pilot plant
Test equipment	Meteorological and other commercial instrumentation for test data collection	No nonstandard instrumentation, meteorological and other commercial instrumentation for station maintenance
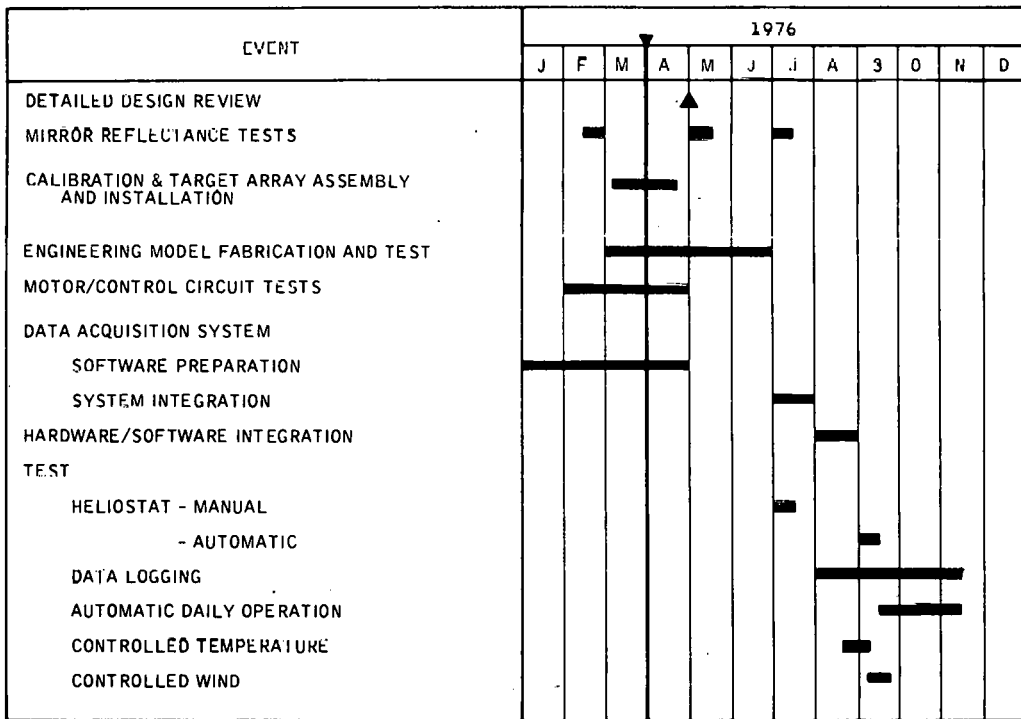
Figure 12. Collector SRE Preparation and
Test Schedule

DESCRIPTION OF THE EXPERIMENT

- The collector SRE is an experimental system of four tracking reflectors that will be used to determine focusing and pointing capabilities of the collector subsystem.

- Table 9 summarizes the collector SRE performance objectives.

Table 9. Collector SRE Performance Objectives

Item	CSRE Specification	Remarks
Far field pointing, mirror normals	2 mr/axis, 1σ	Goal
Optics	1 mr total, 1σ	Goal
Redirected pattern (95% within) (10 a.m. to 2 p.m.)	3.5 m x 7 m	Derived
Surface reflectance (initial)	>80%	
Return to storage	<15 minutes	Derived
Emergency defocus maximum time	<12 sec/3° travel	Derived
Modes:		
Acquisition	-	N/A
Offset pointing	X	
Tracking or following	X	
Synthetic tracking	-	N/A
Emergency shutdown	X	
Manual control single units	X	
Failsafe	X	
Return to storage	X	
Limit control	X	
Calibration and checkout	X	
Initialization	X	Derived
Temperature -- Operate and survive	40°F to 130°F	
Wind:		
Operate:		
Sustained	13.5 m/sec	
Gusts	13.5 m/sec rms	
Survive:		
Sustained	25 m/sec*	
Gusts	54 m/sec rms*	

*To be determined in detail design phase.

Heliostat Array

The collector SRE consists of an array of four heliostats that reflect solar rays to a simulated receiver. The design goal that all heliostats be interchangeable regardless of field position was satisfied through the heliostat configuration shown in Figure 13.

Mirror Module Assembly -- The mirror module assembly drawing was approved during the report period. Four versions of the accepted configuration are being built for evaluation. The first consists of a contoured plywood frame supporting 3mm-thick float glass second-surface mirrors. Figure 14 shows the frame and Figure 15 the assembled module on an assembly gantry.

A second type of module consists of a welded steel frame that provides variable focus of a 4.76mm (3/16-inch) float glass mirror with honeycomb stiffener. The mirror assembly measures 1.829 x 1.829 meters (6 x 6 ft). Figure 16 shows the mirror module structure as received from the manufacturer.

The other two module types are assembled versions purchased from Brunswick Corporation and Parsons Inc., respectively. The Brunswick model has galvanized steel sheet metal ribs and outer skins and shaped Owens Corning Type-300 urethane foam filling. Two variations on this type will be evaluated. The first will have a center beam of paper honeycomb between the support shafts to upgrade stiffness. The second will depend on the shear strength of the foam for stiffness. Delivery of these modules will be made in April.

The Parsons model is a single honeycomb structure with outer skins of aluminum-clad steel. The contour of the mirror will be formed by casting an EPOM-828 and Versamid-140 rigid foam mixture over a contour tool. One of these modules, which appears to be the best approach to the specification, will be used to evaluate a first-surface film reflector applied over the 3mm float glass.

Since mirror modules from the last two sources require transportation of large assemblies over a considerable distance, they will be moved in an angled position to reduce the protective packaging requirements for the 3.175- x 3.175-meter (10.4- x 10.4-ft) units.

Reflective measurements were made on samples of glass mirrors and reflective film using a Cary-14 spectrometer with a tungsten source. The results are being evaluated. Additional samples will be tested.

Outer Gimbal Actuator and Module Drive Assembly -- Two outer gimbal actuator assembly configurations emerged from a design tradeoff study. Both, one ball screw and the other machine screw, will be evaluated. Considerations in the final selection will be efficiency, side-load capability, and self-locking characteristics. Both are competitive from cost and performance standpoints.

17
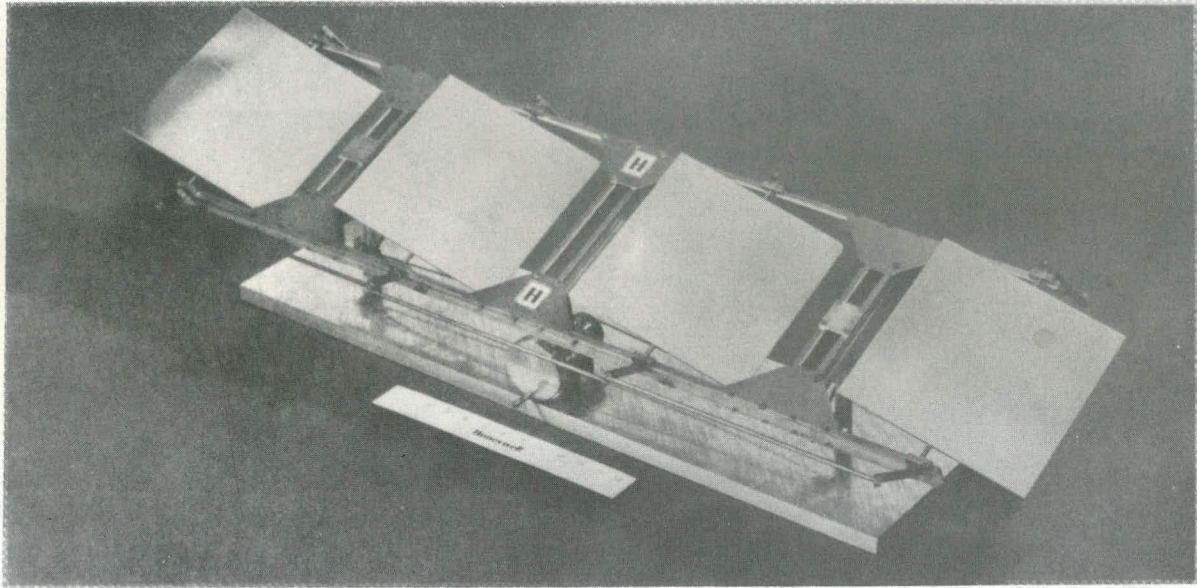
Figure 13. Collector SRE Heliostat Configuration
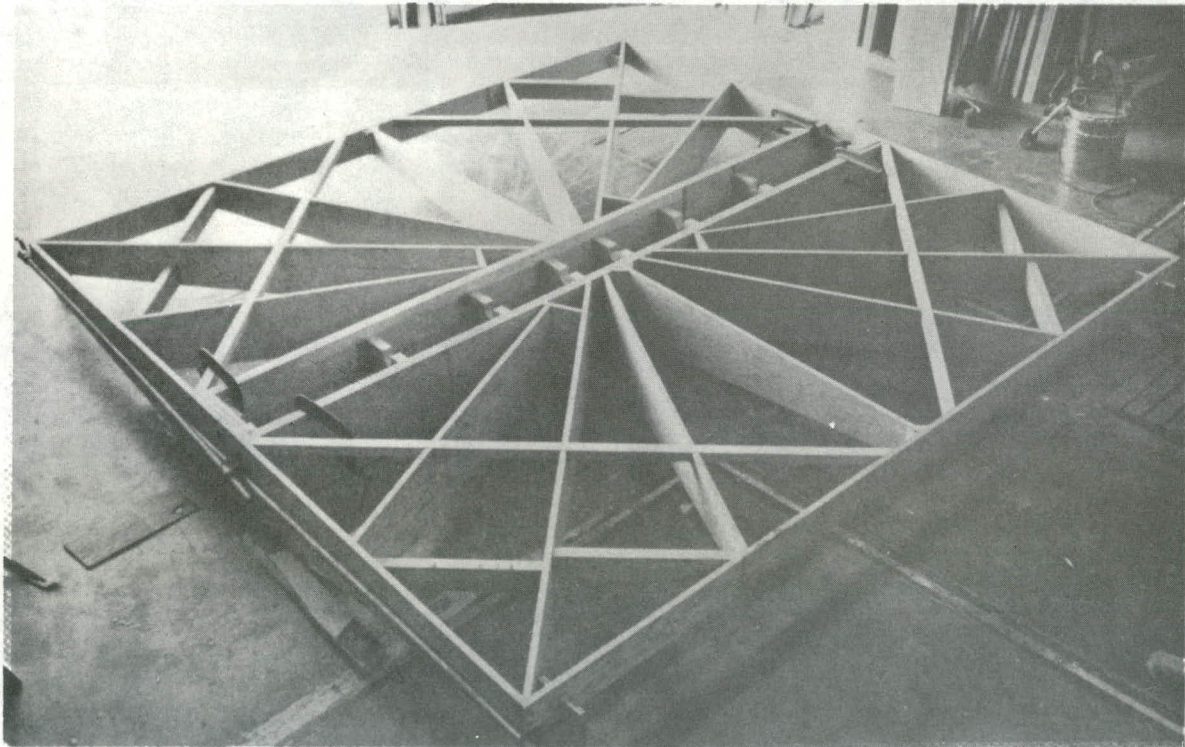
Figure 14. Plywood Mirror Frame
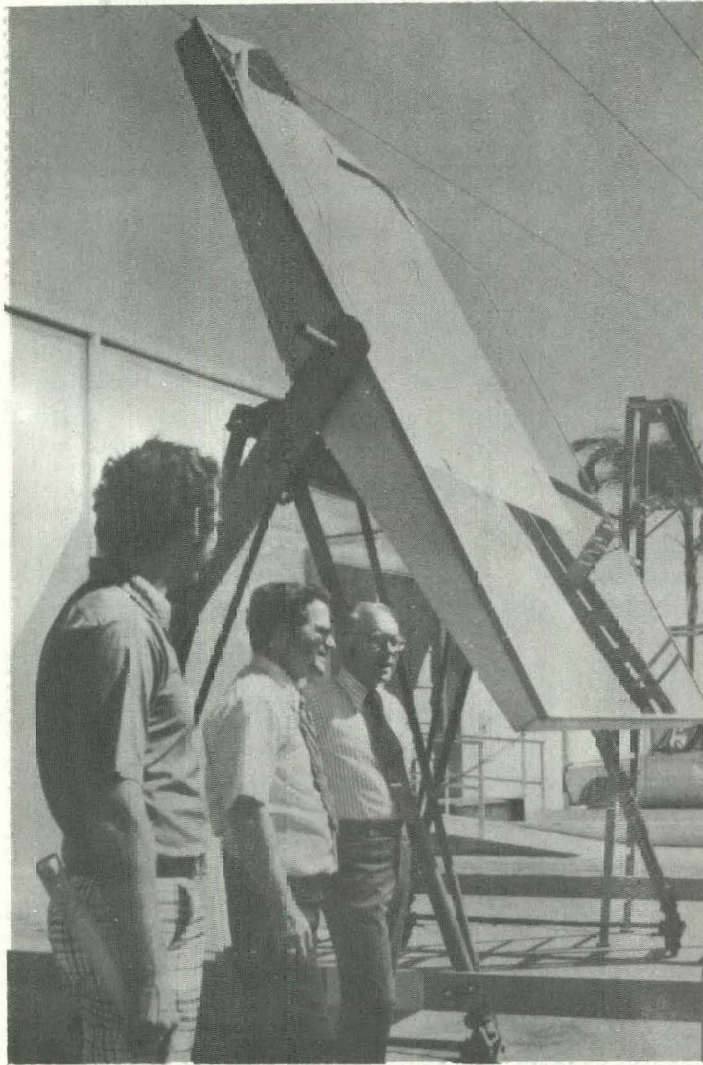
Figure 15. Mirror Module on Plywood Frame
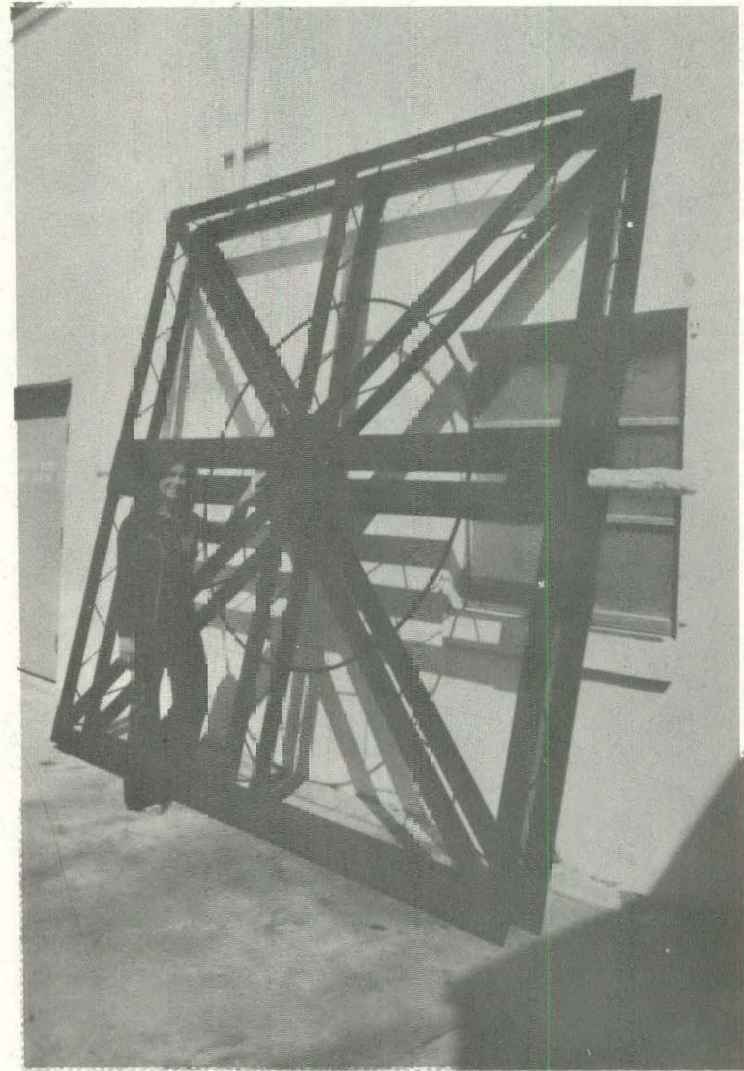
Figure 16. Welded Steel Mirror Frame

18

Mirror module drive system parts were identified, and orders placed for bearings, tie rods, crank arms and retainers, motor, and encoder. Delivery is expected in April. A d-c motor made by Inland Motors was selected for both the outer gimbal axis and the mirror module axis.

Heliostat Electronics -- The design of the heliostat electronics is about half completed. Yet to be finished are the communications, counter control, and up/down counter circuitry. Commercial equipment is being used where practical.

Calibration Array Assembly

The calibration array assembly, incorporating array/computer interface electronics, is nearly complete. The calibration array measures 4.9 x 4.3 meters (16 x 14 ft) and contains 224 photodetectors mounted on a grid with 0.3-meter (1-ft) spacing. The framework is shown in Figúre 17. The array/ computer interface electronics consists of a 240-channel, single-ended, two-tiered analog multiplexer, a differential buffer amplifier, an analog-to-digital converter, a UART for transmitting serial digital data, a line driver for remote operation, and control logic to synchronize operation. Power supplies will be self-contained. The two assemblies will be installed and integrated on top of Bldg. E-2 (Honeywell Aerospace Division, St. Petersburg, Florida) in April. A control room has been set up in the same building with a Honeywell DDP-516 capital computer and peripheral equipment.

Optical Target

An optical target was installed on Bldg. E-2 to provide a reference grid for measuring reflected insolation and determining focus characteristics. Figures 18 and 19 show beam reflection from the plywood mirror module prior to installation of the reference grid.

Weather Instrument Package

A weather instrument package was ordered from Climatronics Corporation. It will be used to provide information on insolation, wind, temperature, and pressure, and will interface directly with the computer complex. Delivery is expected in April.
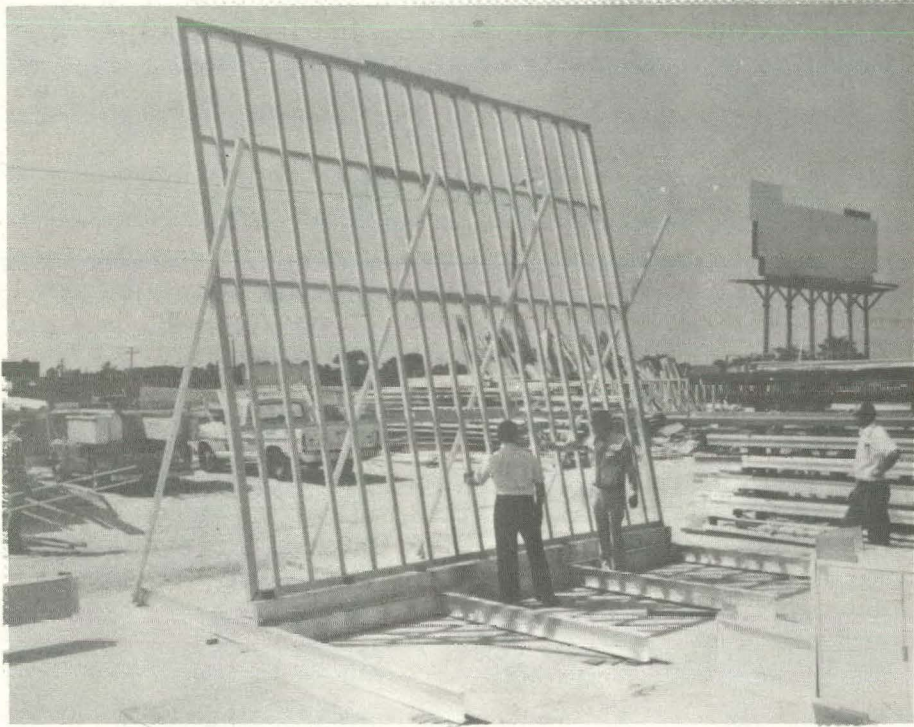
Figure 17. Calibration Array Frame
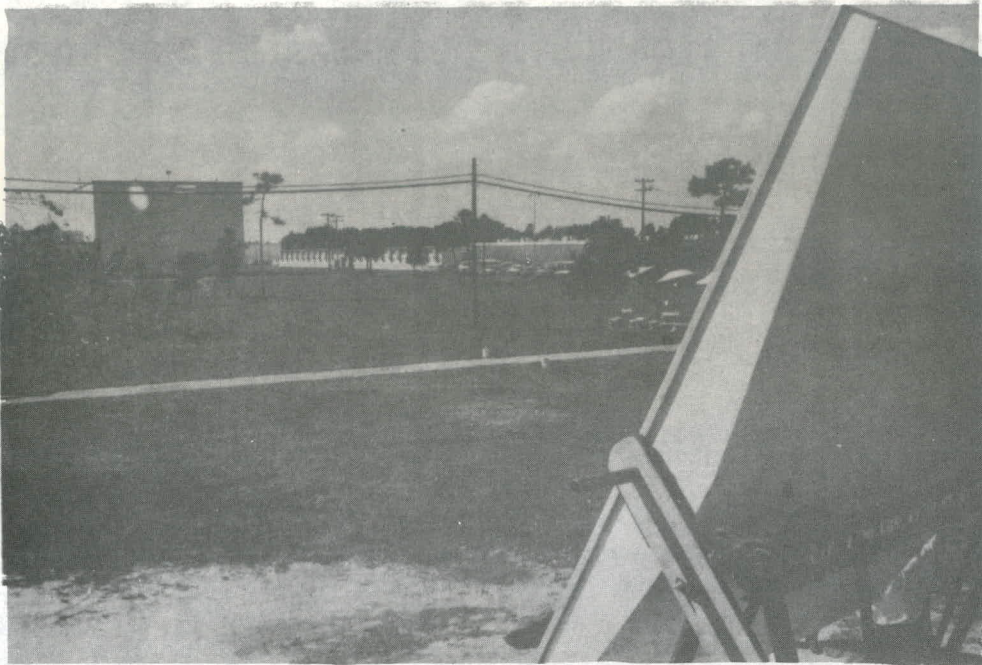
Figure 18. Beam From Mirror Model on Optical Target
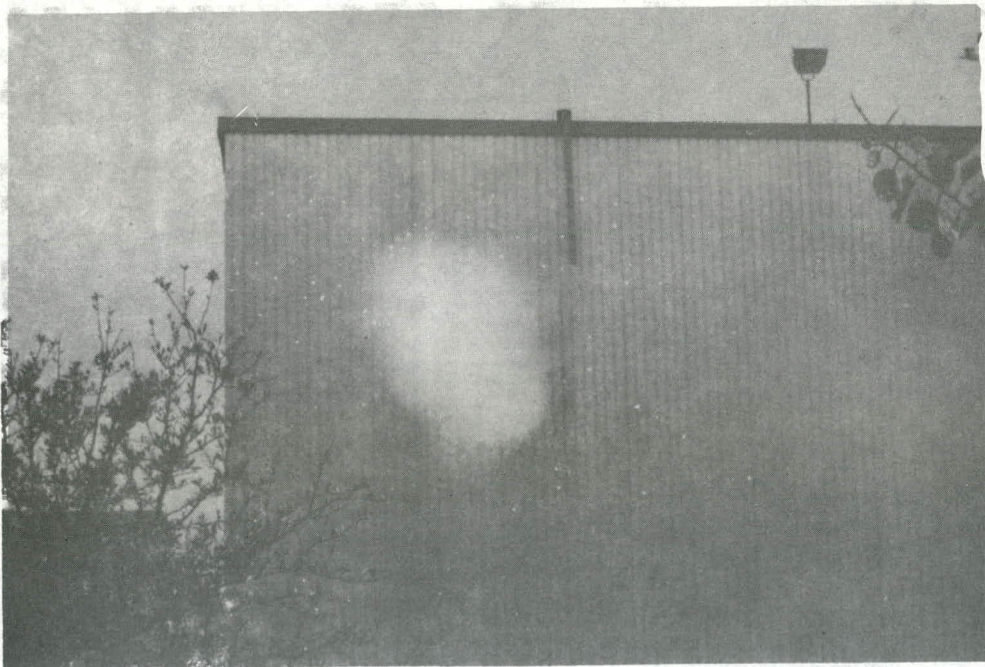
Figure 19. Beam on Optical Target

SECTION IV
STEAM GENERATOR SUBSYSTEM RESEARCH EXPERIMENT

DESCRIPTION OF SUBSYSTEM

The baseline solar steam generator uses existing fossil fuel boiler technology to reduce the risk of failure in critical design areas and expedite the experiment. It has these key features:

- A recirculating drum boiler to facilitate daily startup and shutdown

- Pump-assisted circulation to permit use of smaller boiler tubes

- A helical superheater for relatively free radial thermal expansion and minimization of heat flux maldistribution

- Spray attemperators to control steam temperature between the two stages of the superheater.

A flow schematic of the steam generator is shown in Figure 20.
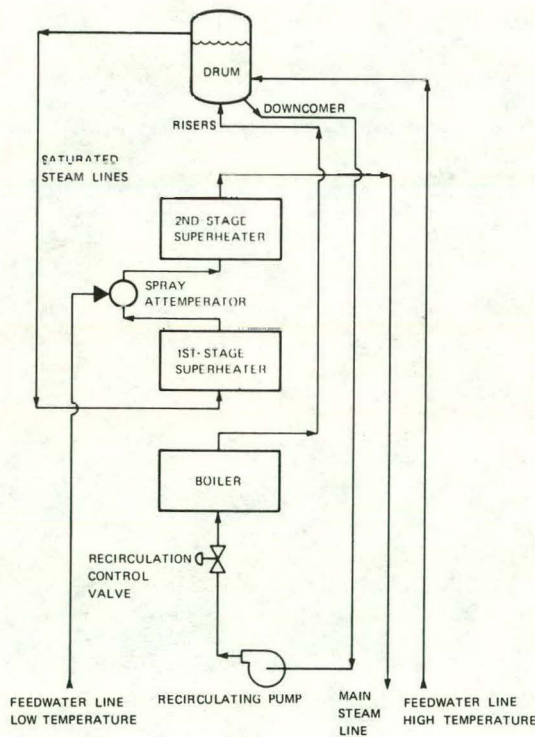
Figure 20. Solar Steam Generator Flow Schematic

OBJECTIVE OF THE EXPERIMENT

The steam generator SRE is designed to prove the validity of the preliminary design by:

- Demonstrating technical feasibility

- Identifying operating procedures

- Confirming fabrication techniques

- Verifying the applicability of standard components and materials and the structural, thermal, and hydraulic analysis of the steam generator

- Verifying the control of the subsystems

- Providing supportive data for system effectiveness studies

The SRE steam generator will, in most parameters, be scaled and matched to the dimensions and materials of the pilot plant version to ensure the validity of the findings of the experiment. A size comparison of the two is shown in Figure 21.
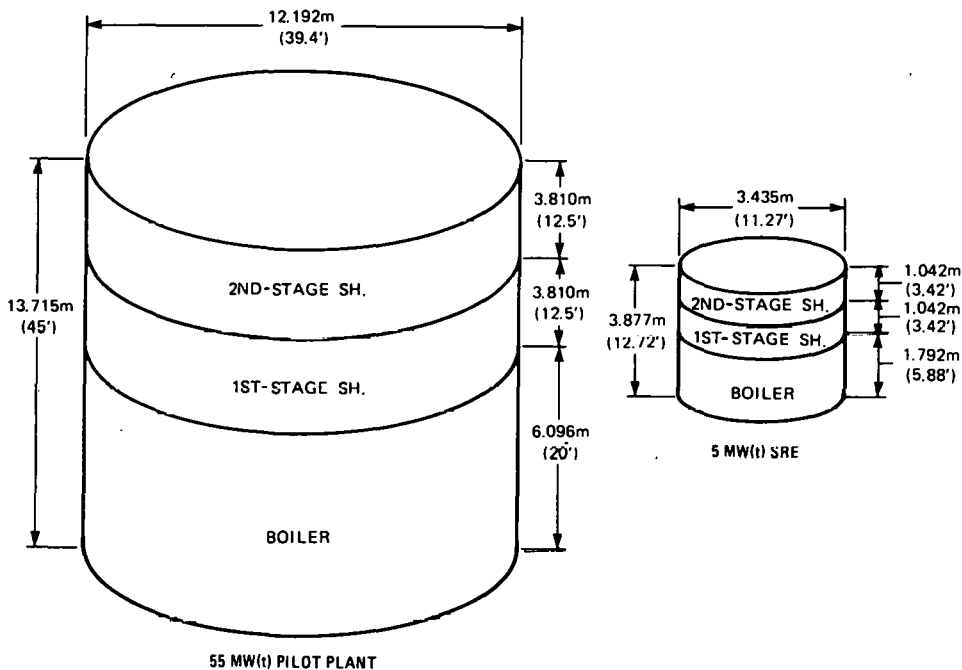
Figure 21. Pilot Plant/Steam Generator SRE
Cavity Size Comparison

STATUS OF THE EXPERIMENT

Design of the steam generator SRE progressed rapidly during the report
period. Long-leadtime materials and components were identified and procure-
ment was initiated. Table 10 shows the status of design and procurement at
the end of the quarter. Figure 22 is the schedule for preparation of the steam
generator test item.

Table 10. Steam Generator SRE Design/Procurement Status

| Component | Percent Completion | | Material Delivery |
	Fabrication Drawings	Materials Ordered	
Boiler section	100	100	4/1 - 7/1
Risers (9)	100	0	Stock
Saturated steam lines (3)	100	0	Stock
Drum and internals	75	0	---
Superheater	75	50	5/21 - 6/21
Recirculation line	50	0	---
Downcomer	50	0	---
Attemperator	0	0	---
Structure	25	0	---
Hangers	25	0	Stock
Pump	100	100	10/1/76
Safety valves	100	100	10/1/76
Recirculation valve	100	0	---
Miscellaneous valves	100	0	---

While delay in completing the conceptual design affected the schedule adversely
(approximately 3 weeks slippage), recovery was sufficient to permit reviewing
the detailed design in early May as originally scheduled. Delivery of the steam
generator and testing are also expected to be on schedule (Figure 23).

In the next quarter, design detailing will be completed and reviewed, all out-
standing materials for the steam generator will be ordered, and fabrication
of all major components will be started.

TASK	DESCRIPTION
1	PILOT PLANT PDBR
2	SRE CDR (TASKS 2.1, 2.2)
2	SRE DETAIL DESIGN (TASK 2.3)
2	SRE DDR
3	FABRICATOR SUBCONTRACTS
3	LONG LEAD MT'L. PROCURM'T.
3	BLR TUBES & HDRS
3	SH TUBES & HDRS
3	DRUM & INTERNALS
3	RECIRC. PUMP
3	PIPE, VALVES, FITTINGS
3	STRUCTURAL STEEL
3	SUPPLIER FABRICATION
3	SRE SUBASSEMBLY FAB.
3	DETAIL DESIGN COORD.
3	FABRICATION
3	SHIPMENT
3	ON-SITE ERECTION, HYDRO, CHEM CLNG.
3	SRE STRESS REPORT
3	SRE OPERATING INSTRUCTIONS
4	SRE TEST SUPPORT & DATA ANALYSIS
4	SRE HOT CHECKOUT
4	SRE TESTING
5	PILOT PLANT PDR
6	SYSTEM/PROJECT MGMT.
6	MEETINGS, REVIEWS, ETC.
7	DESIGN METHODOLOGY DEV.
8	PLANT ESTIMATES
9	QUARTERLY REPORTS

Time scale: FY 1976, FY 1977; CY 1975, 1976, 1977. Months: J A S O N D J F M A M J J A S O N D J F M A M J

LEGEND: △ PLANNED

● ACTUAL

Figure 22. Schedule for Preparation of Steam Generator Test Item

EVENT	1976												1977			
	J	F	M	A	M	J	J	A	S	O	N	D	J	F	M	A
TEST FACILITY PREPARATION																
COMPONENT DELIVERY																
STEAM GENERATOR -																
VALVES, CONTROL																
PIPING																
INSTRUMENTATION																
FILTER, SIM COOLING																
PIPING INSTALLATION																
PIPING TEST																
INSTRUMENTATION INSTALLATION																
INSTRUMENTATION CHECKOUT																
CONTROL CONSOLE INSTALLATION																
DATA ACQUISITION SYSTEM																
HARDWARE DELIVERY																
INSTALLATION IN CONTROL CENTER																
SOFTWARE PREPARATION																
SOFTWARE DEBUG																
OPERATIONAL CHECKOUT																
FACILITY INSTALLATION																
CONTROL CENTER																
DELIVERY TO RIDGWAY																
PREPARATION																
SOLAR SIMULATOR																
SIMULATOR DELIVERY																
SIMULATOR INSTALLATION																
SUBSTATION DELIVERY																
SUBSTATION INSTALLATION																
STEAM GENERATOR TEST ITEM																
DELIVERY																
ERECTION																
STEAM GENERATOR TEST PROCEDURES																
UPDATE																
STEAM GENERATOR TESTS																
INSTALLATION CHECKOUT																
COLD CHECKOUT																
HOT CHECKOUT																
CONTROL SYSTEM VERIFICATION																
CALIBRATION TESTS																
STEADY STATE PERFORMANCE																
TRANSIENT PERFORMANCE																

Figure 23. Steam Generator SRE Preparation and Test Schedule

DESCRIPTION OF THE EXPERIMENT

Critical design parameters of the steam generator SRE are the same as, or proportional to, those of the pilot plant steam generator (Figure 21). The diameter of the model was selected to permit shipment of subassemblies to the test site (NSP Riverside Plant, Minneapolis) by truck. The arrangement of the model (Figure 24) differs from that of the pilot plant only in that the recirculating pump is relocated to the side of the steam generator.
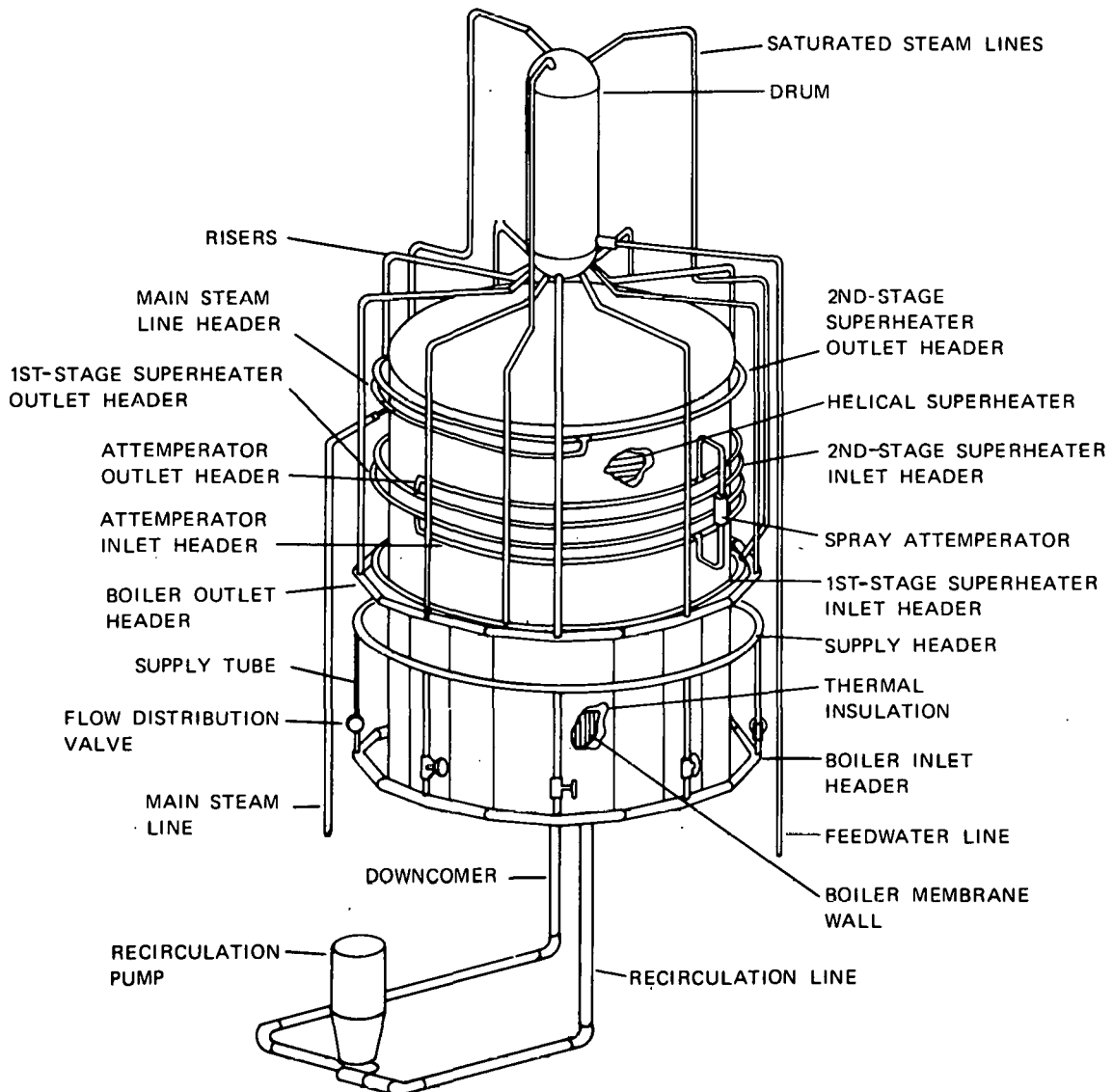
Figure 24. SRE Design Arrangement

Several approved changes have been made to the steam generator SRE since approval of thè conceptual design. These are discussed with other design features in the following paragraphs.

Boiler Section

Figure 25 is a schematic of the revised boiler flow circuit. The pump bypass line was eliminated since it was not required in any of the planned operating modes. The flowmeters on each of the nine boiler flow circuits were also eliminated. Pressure drop across the flow distribution valves and the pressure loss coefficient of the valve will be used to measure flow distribution.
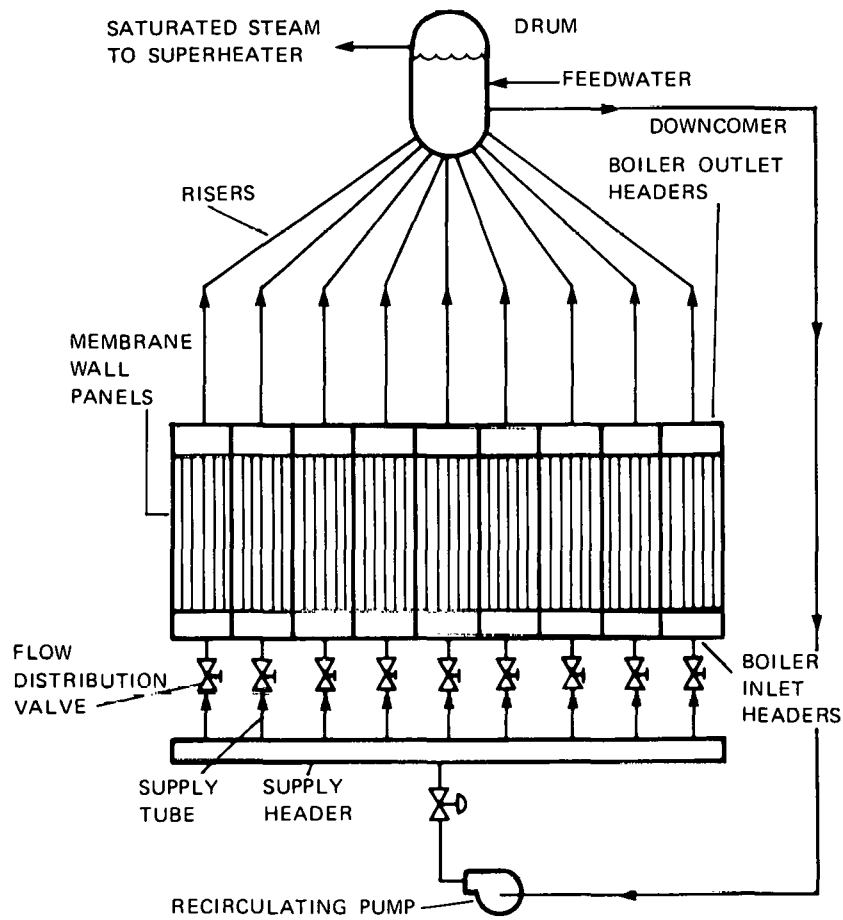
Figure 25. Boiler Flow Circuit

Figure 26 is a cross section of the boiler section membrane wall. The tube material was changed from Croloy 1/2 to carbon steel SA-210, Grade A1CF, since the latter has adequate mechanical properties for this application. The tube-to-tube centerline spacing was changed from 3.493 cm to 3.81 cm to reduce weld interference at the headers. The new spacing gives higher flow per tube and a larger margin to the nucleate boiling (DNB) limit value, while
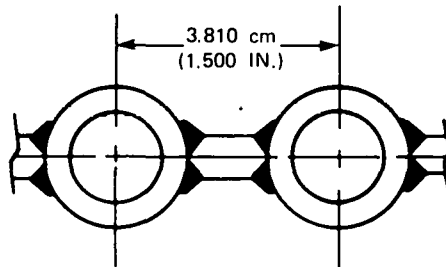
SPECIFICATIONS:

TUBE:

O.D.	2.223 cm	(.875 IN.)
MIN. WALL	0.376 cm	(0.148 IN.)
MAT'L.	SA 210 GRADE A1CF	

WEB:

THICKNESS	635cm (0.25IN.)	
MAT'L.	CARBON STEEL (C1015 C.F.)	

Figure 26. Membrane Wall

maintaining acceptable metal temperatures. Figure 27 shows a typical membrane panel and an isometric view of the panels assembled into an 18-sided polygon. The number of sides was doubled to achieve a better match between the boiler and the circular cross section of the superheater.

Superheater

Figure 28 shows typical superheater tubes for both the steam generator/SRE and the pilot plant. Tube diameter, wall thickness, and material are the same. A steam generator SRE tube makes approximately 3-1/2 turns and is about the same length as a pilot plant superheater tube.

Figure 29 shows the flow circuitry for the superheaters and the interstage attemperator. The first-stage superheater header has two outlet connections rather than three as shown in the CDR. The change was made to reduce the number of attemperators from three to one, thus simplifying temperature control. The number of header connections on the second-stage inlet header and second-stage outlet header were reduced similarly.

MEMBRANE
PANELS

BOILER CAVITY

OUTLET
HEADER

MEMBRANE
PANEL

INLET
HEADER
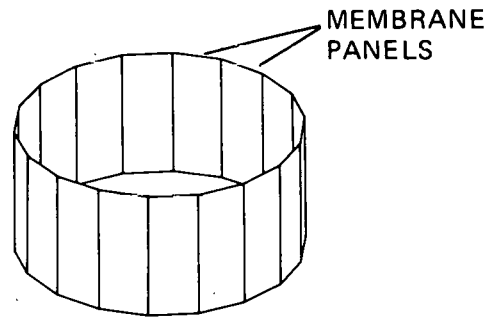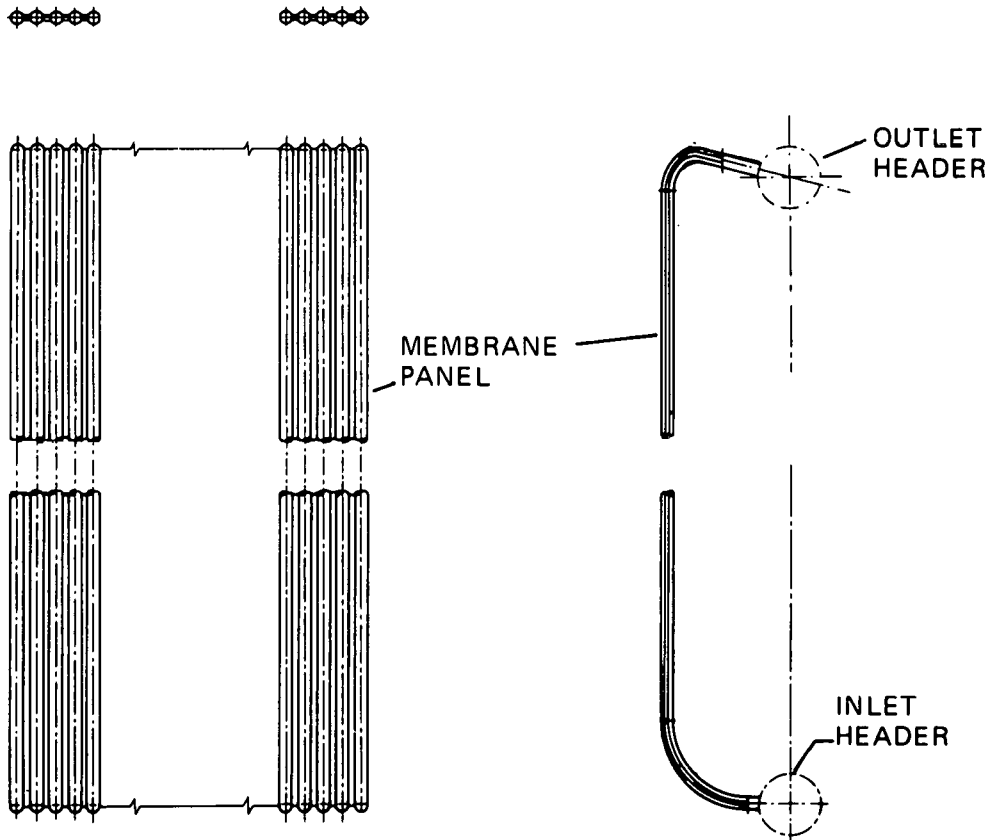
BOILER MEMBRANE PANEL

Figure 27. SRE Membrane Panel Arrangement
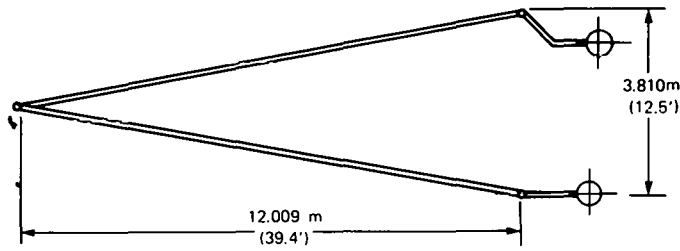
55 MWt — SUPERHEATER HELIX

SPECIFICATIONS:	TUBE O.D.	2.54 cm (1.00") (132 TUBES REQ'D)
	MIN. WALL	0.419 cm (0.165")
	MAT'L	SA213 T22
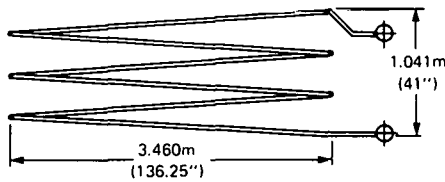
5 MWt — SUPERHEATER HELIX

SPECIFICATIONS:	TUBE O.D.	2.54 cm (1.00") (12 TUBES REQ'D)
	MIN. WALL	0.419 cm (.165)
	MAT'L	SA213 T22

Figure 28. Superheater Heat Transfer Surface
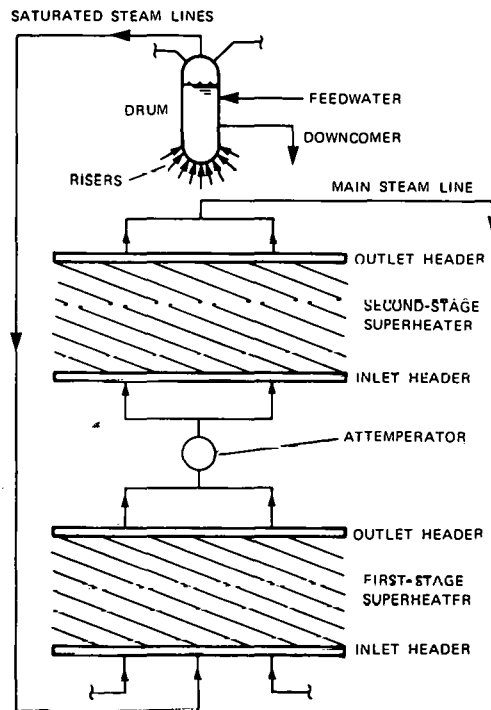
Figure 29. Superheater Flow Circuit

Figure 30 is a plot of superheater design temperatures for the two stages. Superheater outlet steam temperature is increased by 15.6°C (60°F) over the rated steam temperature of 512°C (955°F) to arrive at the design steam temperature. This increase is made to account for tube-to-tube maldistribution. The design metal temperature shown in the figure is the average temperature across the tube wall at the circumferential location of maximum heat flux.
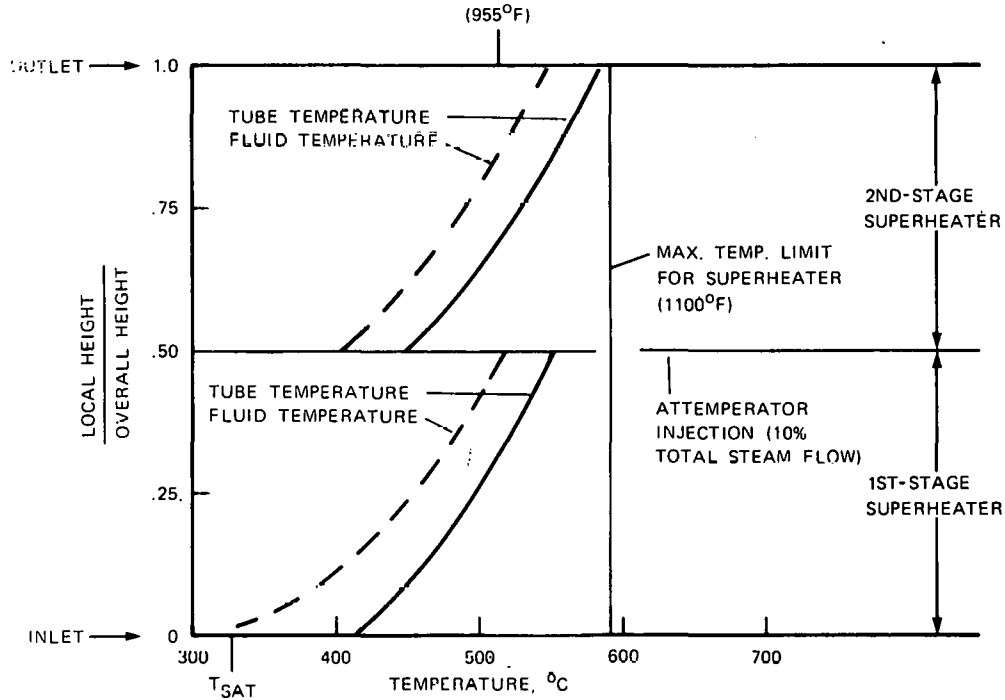
Figure 30. Fluid and O. D. Tube Temperatures - Superheater

As used in the conceptual design, the ability of Croloy 2-1/4 tubes to resist spalling at cyclic operating conditions was questioned. Further investigation indicates that fossil boilers with Croloy 2-1/4 superheater tubes operating under cyclic conditions do not exhibit unusually high rates of oxidation. Since this type of tube meets all requirements of the steam generator, and at less than half of the cost of high-alloy tubing, it will be used in the steam generator SRE. Superheater tubes will be observed during the tests to determine if there is a tendency to spall.

Heat Transfer Surface Supports

Figure 31 shows the concept for support of the boiler and superheater sections. The superheater headers have been relocated to permit draining the super-heater.
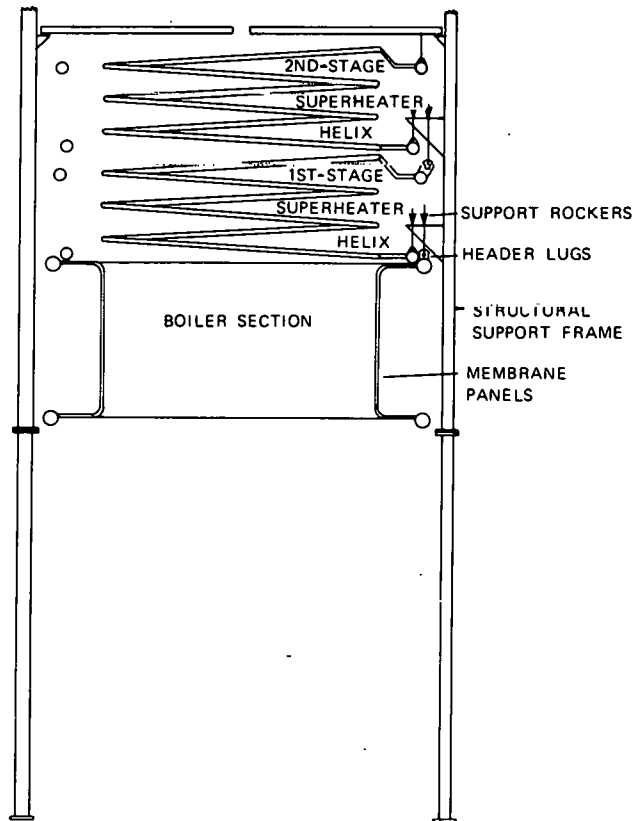
Figure 31. SRE Support Concept

Drum and Internals

The drum and internals are shown in Figure 32. The design has been changed to permit use of a stock hollow forging for the drum shell and pressed hemispherical heads rather than the pipe and pipe caps selected originally. This change was made because the pipe and caps did not meet the requirements of the ASME Code for boiler drums.
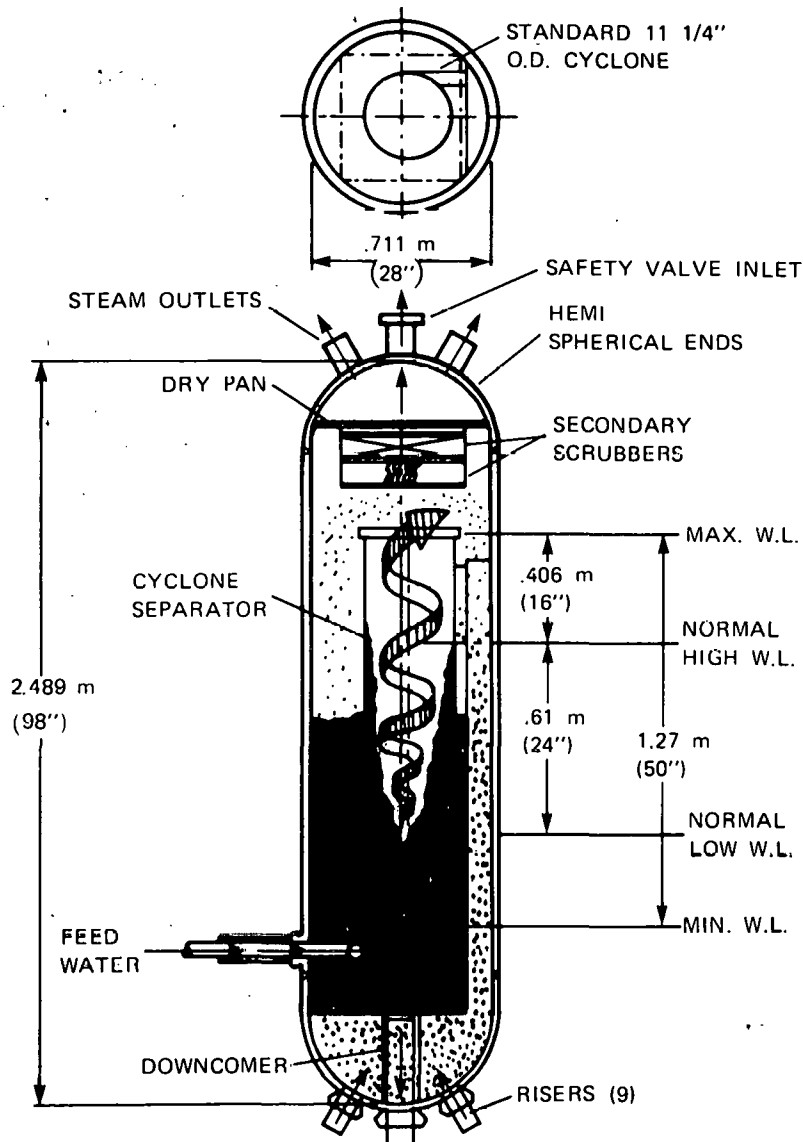
Figure 32. SRE Drum and Internals

Test Parameters

Solar Simulator -- The solar simulator design was modified to simplify it and provide better control. The number of manual/automatic programming sections on the control console was increased from three to four. Each section corresponds to one lamp array zone, which is arranged as shown in Figure 33. Individual lamp and facet structure are shown in Figure 34.
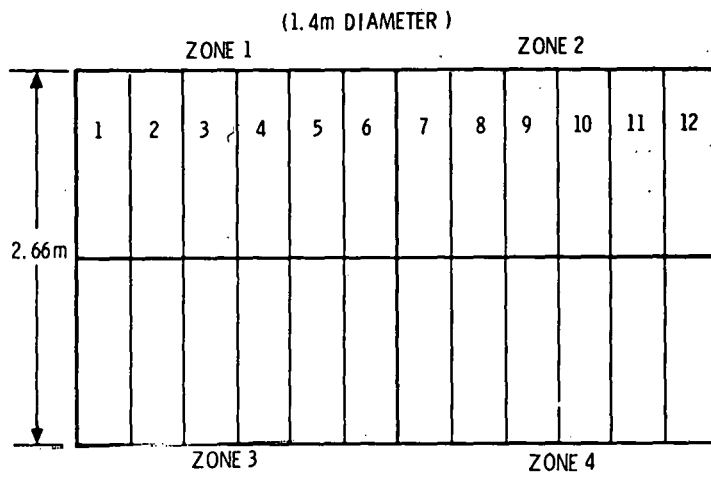
Figure 33. Solar Simulator Array Zone/
Facet Orientation
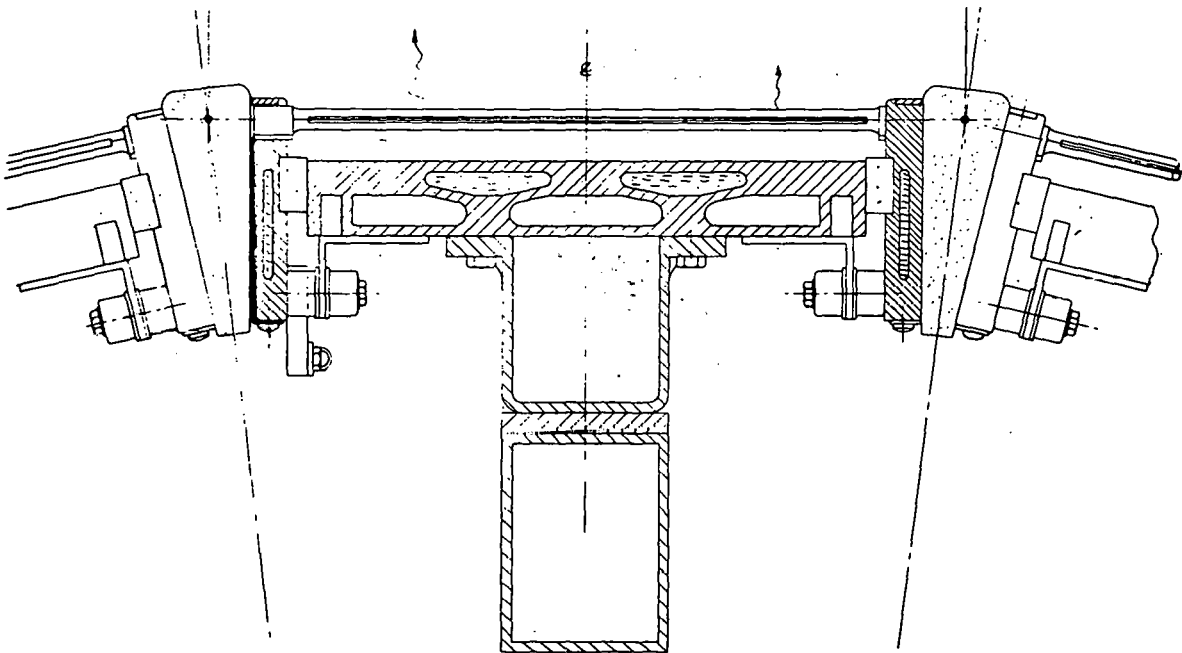
Figure 34. Lamp and Facet Detail

Test Plan -- Steam generator SRE testing will include the following steps to ensure safety and proper instrumentation performance, and to verify steady-state and transient performance of the steam generator:

- Initial debugging
- Cold checkout
- Hot checkout
- Control system tune-up
- Initial calibration tests
- Steady-state performance tests
- Transient performance tests

SECTION V

THERMAL STORAGE SUBSYSTEM RESEARCH EXPERIMENT

DESCRIPTION OF THE SUBSYSTEM

Storage Concept

The thermal storage concept uses the latent heat of fusion of a eutectic salt to store thermal energy. Energy to charge the salt is obtained as heat of condensation from steam supplied by the steam generator (receiver) subsystem. The banks of condenser tubes are located at the bottom of the storage tank. Heat transfer to the salt is by natural convection.

Heat energy in the tank is discharged by circulating feedwater through boiler tubes located at the top of the tank to obtain saturated steam. Salt buildup on the tubes is removed mechanically.

Pilot Plant Design and Performance Features

The basic design features of the pilot plant thermal storage subsystem include:

- 315-MWhr(t) storage capacity
- Salt phase-change materials $NaNO_3$ - $NaOH$
- Array of five insulated cylindrical tanks
- Ground-level storage
- Modular heat exchangers
- Self-regulating control system
- 40-year storage life
- One holdup storage tank

The basic performance features include:

- Deliver 7 MW(e) net - 6 hours
- Provide 28°C superheat
- 6.5 MPa/307°C discharge cycle
- 12 MPa/510°C charge cycle
- Handle 31.5-MW(t) charge rate
- Heat loss <0.35 percent per hour

Phase-Change Material

A mixture of 99 percent by weight of sodium nitrate (NaNO3) and 1 percent by weight of sodium hydroxide (NaOH) was selected as the storage medium because of its desirable characteristics (solid plus liquid phase) in the operating temperature range.

OBJECTIVE OF THE EXPERIMENT

The thermal storage SRE is designed to give maximum information for evaluating the design, performance, and operating parameters of the proposed pilot plant configuration.

The pilot plant configuration selected makes it possible to design, construct, and test a full-size heat exchange module. The module will contain the same salt mixture as the pilot plant cell and will exchange heat with identical vaporizer and condenser heat exchangers. The same control system will be used and will operate on the same basic charge and discharge-cycle conditions. The performance of the SRE model can be evaluated and the operating characteristics defined and directly applied to the pilot plant design. The operating experience gained during the testing phases will permit a realistic assessment of equipment reliability and maintenance. This will enable expected subsystem availabilities to be determined as a function of the key plant operating parameters. A comparison of the pilot plant and SRE parameters is presented in Table 11.

Table 11. Pilot Plant -- Thermal Storage
SRE Comparison

	Pilot Plant	SRE
Design	• 315 MWhr(t) main storage capacity • Salt PCM - NaNO3 - NaOH • 235 modular exchangers housed in 5 cylindrical storage tanks • 15-MWhr(t) superheater capacity • Self-regulating control system • Ground-level storage	• 1.34-MWhr(t) storage capacity • Same salt PCM - NaNO3 - NaOH • Single PP modular exchanger in a rectangular tank • Based on test results and analysis • Same control system • Above-ground storage with insulation/variable heat loss control system
Performance	• Deliver 7 MW(e) net or 31.58 MW(t) discharge rate - 6 hours • Provide 28C° superheat • 6.5 MPa/307°C discharge cycle • 12 MPa/510°C charge cycle • 31.58 MW(t) charge rate • Heat loss <0.35%/hr	• 134 kW(t) discharge rate - 6 hours • Based on test results and analysis • Same discharge cycle • Same charge cycle • 134-kW(t) charge rate • Variable heat loss

STATUS OF THE EXPERIMENT

Significant progress was made during the report period in refining the thermal storage SRE concept preparatory to carrying it into detailed design.

The conceptual design was reviewed initially on 17 December 1975. Since there had been time for only limited experimentation with an engineering model prior to the review, it was felt more information was needed to evaluate the approach. Areas requiring further work were:

- Analysis of the system using an $NaNO_3$ mixture with higher melting temperature than $NaNO_3$ - $NaCl$ - Na_2SO_4

- Definition of scraper design and energy recovery with the $NaNO_3$ mixture

- Evaluation of the $NaNO_3$ mixture in additional cycling and decomposition tests

- Understanding the freezing response process.

These and other questions pertaining to the thermal storage SRE were addressed on 29 January and 9 March after further analysis and experimentation. The new and amended data were incorporated in the Thermal Storage Conceptual Design Report, which was resubmitted for approval on 22 March.

Assuming approval, detailing of the design will be initiated. Preparation for SRE testing is proceeding in accordance with the schedule shown in Figure 35.

DESCRIPTION OF THE EXPERIMENT

Thermal Storage Unit

The original concept called for scaling the SRE storage unit to the pilot plant baseline. However, the configuration selected for the latter makes it feasible to build and test a full-size heat exchange module in the SRE. The conceptual design was so modified during the report period.

Tank -- The cube-shaped tank (Figure 36) is readily manufactured and transported and lends itself to efficient vaporizer and condenser designs. Figure 37 shows tank design pressure and Figure 38 heat loss as a function of tank insulation. The tank assembly is shown diagrammatically in Figure 39.

EVENT	1976												1977			
	J	F	M	A	M	J	J	A	S	O	N	D	J	F	M	A

TEST FACILITY PREPARATION
  COMPONENT DELIVERY
    VALVES
    PIPING
    DESUPERHEATER
    INSTRUMENTATION
  PIPING INSTALLATION
  PIPING TEST
  INSTRUMENTATION INSTALLATION
  INSTRUMENTATION CHECKOUT
  CONTROL CONSOLE INSTALLATION
DATA ACQUISITION SYSTEM
  HARDWARE DELIVERY
    INSTALLATION IN CONTROL CENTER
  SOFTWARE PREPARATION
  SOFTWARE DEBUG
  OPERATIONAL CHECKOUT
  FACILITY INSTALLATION
CONTROL CENTER
  DELIVER TO RIDGWAY
  PREPARATION
STORAGE TEST AREA
  CONSTRUCTION
STORAGE TEST ITEM
  DELIVERY
STORAGE TEST PROCEDURES
  UPDATE
STORAGE TESTS
  INSTALLATION CHECKOUT
PRE-OPERATION TESTS
  PERFORMANCE

Figure 35.   Thermal Storage SRE Preparation
and Test Schedule
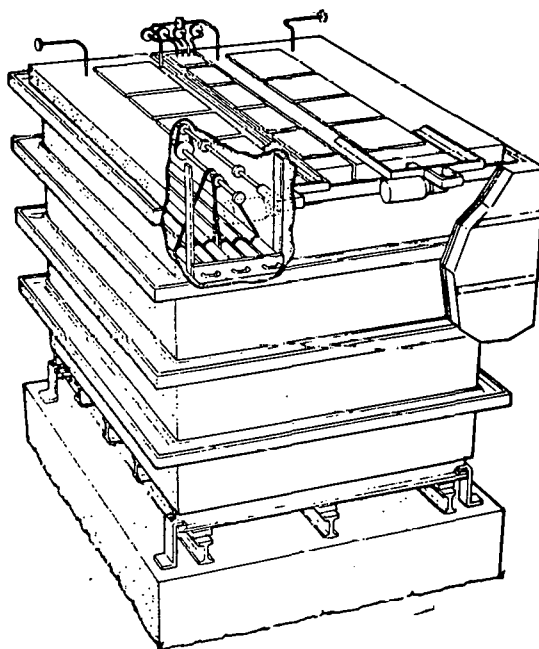
Figure 36.   Thermal Storage Tank

41
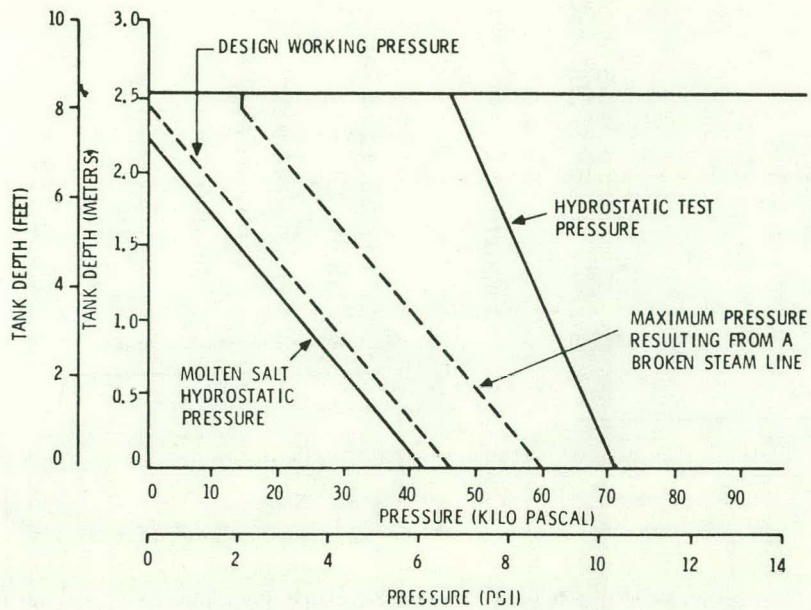
Figure 37. Thermal Storage Tank Design
Pressure
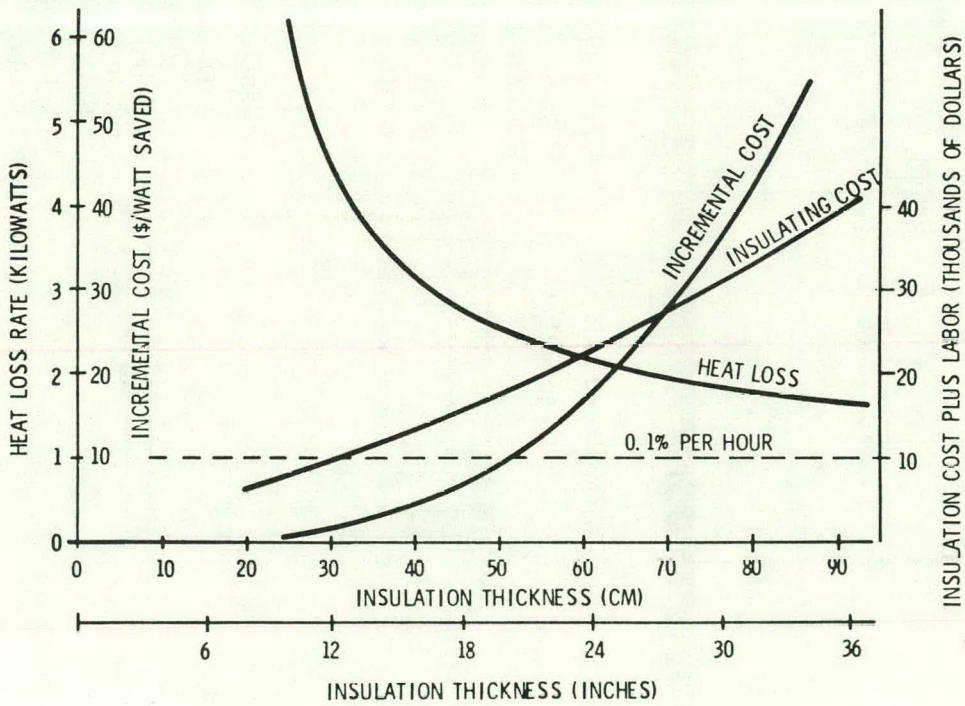
Figure 38. Heat Loss versus Tank
Insulation

Temporary Covers
With Gasketed
Access Hatches

Temporary Test Cover
Setup

Vaporizer Cover & Support

Vaporizer Cover Seal

Counter Shaft

Shaft Drive

Sprocket

Scraper Drive
Motor & Reducer

Scraper Chain
Drive

Vaporizer
Tube Support

Tank Reinforcing
Beam

Fully Charged Salt
Liquid Line

Discharge Salt
Liquid Line

Chain Drive

Insulation

Vaporizer Tube
& Scraper

Tank Drain

Guard Heater

Downcomer
Steamline

Marinite
(Or Equiv)
Insulation Blocks

Condenser

Condensate Drain
Line

Tank Base
Anchor

Concrete Base Pad

Secondary Tank Heater
& Liquid Relief Path
Generator

Cross-Support Beam

Figure 39. Thermal Storage SRE Tank Design

42

Vaporizer -- The vaporizer unit of the thermal storage SRE is one of 235 pilot plant heat exchanger modules. Operating under identical conditions, it has 1/235th of the pilot plant output. Vaporizer design parameters are summarized in Table 12. Design details are listed in Table 13.

Table 12. Vaporizer Design Parameters

	Parameter	Pilot Plant	SRE
Performance Requirements	Discharge rate	$1.078(10)^8$ Btu/hr	$4.59(10)^5$ Btu/hr
	Temperature difference	31°F	
	Operating pressure	1000 psi	
	Pipe size	1.0 O.D. /0.87 I.D.	
	Steam quality	0.20	
	Water velocity	5 ft/sec	
Physical Limitations	Energy density	9000 Btu/ft^3	
	Heat recovery	0.6	
	Salt heat flux	6500 Btu/hr ft^2	
	Heat transfer coefficient	670 Btu/hr ft^2 °F	
Design	Number of modules	235	1
	Surface area	16,584 ft^2	70.5 ft^2
	Salt depth	7.25 ft	7.25 ft
	Length of pipe	19,825 ft	84 ft

Table 13. Vaporizer Design Detail

Parameter	Value
Number of rows	1
Number of serpentines	1
Number of legs	12
Length of legs	2.13 m (7 ft)
Tube center spacing	
Scraper length	53 cm (21 in.)
Number of scrapers	48
Number of drive motors	2
Type of tubing	ASTM A214
Corrosion allowance	0.03 cm (0.012 in.)/12 yr

The scrapers are ganged and chain-driven by two motors. The current scraper configuration is shown in Figure 40, but other configurations and salt removal techniques will be evaluated during the detail design phase. Any changes will be reflected in the pilot plant design to ensure uniformity.
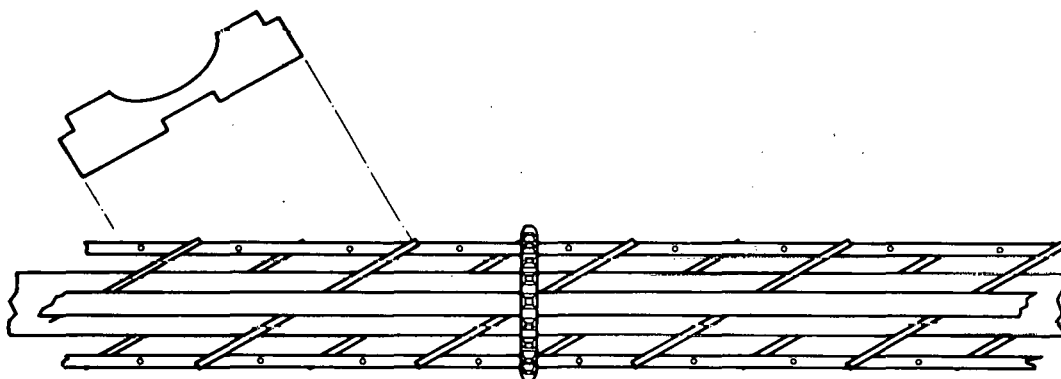
Figure 40. Split-Design, Inclined-Plate
Rotary Scraper

Condenser -- The condenser unit of the thermal storage SRE is a full-scale model of a pilot plant condenser module. Design parameters are listed in Table 14, and design details in Table 15. Pipe wall thickness was calculated from empirical formulae and the table of pressure-temperature ratings (ASME Boiler and Pressure Vessels Code, Section VIII, Table ACS-1).

Table 14. Condenser Design Parameters

Parameter	Value for Module	Factor for Selection of Value
Heat rate	134 kW(t) (4.57 x 10^5 Btu/hr)	Same charge and discharge rate strategy
Steam conditions	12.3 MPa/327°C (1780 psia/620°F)	Steam conditions at receiver and salt temperature
Steam rate	4.12 kg/hr (908 lb/hr)	Charge rate
Pipe size	2.54 cm O.D. x 2.01 cm I.D. 0.27 cm wall (1-in. O.D. x 0.79-in. I.D.)	ANSI code and available sizes*
Module size	166 m (544 ft) tube length in a single serpentine of 71 legs and 2 rows	Free convection heat transfer coefficients and overall ΔT

*For power piping in conditions beyond scope of ASME code.

Table 15. Condenser Design Details

Parameter	Symbol	SI Units		English Engineering Units	
		Units	Condenser Module	Units	Condenser Module
Storage Capacity		MWhr(t)	1.34	Btu	4.57×10^6
Tank Size:					
Length	L	m	2.56	feet	8.4
Width	W	m	2.56	feet	8.4
Height	H	m	2.56	feet	8.3
Pipe Size:					
Outside diameter	D_o	m	0.0254	inches	1.000
Inside diameter	D_i	m	0.0201	inches	0.790
Wall thickness	t_w	m	0.0026	inches	0.105
Exterior area/length	A_o/L	m^2/m	0.0798	ft^2/ft	0.2618
Interior area/length	A_i/L	m^2/m	0.0630	ft^2/ft	0.2068
Condenser Module:					
Total pipe length	L_p	m	165.8	feet	544
No. of serpentines	---	---	1	---	1
Leg length	---	m	2.33	inches	92
No. of legs	---	---	71	---	71
Center-to-center spacing between legs	---	m	0.063	inches	2.48
No. of rows	---	---	2	---	2
Input Parameters:					
Steam rate/module	W	kg/hr	412	lb/hr	908
Entrance steam velocity	---	m/sec	5.0	ft/sec	16.4
Condensate loading	Γ	kg/hr-m	2.48	lb/hr-ft	1.67
Heat rate/module	q	Watts	1.343×10^5	Btu/hr	4.587×10^5
Heat rate/length	q/L	W/m	804.4	Btu/hr-ft	838
Heat flux to:					
Outside area	q/A_o'	W/m^2	10,160	$Btu/hr\text{-}ft^2$	3221
Inside area	q/A_i'	W/m^2	12,862	$Btu/hr\text{-}ft^2$	4077
Charge time (for complete meltdown)	---	hr	10	hr	10
Heat Transfer Coefficients:					
Inside	h_i	$W/m^2\text{-}C°$	13,855	$B/hr\text{-}ft^2\text{-}F°$	2440
Tube wall conductance	h_{w_i}	$W/m^2\text{-}C°$	18,297	$B/hr\text{-}ft^2\text{-}F°$	3222
Fouling coefficient (assumed) (inside and outside)	h_f	$W/m^2\text{-}C°$	5678	$B/hr\text{-}ft^2\text{-}F°$	1000
Outside	h_o	$W/m^2\text{-}C°$	519.6	$B/hr\text{-}ft^2\text{-}F°$	91.5
Overall coefficient	U_i	$W/m^2\text{-}C°$	548.0	$B/hr\text{-}ft^2\text{-}F°$	96.5
Conductance/length	UA/L	$W/C°\text{-}m$	34.6	$B/hr\text{-}F°\text{-}ft$	20.0
Estimated Temperature Drops:					
$t_{sat} - t_{wi}$	Δt_i	C°	0.9	F°	1.67
$t_{wi} - t_{wo}$	Δt_{wf}	C°	2.9	F°	5.25
$t_{wo} - t_{salt}$	Δt_o	C°	19.5	F°	35.0
Overall $\Delta T = (t_{sat}-t_{salt})$	ΔT	C°	23.3	F°	42
Salt temperature	t_{salt}	°C	303.3	°F	578
Steam temperature	t_{sat}	°C	327.6	°F	620
Steam pressure	P	kPa	12,273	psia	1780

The pipe material is A106B carbon steel. Corrosion tests with an $NaNO_3$ - NaOH mixture yielded a corrosion rate of 0.2 mm/year. Using a corrosion allowance of 0.0762 cm (40-year life) and a working pressure of 12.3 MPa, the pipe wall requirement was determined to be 0.267 cm (12-gage tubing).

Phase-Change Material -- Laboratory experiments have shown that it is necessary to have a salt composition that forms a slurry during the freezing process. The salt mixture must allow a large percentage of the material to freeze over a narrow temperature range and yet not form a complete solid above the surface temperature of the heat exchanger. A slurry or slush must be formed which retains a small amount of liquid to prevent the formation of a strong rigid material that cannot be scraped.

A mixture of $NaNO_3$ (99 percent by weight) and NaOH (1 percent by weight) was selected because it meets the above requirements. Melting and freezing characteristics are shown in Figures 41 and 42. The former is based on experimental results, and the latter on differential scanning calorimetry (DSC).

Figure 41 shows that the bulk of the energy is transferred over a small temperature range while a small portion of energy is held in the liquid to a much lower temperature. The dashed lines compare the experimental results with the scan. The scan temperatures are shifted because of high-speed heat transfer in the test tubes.
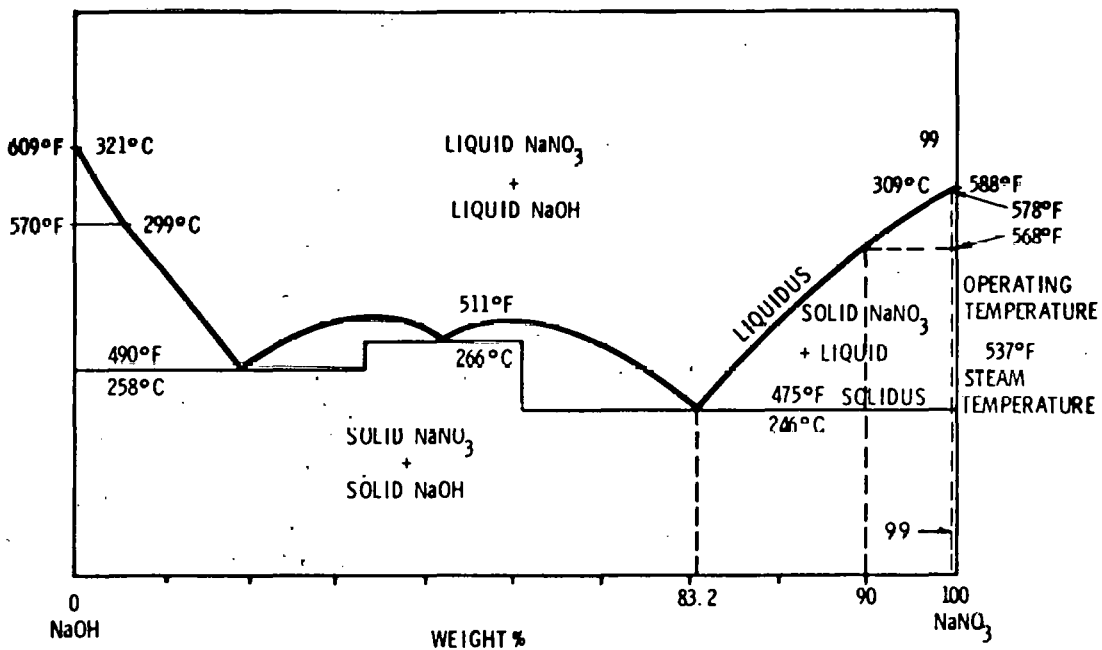

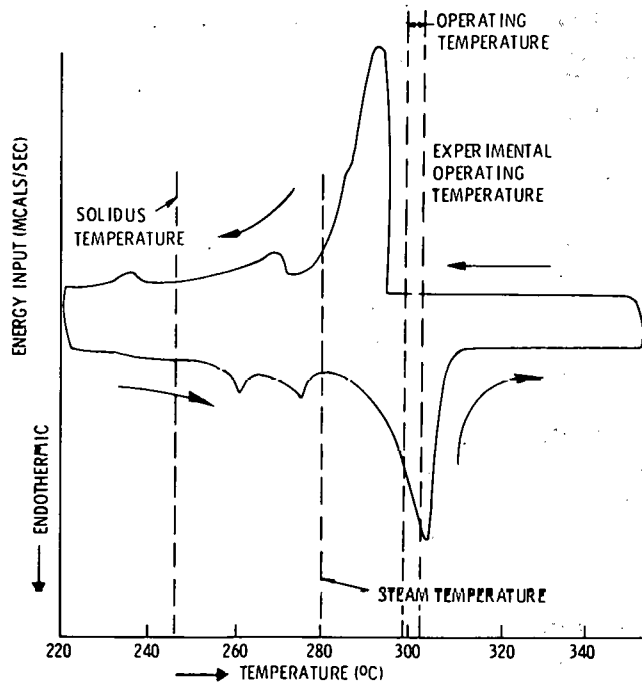Figure 41. $NaNO_3$ - NaOH Phase Diagram

Figure 42. DSC Scan of NaNO₃ + NaOH (1% By Weight)

Since selection of the right phase-change material is essential to thermal storage from both performance and economic standpoints, considerable time was spent on it during the report period. The experimental data are summarized in Table 16 and the DSC data in Appendix B.

Steam Drum

The steam drum design is based on the proper separation of the entrained water in the two-phase flow, the liquid holdup requirements (capacity), and the fluid flow and state parameters.

Steam Drum Separator -- The steam drum separator (Figure 43) consists of a liquid receiver tank and an internal entrainment separator. The liquid receiver has a capacity of 189 liters (50 gallons) of water and an internal volume of 610 liters (21.5 cubic feet). The entrainment separator, based on off-the-shelf elements, is an efficient, large-volume, two-stage unit with a great deal of flexibility in usage. Two noteworthy features are that is has no moving parts and is self-cleaning, thus eliminating maintenance and replacement costs.

Table 16. Engineering Model Test Summary

Parameter	Pilot Plant	1030A*	1125A	0108A-1	0126B	0130B	0202A	0211B	0216B	0220A	0221A	0223A	0226A	0227B	0301A
Composition (component, wt %)	$NaNO_3$?	$NaNO_3$ 83 $NaOH$ 17	$NaNO_3$ 85 $NaOH$ 15	$NaNO_3$ 99 NaC 0.39 Na_2SO_4 0.51	$NaNO_3$ 98 $Ca(NO_3)_2$ 2	$NaNO_3$ 96 $Ca(NO_3)_2$ 4	$NaNO_3$ 81 Na_2SO_4 8 $NaCl$ 5 KNO_3 4 $Ca(NO_3)_2$ 2	$NaNO_3$ 84 Na_2SO_4 8 $NaCl$ 5 KNO_3 2	$NaNO_3$ 82 Na_2SO_4 8 $NaCl$ 5 KNO_3 2 $Ca(NO_3)_2$ 2	$NaNO_3$ 99 $NaOH$ 1	$NaNO_3$ 99 $NaOH$ 1	$NaNO_3$ 99 $NaOH$ 1	$NaNO_3$ 99 $NaOH$ 1	$NaNO_3$ 79 $NaCl$ 5 Na_2SO_4 8 KNO_3 4 $Ca(NO_3)_2$ 4	$NaNO_3$ 99 $NaOH$ 1
Operating temperatures (salt, tube-wall, °F)	549-514	479 474	488 465	577 565	580 574	575 570	545 521	545 540	550 535	576 514	576 542	578 540	578 536	548 515	578 539
Minimum wall temp (°F)	<514	474	465	550	563	531	511	539	514	473	475	475	475	513	475
Pipe heat flux (Btu/hr-ft^2)	21,000	3200	3000	5100	7800	3000	9600	7500	9000	36,600	24,900	25,500	24,000	16,500	24,000
Salt heat flux (Btu/hr-ft^2)	13,000	1100	1000	1700	2600	1000	3200	2500	3000	12,200	3000	8500	8000	5500	8000
Heat recovery (%)	85	---	---	54	53	70	37	41	54	31 (43)	38	53	63	56	65
Ext. heat transfer coefficient	609	165	1200	503	1200	500	400	850	550	600	300	850	900	590	800
Scraper speed (rpm)	?	80	160	60	160	40	120	40	110	120	120	120	120	120	120

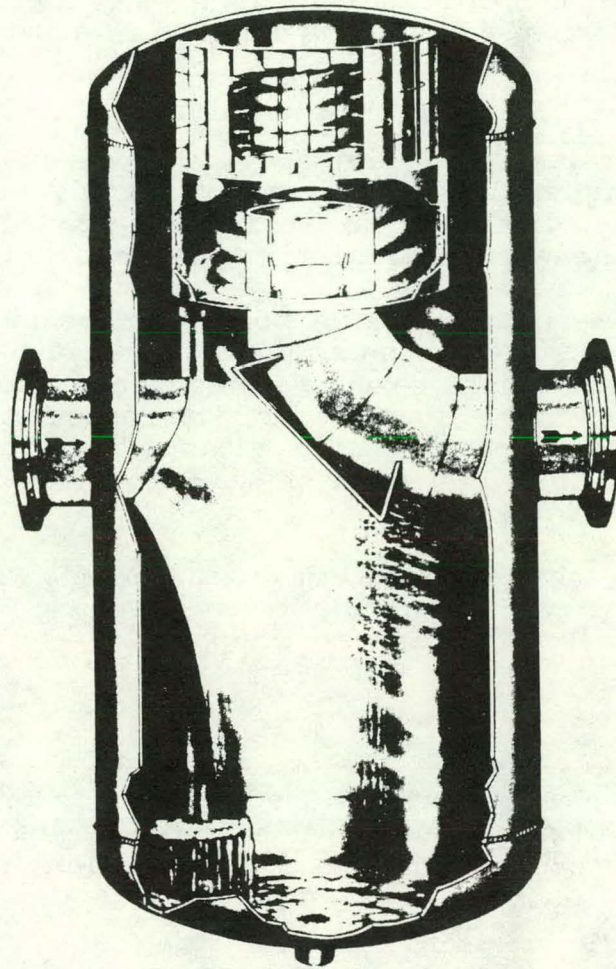*Designator indicates test date and sequence.

Figure 43. Wright-Austin Entrainment Separator Receiver

Recirculation Control -- The steam drum pressure can be allowed to circulate between the design point and the limit of salt temperature, or it can be controlled by using recirculation rate as a control variable.

If the recirculation rate is held constant, steam drum pressure will have an equilibrium value proportional to the rate at which steam is being used. If the recirculation rate is constant, the heat transfer coefficient will be constant. Therefore, the temperature differential (T_{sat} - T_{salt}) will vary with the discharge rate. The steam drum pressure is directly related to ΔT. At low discharge rate, ΔT will go to zero. In that condition the steam temperature will equal the salt temperature.

On the other hand, steam drum pressure can be held constant by varying the heat transfer coefficient by varying circulation rate. Then the ΔT will be held

constant. In that case, the recirculation rate and steam quality will go to equilibrium values determined by the output steam rate and the overall heat transfer coefficient.

Steam Drum Level Control -- The liquid level in the steam drum is controlled by the feedwater flow rate. The feedwater flow response is reduced by including liquid level rate feedback to the flow control valve. Liquid level rate feedback is achieved by adding a signal from the output steam flow rate to the liquid-level signal. The output steam rate is proportional to liquid rate.

Steam Charge Control -- In the charging mode, the thermal storage unit receives steam at pressures and temperatures above the design conditions. The steam is conditioned with a pressure regulator and a desuperheater. The steam is then condensed in the storage cell. The condensate flows into a trap that discharges condensate without passing steam. The condensate is still at fairly high pressure and partially vaporizes as it goes through the throttling to a low-pressure return line.

The input steam at the test site (Northern States Power's Riverside Plant) will be reduced through a pressure regulator to design values. An air failure-to-close isolation valve will protect the test equipment.

Test Instrumentation

Temperature -- Thermocouples will be used to measure boiler temperatures, condenser tube temperatures, tank wall temperatures, and salt temperatures within the tank. Thermocouple locations will be as follows:

- Tank (outside) - 28
- Condenser - 26
- Boiler - 10
- Bulk Fluid - 58

Thermal Capacity -- Liquid surface level will be used as an indicator of the percentage of storage capacity that is melted.

Figure 44 shows the basic measurement scheme. A small dip tube is supplied with dry nitrogen through a regulator and orifice. A differential pressure gage measures the pressure necessary to bubble nitrogen out of the dip tube. The pressure will be a direct function of the liquid level above the end of the tube and the fluid density.
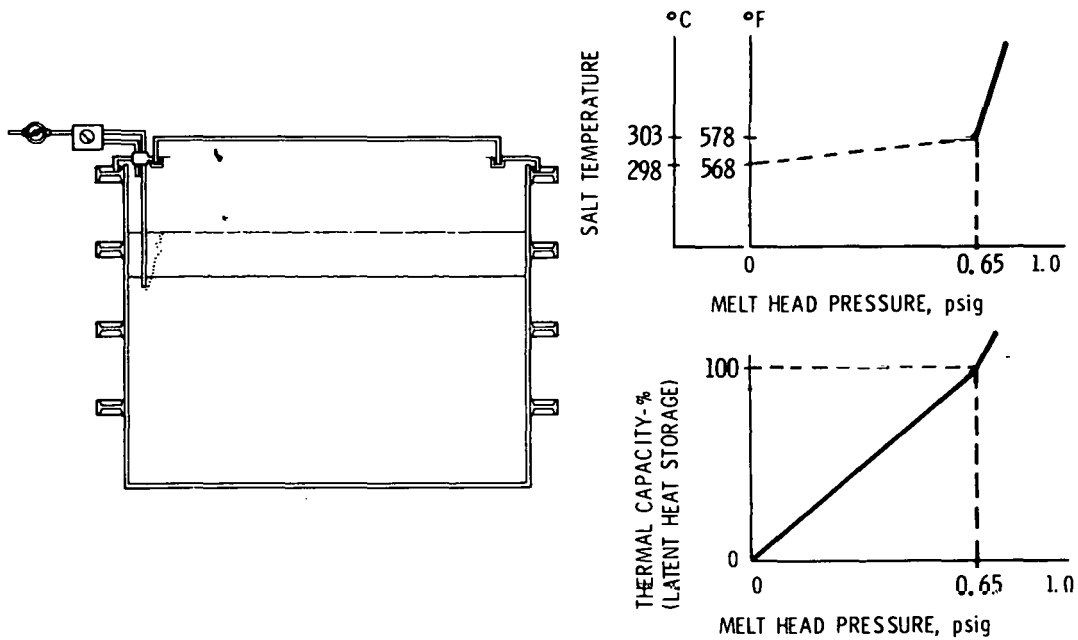
Figure 44. Thermal Capacity Measurement

Heat Loss -- Heat flux meters will be attached to the sides, top, and bottom of the insulation to determine overall heat loss rate. Measurement of tank surface temperatures, insulation outer jacket temperatures, and guard heater power input will give a good calibration of the heat flux meters. The latter can then be used to adjust guard heater power levels at other temperatures.

Salt Buildup on Tank Walls -- To measure salt buildup on the walls, mechanical probes will be used through the access ports. If needed, additional probing parts will be included to facilitate this work.

Safety

The following safety aspects have been thoroughly considered and appropriate safeguards incorporated in the test arrangement:

- Personnel safety
- Fire
- Condenser leakage
- Vaporizer leakage

52

SECTION VI
ELECTRICAL GENERATION AND PLANT INTEGRATION

ELECTRICAL GENERATION SUBSYSTEM

The electrical generation subsystem is being designed to generate electrical power using a water/steam cycle with the thermal energy being supplied by solar radiation, either directly through the receiver or indirectly through the thermal storage subsystem. The operating modes are listed in Table 17.

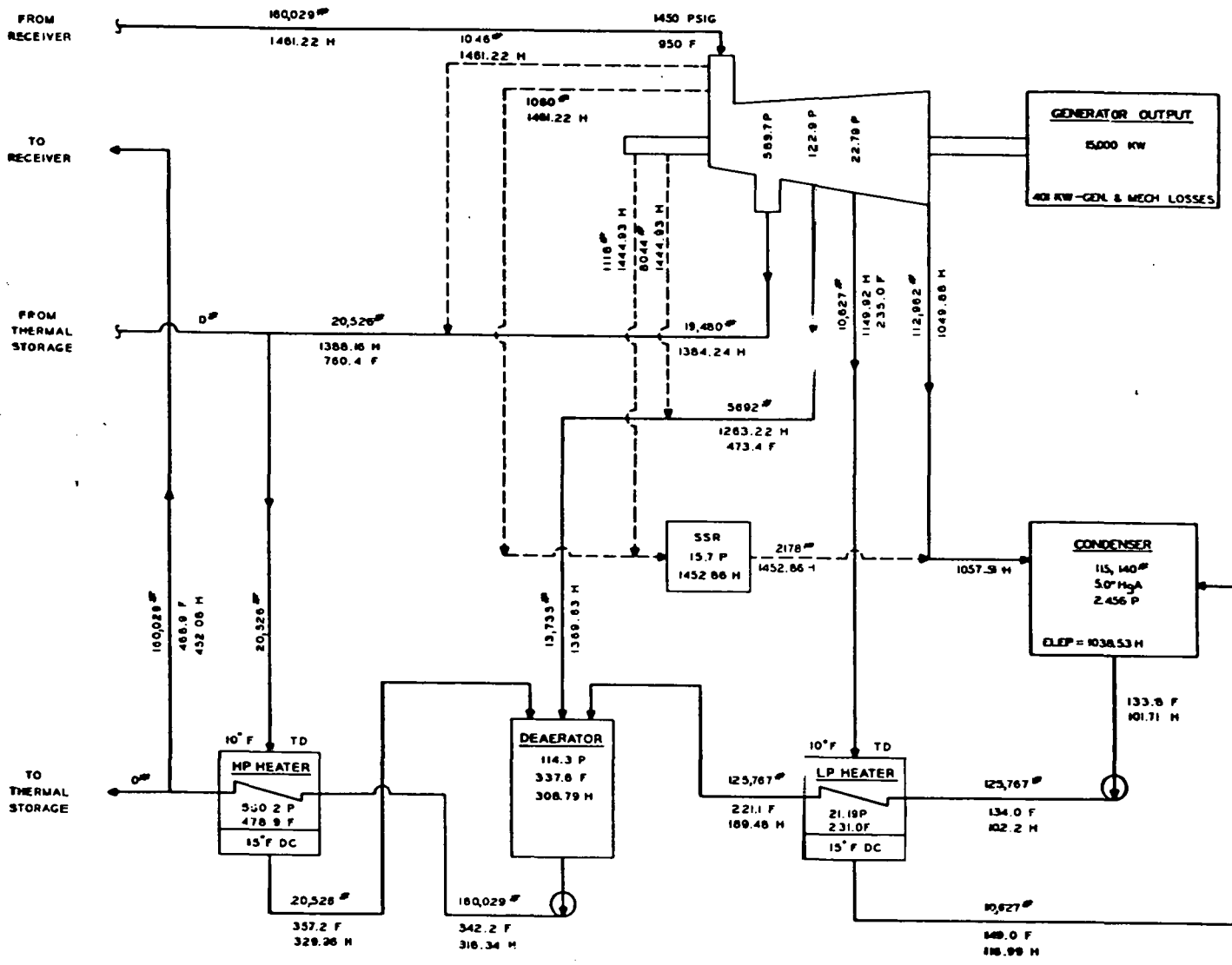Table 17. Solar Power Plant Steady-State Operating Modes

Subsystem	Steady-State Mode					
	A	B	C	D	E	F
Receiver	On	On	On	Off	On	Off
Turbine	On (Receiver steam)	On (Receiver steam)	On (Receiver and storage steam)	On (Storage steam)	Off Off	Off Off
Storage	Holding	Charging	Discharging	Discharging	Charging	Holding

Work being done under this heading includes:

- Performance requirements and operational analysis
- Mechanical design
- Electrical design
- Structural design
- Control and instrumentation
- Plant and support services

Performance Requirements and Operational Analysis

A computer model of the General Electric 15-MW(e) heat balance (Figure 45) was nearly complete at the end of the report period. Figures 46 and 47 are, respectively, an approximate backpressure correction curve and generator output/steam flow curve.

FROM RECEIVER

180,029 # 1450 PSIG
1461.22 H   950 F
1046 #
1461.22 H

1080 #
1461.22 H

GENERATOR OUTPUT

15,000 KW

401 KW - GEN. & MECH LOSSES

TO RECEIVER

589.7 P   122.9 P   22.79 P

1116 #   1444.93 H
8044 #   1444.93 H

1149.92 H   235.0 F
112,962 #
1049.86 H

FROM THERMAL STORAGE

0 #   20,526 #
1388.16 H
760.4 F

19,480 #
1384.24 H

10,627 #

5692 #
1263.22 H
473.4 F

180,029 #
466.0 F   452.06 H

20,526 #

15,735 #   1369.63 H

SSR
15.7 P
1452.86 H

2178 #
1452.86 H

1057.51 H

CONDENSER
115, 140 #
5.0" HgA
2.456 P

CLEP = 1038.53 H

133.8 F
101.71 H

TO THERMAL STORAGE

0 #

HP HEATER
550.2 P
478.9 F
15°F DC

10° F   TD

DEAERATOR
114.3 P
337.6 F
308.79 H

125,767 #
221.1 F
189.48 H

10°F   TD

LP HEATER
21.19 P
231.0 F
15° F DC

125,767 #
134.0 F
102.2 H

20,526 #
357.2 F
329.26 H

180,029 #
342.2 F
316.34 H

10,627 #
149.0 F
116.99 H

LEGEND: H - ENTHALPY, BTU/LB
          # - FLOW, LB/HR
          P - PRESSURE, PSIA
          F - TEMPERATURE, F

GROSS HEAT RATE = 180,029 (1461.22 - 452.06)/15,000 = 10,766 BTU/KW HR

7021 - 102875 - 1
LTSD - 2538A - 3

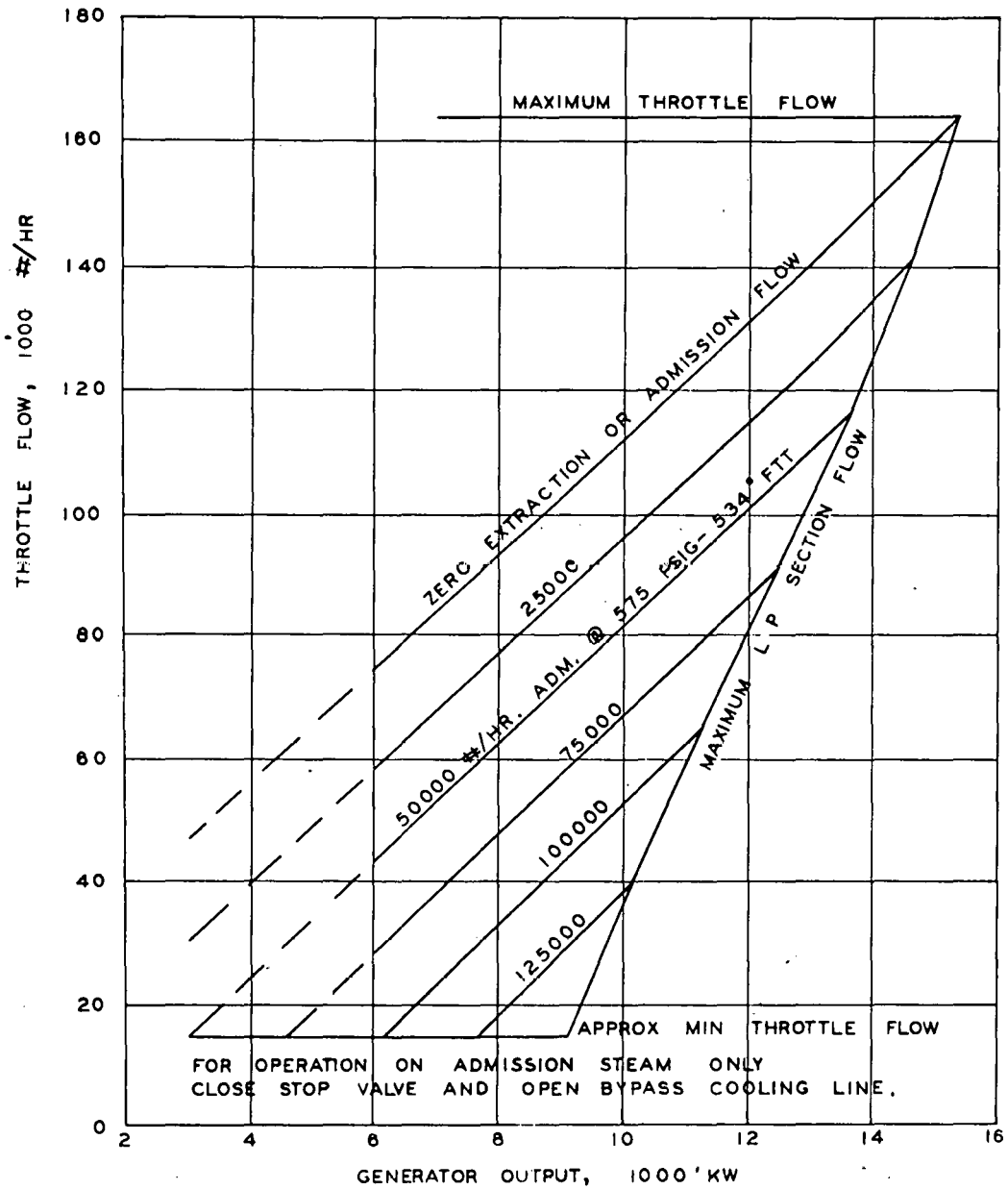Figure 45. General Electric 15,000-kW Heat Balance
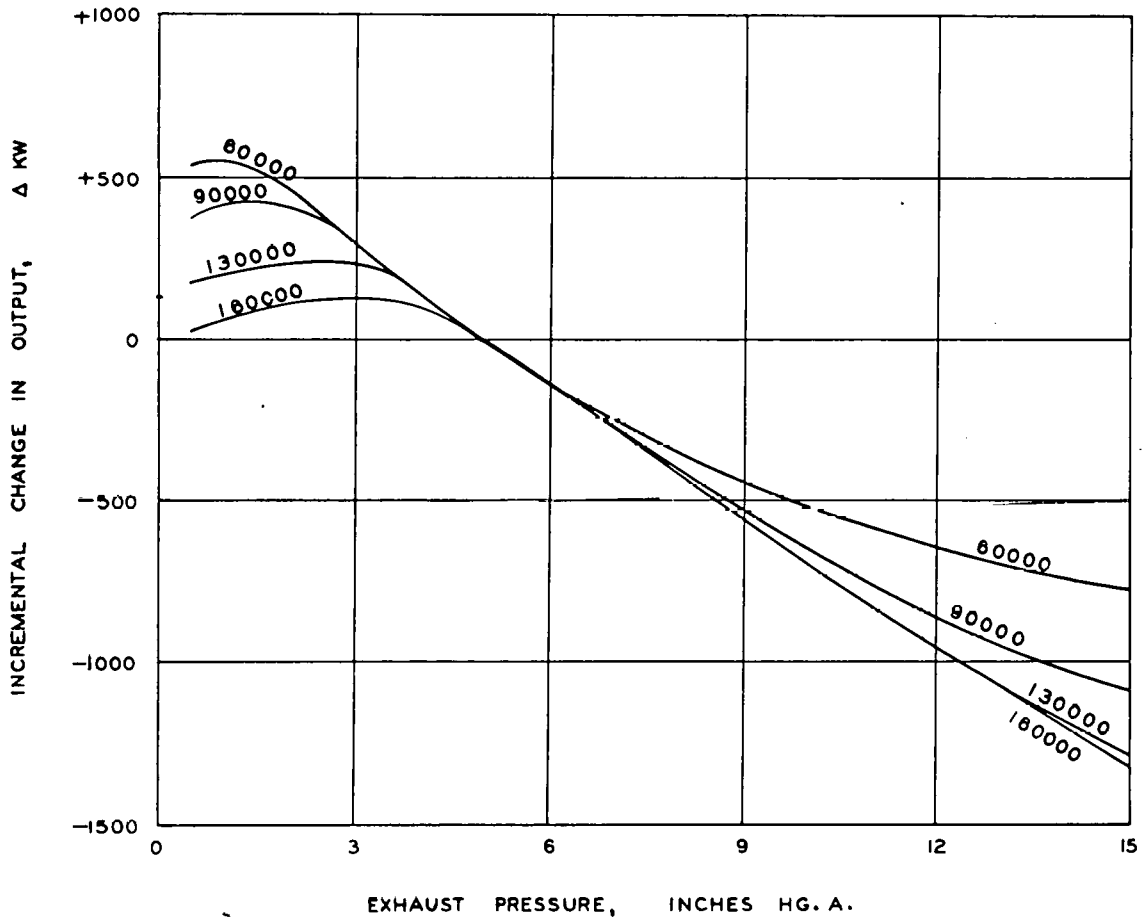
15000 KW
1450 PSIG-950° FTT-5.0" HG. A.
A. E. @ 575 PSIG

LTSD-2538A-6 REV.

NOTE :

1. FIGURES ON CURVES DENOTE VALUES OF APPARRENT
L P SECTION FLOW WHICH IS DEFINED AS THE
SUM OF THE THROTTLE FLOW AND SIMULTANEOUS
ADMISSION FLOW (IF ANY).

2. THE CORRECT OUTPUT AT VARIANT PRESSURE IS
EQUAL TO THE BASE OUTPUT FROM PERFORMANCE
CURVE PLUS THE Δ KW FOR VARIANT - EXHAUST PRESSURE.

Figure 46. Approximate Correction Curve for Variant
Exhaust Pressure

Figure 47. Generator Output versus Steam Flow

A scheme developed for condenser evaluation analysis was revised to incorporate cost parameters and collector, receiver, and 'hermal storage values. The computer program flow chart for condenser analysis is shown in Figure 48. Figure 49 is a typical condenser performance curve.

Mechanical Design

This encompasses definition of cycle efficiency, a feedwater pump analysis, obtaining turbine data, and developing piping and instrument diagrams.

Several cycle and plant efficiencies were defined relative to the current General Electric turbine cycle during the report period.

Several feedwater pump arrangements are under study. The high-head, low-flow condition resulting from tower height and receiver drum pressure represents an unusual pump application. Preliminary information indicates that at least two pump manufacturers can satisfy one or more of the alternative arrangements.

Preliminary versions of four piping and instrument diagrams were developed during the report period. They include service air (compressed), control air (compressed), turbine lubricating oil, and service and fire water. Descriptions to complement the diagrams have been started.

Electrical Design

Information was obtained from equipment manufacturers to update the total auxiliary power requirement. The current estimated peak value auxiliary power requirement is 1850 kW. This will change when more information from manufacturers becomes available.

Structural Design

Preliminary plant arrangement drawings were generated for the pilot plant baseline design. Additional design information from equipment manufacturers and possible location of the pilot plant with an existing facility will (could) have major impacts on the arrangement.

A preliminary design for the turbine foundation was completed. Figure 50 is an outline drawing of the foundation.
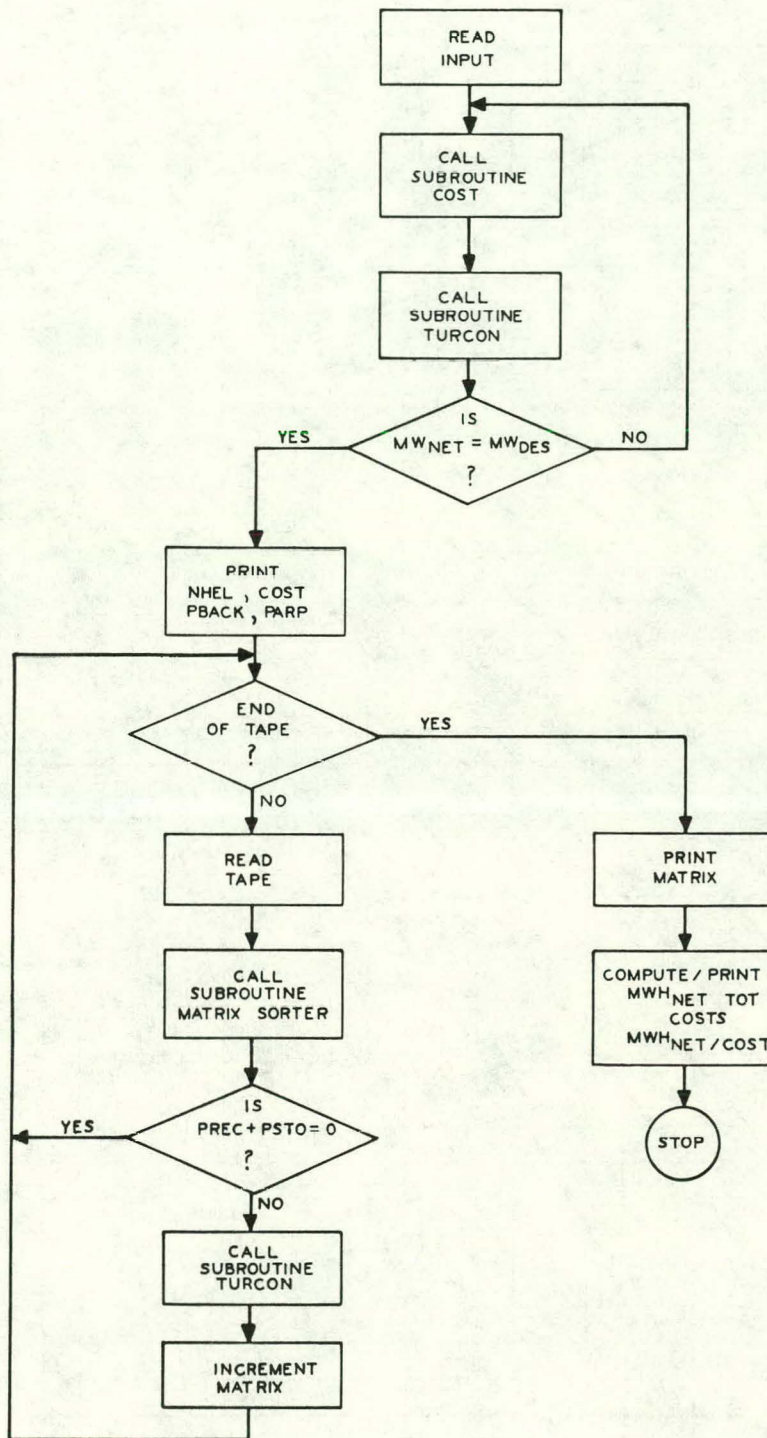
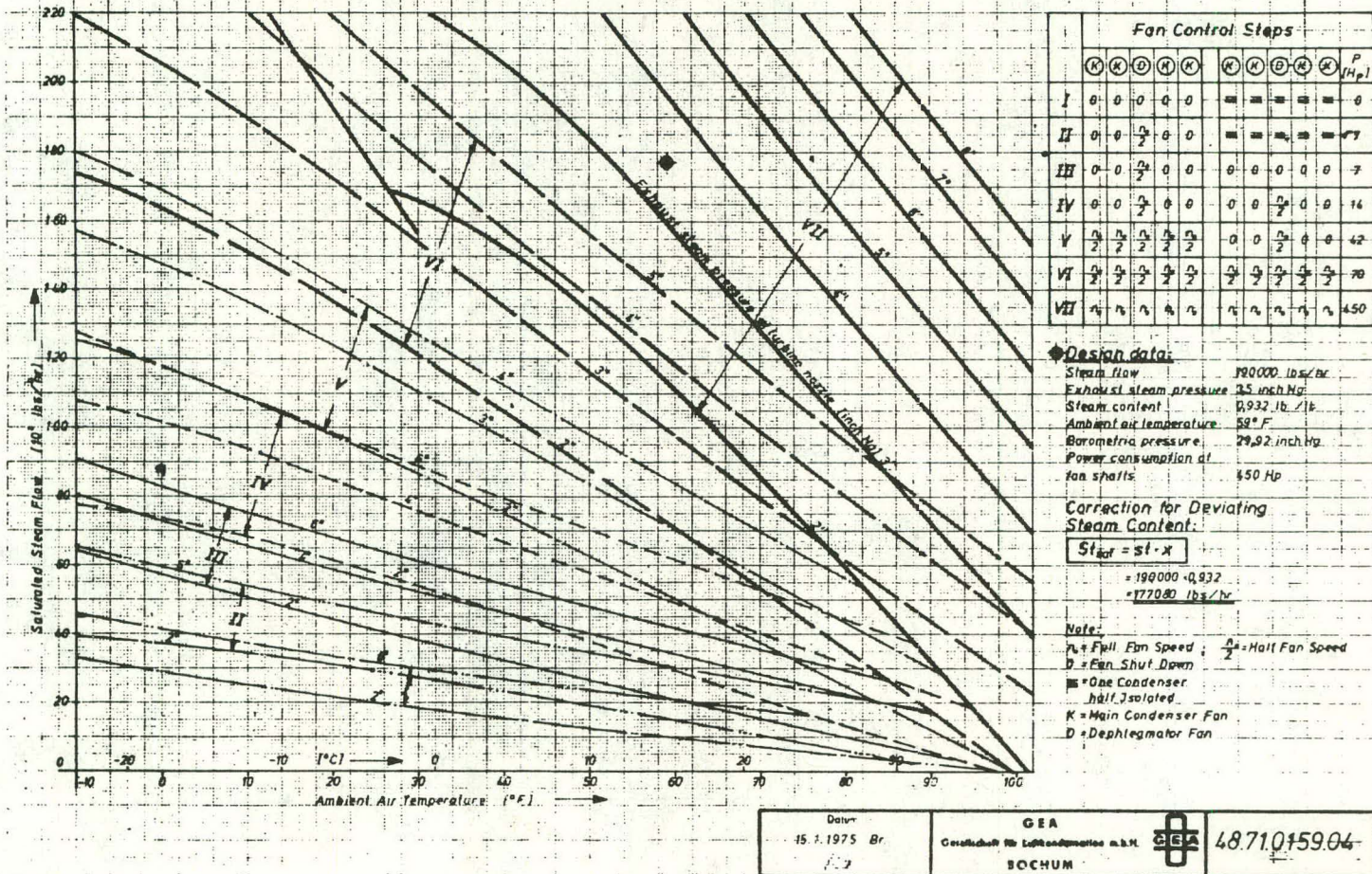Figure 48.   Condenser Analysis Program Flow Chart

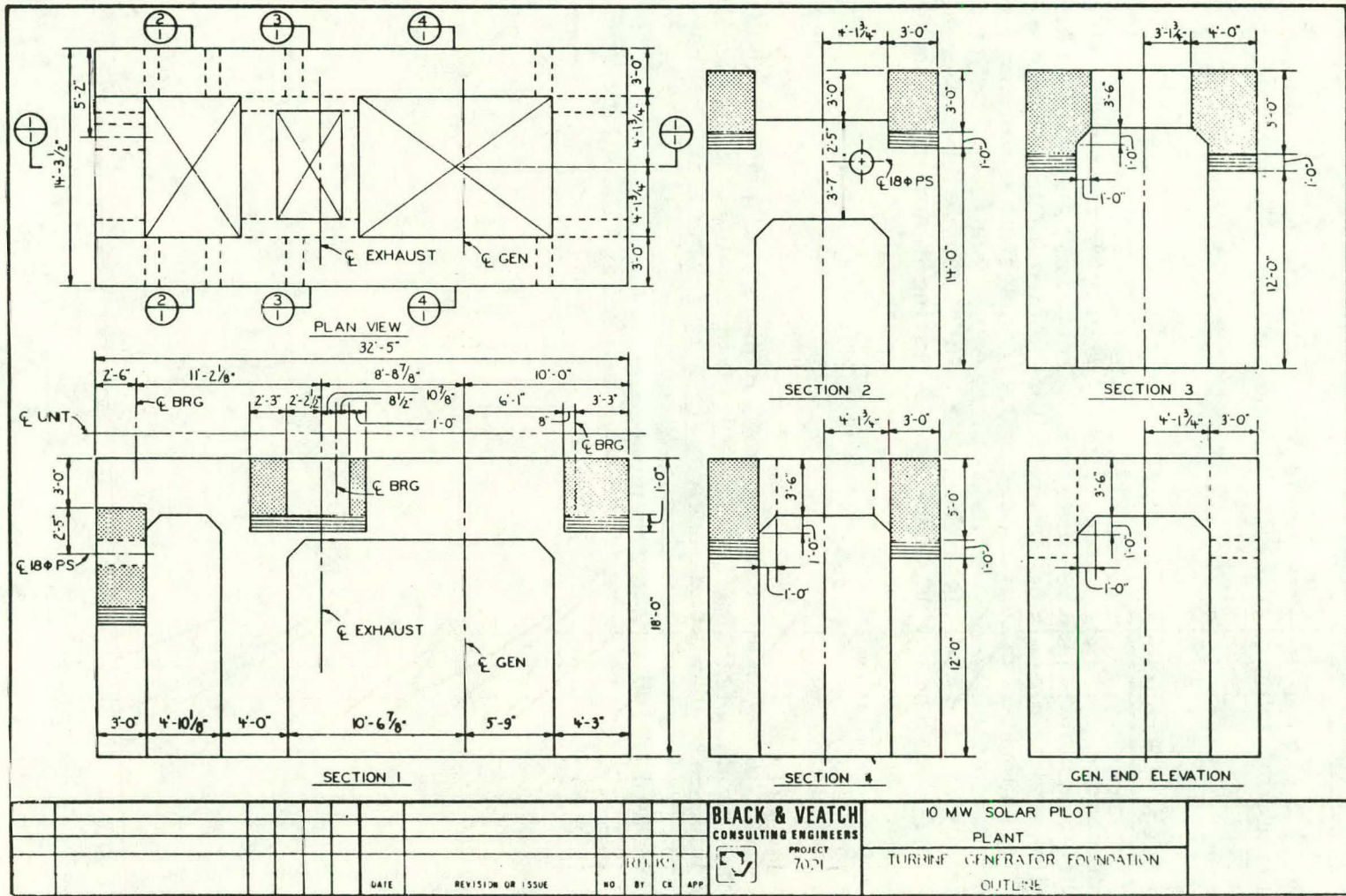Figure 49. Typical Condenser Performance Characteristics

Figure 50. Turbine Generator Foundation Outline

Control and Instrumentation

Black & Veatch has begun development of a control philosophy document. It will include a discussion of tradeoffs between analog and digital control for the pilot plant.

Plant and Support Services

Design information pertinent to the auxiliary cooling water system was received from an equipment manufacturer. The design includes an air-cooled water chiller and an air-cooled water cooler. At air temperatures above $21^{\circ}C$ ($70^{\circ}F$), the water chiller is required to remove the estimated 5 million Btu/hr heat load associated with major plant equipment (e.g., boiler feedpump bearings). At air temperatures below $70^{\circ}F$, the water cooler will handle the heat load, resulting in substantial saving in auxiliary power requirements.

PLANT INTEGRATION

The preliminary long-leadtime study was completed. A preliminary finding was that the turbine generator is the key item in the electrical generation (including balance of plant) and receiver (less steam generator) subsystems. A related finding was that if the Sandia-Livermore schedule is to be met, the turbine generator specification document must be started during Phase I. Figure 51 is the latest revision of the procurement and installation schedule.

FILE NO. | **DESCRIPTION**

Years across top: 1977 | 1978 | 1979 | 1980 (months J F M A M J J A S O N D repeated)

EQUIPMENT PROCUREMENT
- TURBINE·GENERATOR — X ... C
- FEEDWATER HEATERS — C
- PIPING — C
- GENERATOR TRANSFORMER — C
- VALVES — C
- CONDENSER — C
- PUMPS — C
- DEAERATOR — C
- SECONDARY UNIT SUBSTATION — C
- PLANT SERVICES EQUIPMENT — C
- CONTROL / INSTRUMENTATION — C
- ELEVATORS — C
- MOTORS — C
- WATER TREATMENT — C
- BATTERIES — C
- MOTOR CONTROL CENTER — C

FIELD CONSTRUCTION
- CONSTRUCTION FACILITIES
- SITE PREPARATION

FOUNDATIONS
- RECEIVER TOWER
- TURBINE·GENERATOR

SUPERSTRUCTURE
- RECEIVER TOWER
- TURBINE AREA
- CONTROL / SERVICES

(Vertical notes: PHASE I / END OF PHASE I / START OF PHASE II / INITIAL OPERATION / NORMAL OPERATION)

Legend:
X - INITIATION OF SPECIFICATION DOCUMENT
C - CONTRACT AWARD
— - INSTALLATION

BLACK & VEATCH
CONSULTING ENGINEERS
B&V PROJECT 7021

ENERGY RESEARCH AND DEVELOPMENT ADMINISTRATION
10 MWe SOLAR PILOT PLANT
PRELIMINARY PROCUREMENT AND INSTALLATION SCHEDULE

REVISION - A

DATE | REVISION OR ISSUE | NO. | BY

61

Figure 51. Pilot Plant Preliminary Procurement and Installation Schedule

SECTION VII
PROGRAM DOCUMENTATION

In addition to this report, the Solar Pilot Plant program was documented by the following CDRL items during the first quarter of 1976:

- Preliminary Design Baseline Report (PDBR), Revised, 30 January - CDRL Item 1

- Steam Generator SRE Conceptual Design Report Amendment, 29 January, and Steam Generator SRE CDR, Approved, 16 February - CDRL Item 4

- Thermal Storage SRE Conceptual Design Report Supplement, 29 January, SRE Complement, 9 March, and Thermal Storage SRE CDR, Revised, 22 March - CDRL Item 5

- Preliminary Design Report (Preliminary Cost Estimate), 8 March - CDRL Item 2

- Program Plan Update, 9 March - CDRL Item 9

- Project Review No. 4, 9 March - CDRL Item 10

The initial presentation of the Collector SRE Detailed Design Report (DDR) is scheduled for 4 May, that of the Steam Generator for 6 May, and that of the Thermal Storage for 9 June. These are CDRL items 6, 7, and 8, respectively.

The next Quarterly Technical Report, covering the second quarter of 1976, will be issued on 20 July.

APPENDIX A
PRELIMINARY STRUCTURAL DESIGN AND SEISMIC
ANALYSIS OF RECEIVER SUPPORT TOWER

INTRODUCTION

Purpose

This appendix summarizes the preliminary baseline design and the preliminary seismic and wind analyses of the receiver subsystem. The pilot plant design calls for a central receiver located on top of a tower. Generally, the term tower refers to the reinforced concrete chimney-type structure which supports the receiver. The foundation mat is also considered along with the tower. The receiver consists of the steam generator, the steam generator housing, and the steam generator supports. The receiver subsystem must be designed to survive the effects of earthquakes and wind loadings. Black & Veatch has the responsibility of providing a conceptual design of the tower and the receiver and of analyzing the effects of seismic and wind loadings on the tower and the receiver. The design of the steam generator is the responsibility of Babcock & Wilcox.

Scope

This report presents the design criteria used in the designs and analyses of the tower and the receiver. The design of each element, namely the tower, the foundation mat, the steam generator, steam generator housing, and the steam generator supports, is presented. The seismic and wind loading analyses are discussed. Finally, conclusions reached as a result of the study are presented.

DESIGN CRITERIA

Plant Site Criteria Affecting the Structural Design

RFP 75-125 required that the pilot plant be designed to survive in Seismic Zone 3 as specified in the Uniform Building Code. The pilot plant is to be operational when the wind velocity at 30 feet above the ground is 30 mph. At greater velocities it is assumed that the heliostat field will be shut down. Seismic loads are assumed to be more critical to tower and receiver survival than extreme wind. The allowable soil-bearing pressure is 2 tsf.

Design Codes and References

(a) Building Code Requirements for Reinforced Concrete (ACI 318-71) for design of reinforced concrete

(b) Specifications for the Design and Construction of Reinforced Concrete Chimneys (ACI 307-69) for seismic analysis of reinforced concrete chimney

(c) AISC Steel Construction Manual for structural steel design

(d) Nuclear Regulatory Commission (NRC) Regulatory Guide 1.60 for design response spectra

(e) Black & Veatch Standard Practices Manual S-419.01 for wind pressures

Structural Materials

(a) Concrete: f'_c = 4000 psi (reinforced tower)*
f'_c = 3000 psi (foundation mat)*

(b) Reinforcing Bars: Grade 60 (main tension reinforcement)
Grade 40 (ties and shear reinforcement)

(c) Structural Steel: A36

TOWER DESIGN

Original M.W. Kellogg Design

The original M.W. Kellogg design called for a 410-foot reinforced concrete tower with octagonal foundation mat. The foundation mat was designed to be a 90-foot octagonal mat 8 feet thick. The results of the M.W. Kellogg program are summarized later in this appendix, in Table A-1. It should be noted that the M.W. Kellogg design has not accounted for the seismic loads from the steam generator housing and is therefore not conservative.

---

*Minimum-specified 28-day ultimate strength of concrete.

Revised M. W. Kellogg Design

Since the M. W. Kellogg computer analysis was performed, the tower height was increased from 410 feet to 480 feet. To account for the corrected height, the M. W. Kellogg tower was assumed to be the top 410 feet of the 480-foot tower and the base diameter was proportionately increased from 40.5 feet to 44 feet.

Geometry of Revised Tower

The reinforced concrete tower is 480 feet in height as shown in Figure A-1. The outside diameter at the top of the tower is 20 feet, increasing linearly to 44 feet at the base. The nominal thickness is 1/24 of the outside diameter, except that the thickness of the top 40 feet of the tower was increased to 24 inches to provide a rigid base for the three steam generator housing support legs and adequate anchorage thickness for the embedments.

FOUNDATION MAT

Loading Conditions

Under seismic loading there should be no uplift of the foundation. Also, the maximum foundation pressure must not exceed the allowable bearing pressure of 2 tsf. The thickness of the foundation is controlled by the allowable shear stress of 60 psi for 3000-psi concrete. The foundation was designed for a seismic over-turning time history method (THM) moment of 574,970 foot-kips reduced by a ductility factor of 1.6. This yielded a service load moment of 360,000 foot-kips. The total gravity load of the tower (excluding the foundation mat weight) is approximately 10,840 kips.

Analysis and Design Procedure

For the vertical gravity loads (including the foundation mat weight) and seismic moments, the combined stresses were computed for trial sizes of octagonal mats. The process is an iterative one. It is necessary that:

$$\frac{P}{A} + \frac{Mc}{I} \leq 2 \text{ tsf} \qquad \text{(bearing)}$$

and

$$\frac{P}{A} - \frac{Mc}{I} \geq 0 \qquad \text{(no uplift)}$$

The shear stress at a distance of one-half of the mat thickness away from the tower should be less than 60 psi.

66
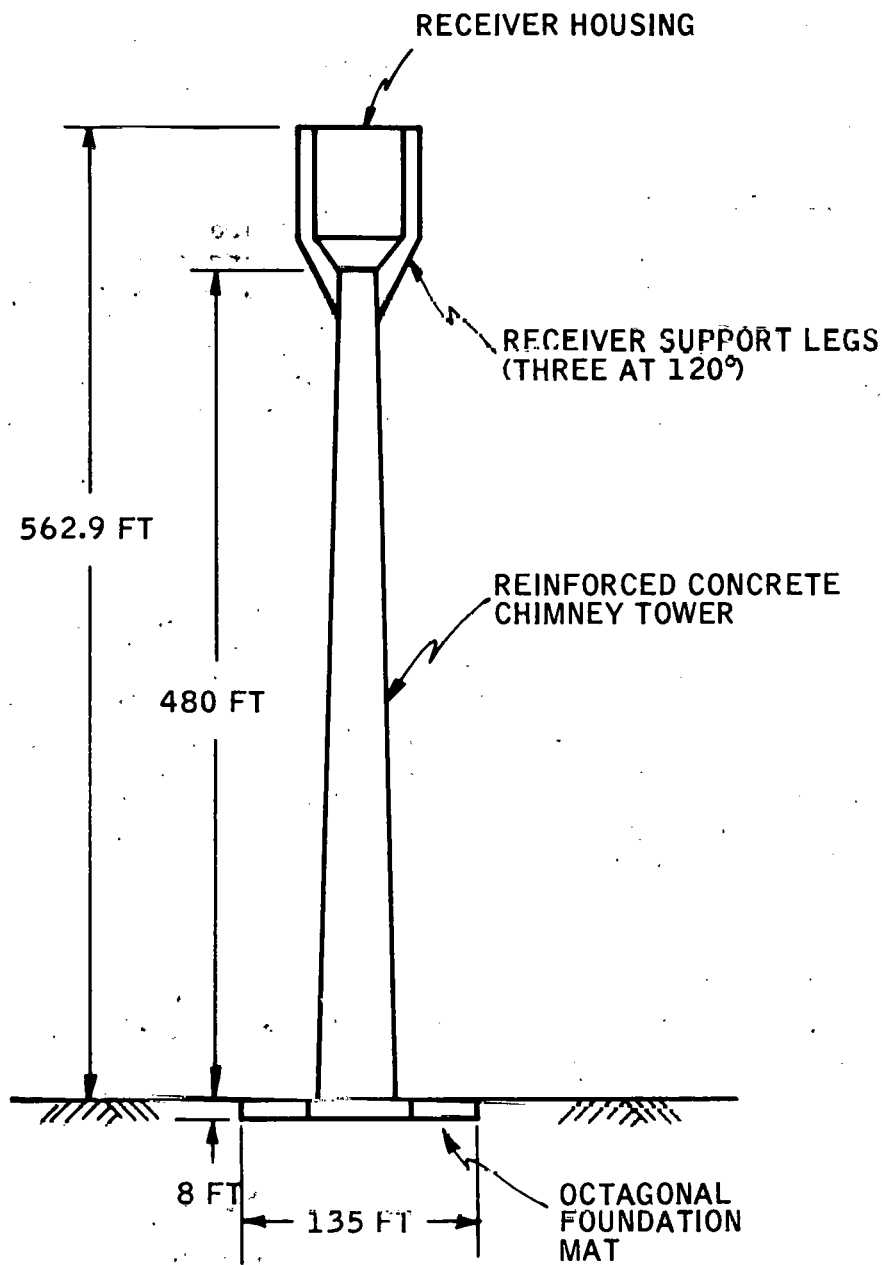
Figure A-1. 480-Foot Solar Tower

Results of Analysis

An octagonal mat (see Figure A-1) with a 135-foot diameter and 8-foot thickness gave the following results for combined seismic and gravity loads:

- Bearing: 1.63 tsf < 2 tsf
- Uplift: 0.29 tsf > 0
- Shear: 59 psi < 60 psi

It should be noted that in order to maintain a soil-bearing pressure less than 2 tsf with no uplift, the foundation mat size was increased considerably over the original M. W. Kellogg design (from a 90-foot to a 135-foot octagonal mat 8 feet thick).

STEAM GENERATOR AND STEAM GENERATOR HOUSING GEOMETRY

Geometry of Steam Generator

The B&W steam generator design is in the shape of a right circular cylinder, is 46 feet in height, 39.4 feet in diameter, and weighs approximately 440 kips. The steam generator, as shown in Figure A-2, consists of a boiler section and two superheater sections. A steam drum is located above the upper superheater. Headers, piping, and spray attemperators surround the boiler and superheater sections.

Geometry of Steam Generator Housing

A perspective view of the steam generator housing is shown in Figure A-3. For the preliminary baseline design, the steam generator housing is 65 feet in height with an outside diameter of 48 feet, as shown in Figure A-4. The main shell is constructed of A36 structural steel 1/2-inch thick. Ring stiffeners (to be designed later) are located at intermediate positions.

STEAM GENERATOR SUPPORT DESIGN

Low-Frequency Support System for Steam Generator

A low-frequency (soft) support system such as a pendulum or sliding-surface system was considered. In order for such a system to function properly, its natural frequency would have to be no greater than one-fifth of the first fundamental frequency of the tower, or approximately 0.07 Hz. Design of a support system with such a low frequency was judged to be impractical and will not be considered further.

68
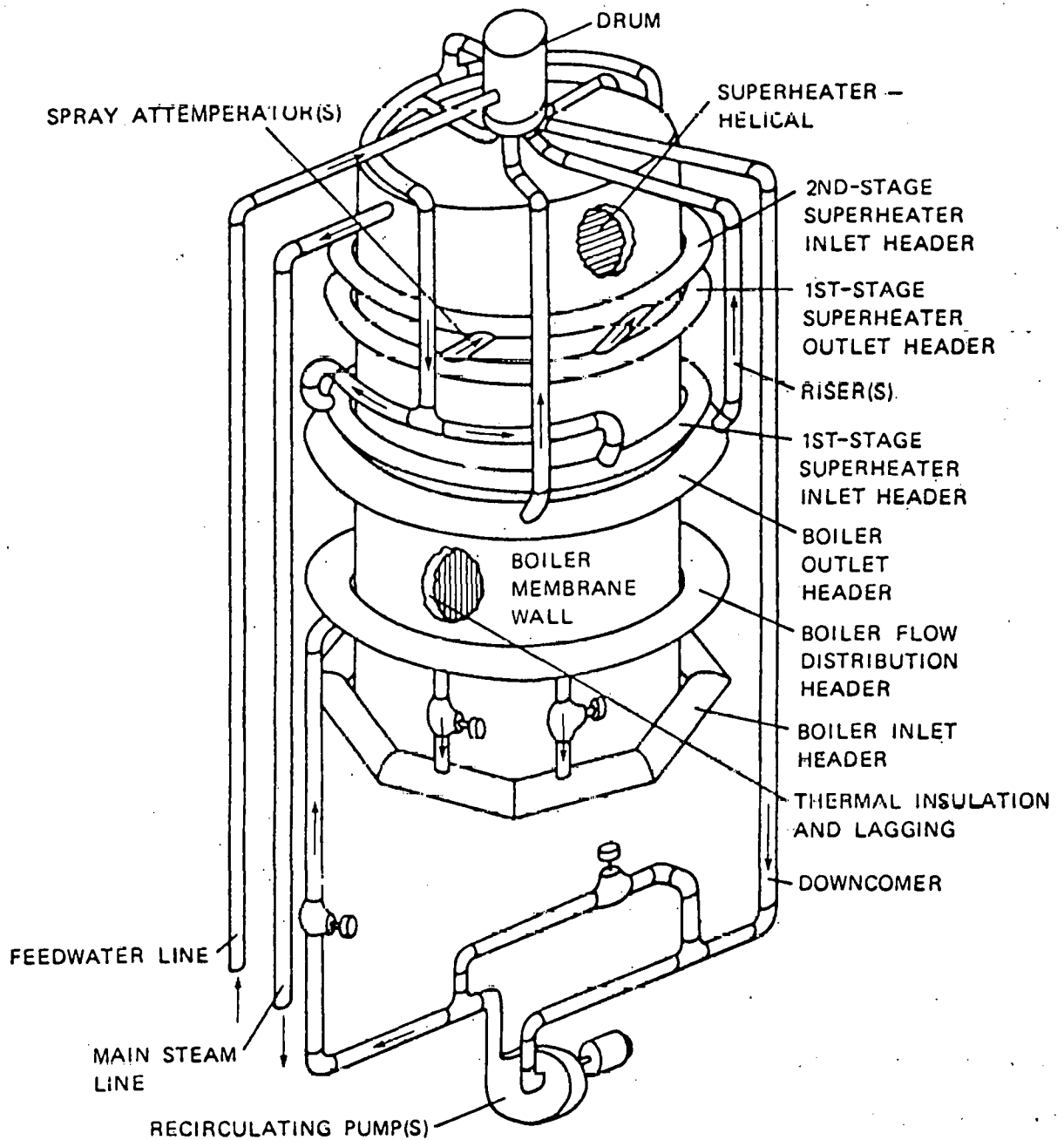
Figure A-2. Steam Generator

69
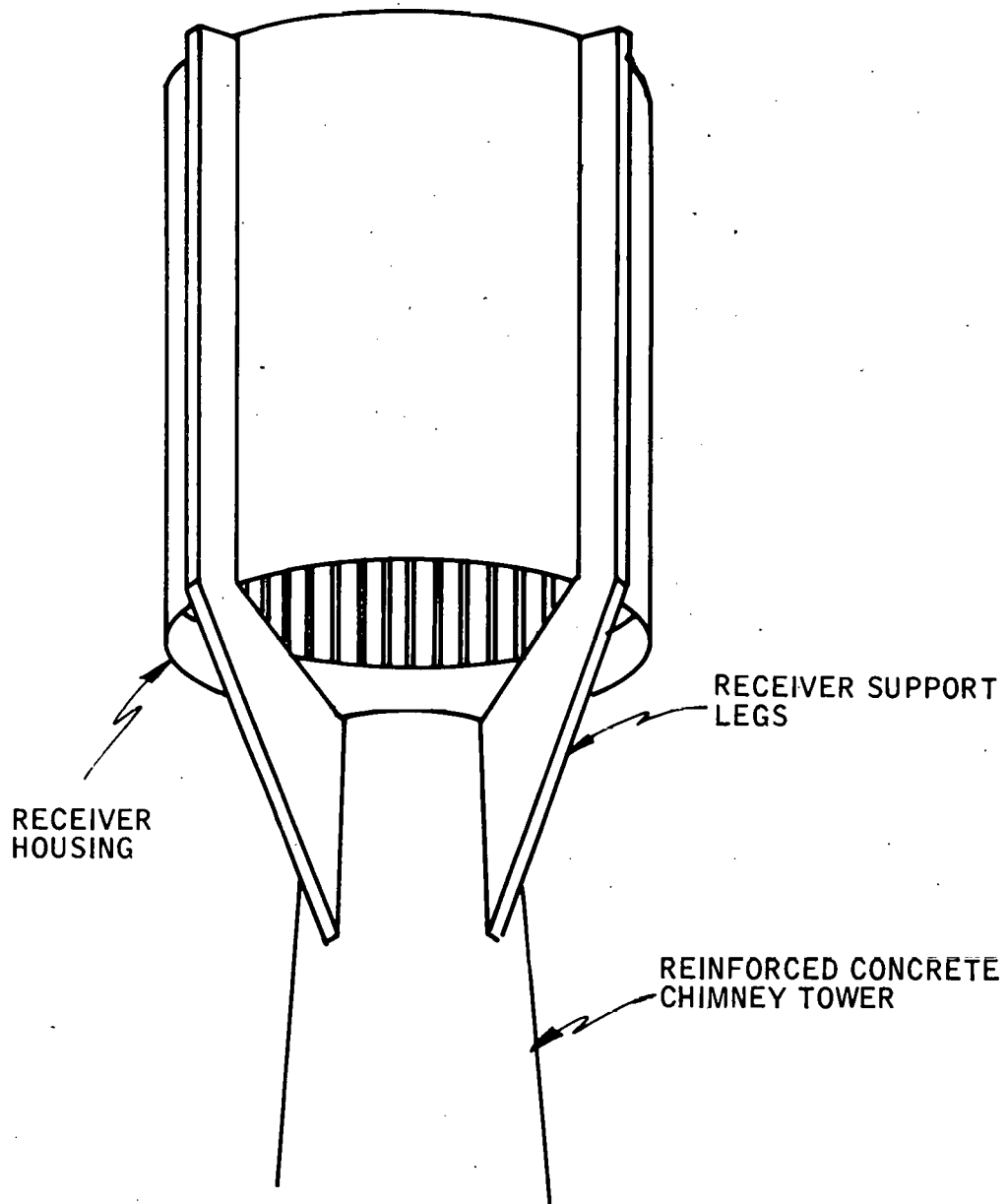
Figure A-3. Perspective View of Receiver Housing

70
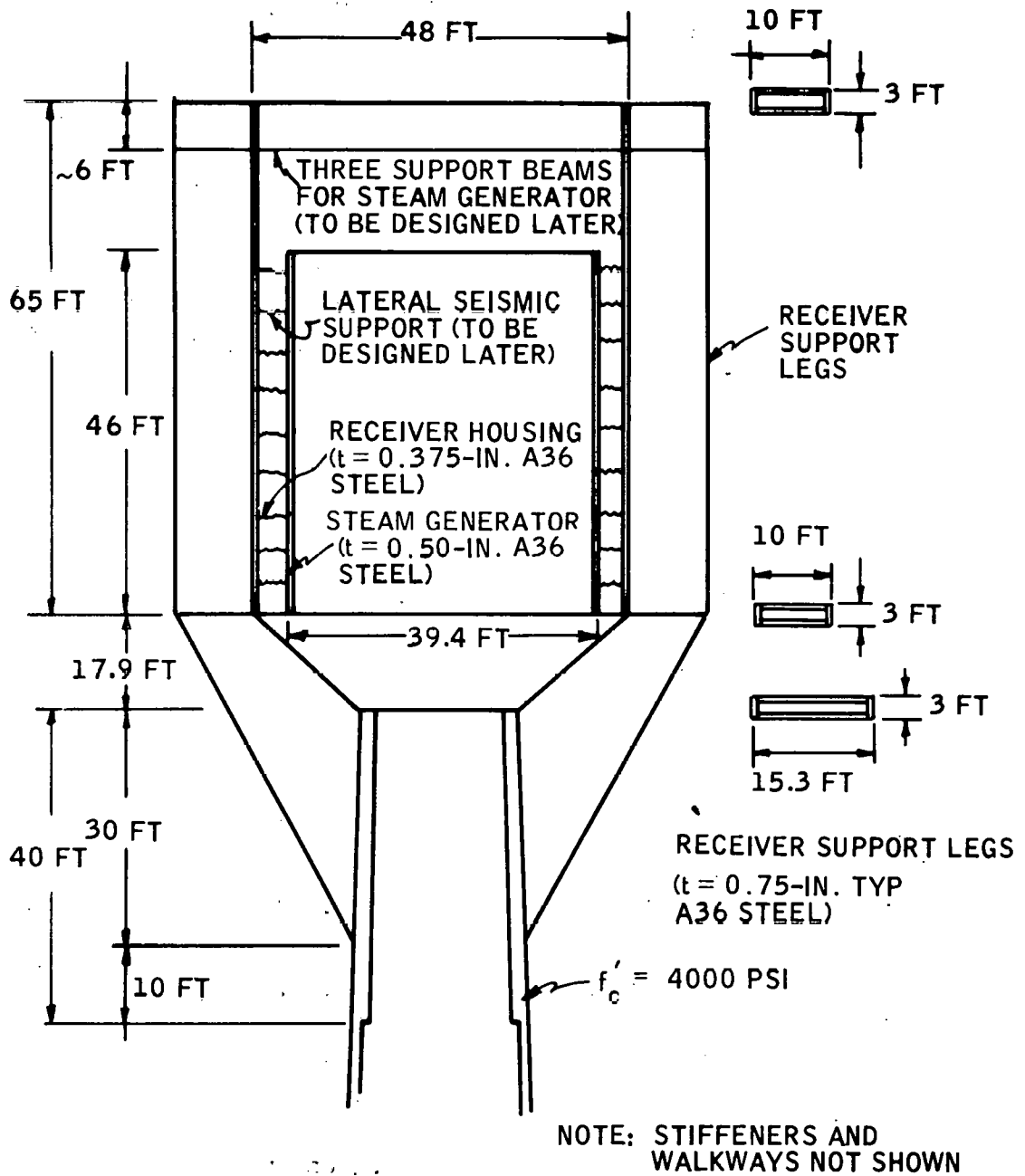
Figure A-4. Section of Receiver Housing and Steam Generator

Rigid Support System for Steam Generator

The steam generator will be rigidly connected to and hung from the top of the steam generator housing as shown in Figure A-4. Lateral support (to be designed later) will be provided to prevent the steam generator from colliding with the inside face of the steam generator housing. The lateral support will be designed to withstand the full seismic force induced by the steam generator.

Geometry Limitations on Support Legs

The steam generator housing will be supported by three legs at 120 degrees extending from the tower to the top of the steam generator housing (see Figure A-4). The legs will extend as far down the tower as necessary for structural strength. The legs may extend as far away from the tower as required but must be limited to a structural width of 3 feet.

Preliminary Design of Support Legs

The support legs are to be constructed from A36 structural steel. The decision to use structural steel instead of reinforced concrete was due, at least in part, to the requirement for an access way through the legs to the steam generator and steam generator housing. For the preliminary baseline design, a box section made from 3/4-inch steel plates was chosen as shown in Figure A-4. It is anticipated that intermediate stiffeners or bracing will be required at various locations. Radiation shielding will be required on the outside faces of the legs.

Results of Analysis of Support Legs

Results of the preliminary seismic analysis indicate that stresses in the legs are acceptable, although the design may not be the most efficient one possible. Hand calculations based on the computer analysis show a maximum axial stress of around 16 ksi and a maximum shear stress of around 6 ksi due to combined gravity and seismic loads. These stresses compare favorably with allowables of 21.6 ksi and 14.4 ksi, respectively, for A36 steel.

WIND DEFLECTIONS

The wind drift at the top of the 480-foot tower was computed using the average wind load per foot of tower height plus a concentrated load at the top to account for the larger diameter of the steam generator housing. The average moment of inertia was assumed to be the value at mid-height of the tower. Obviously these approximations are intended only to compute quickly the order of magnitude of the deflection. An analysis of the tower approximated as a cantilever beam of uniform cross-section indicated that the total deflection at the top of the tower under a 30-mph wind (specified at 30 feet above the ground) is of the order of 7 inches (see Figure A-5). A deflection of 1 foot or less was assumed to be adequate.
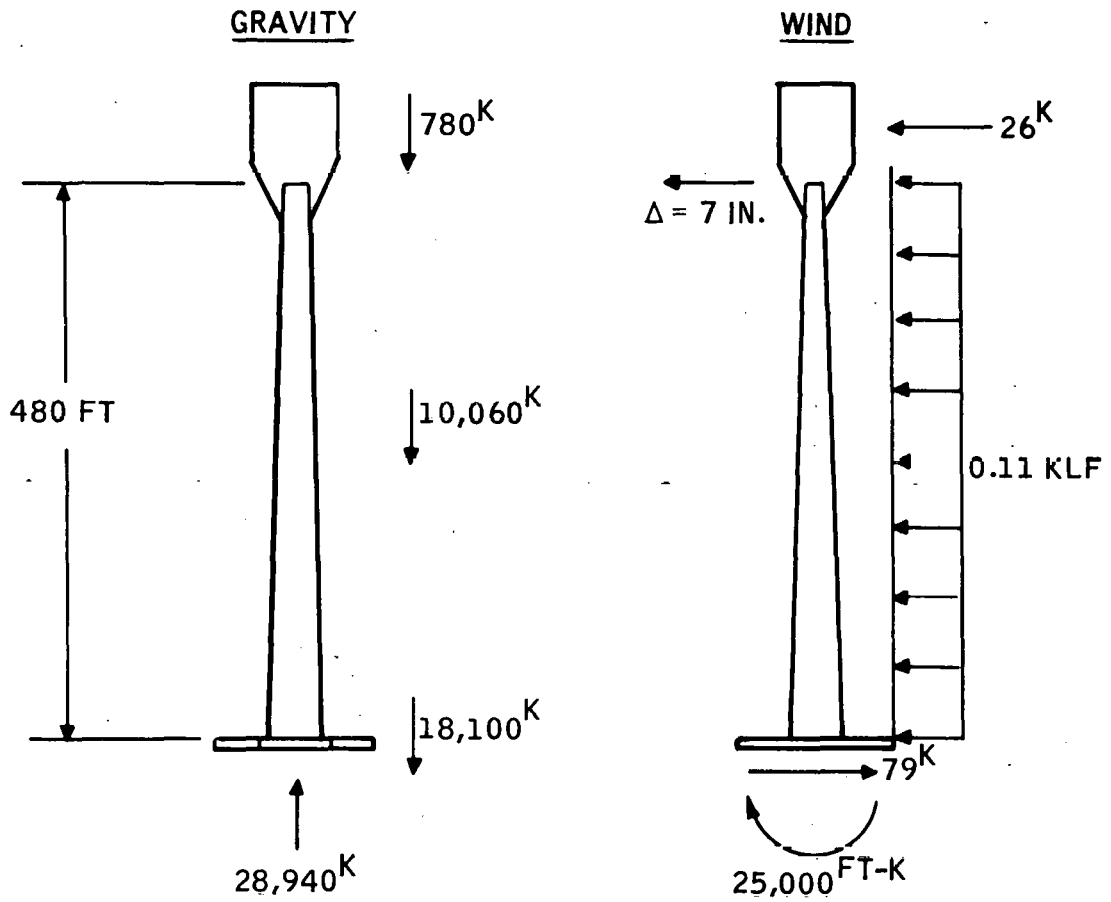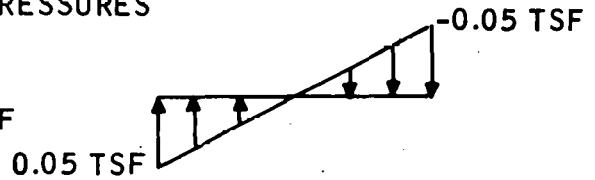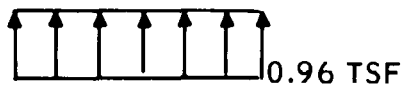
GRAVITY

780^K

480 FT

10,060^K

18,100^K

28,940^K

WIND

26^K

Δ = 7 IN.

0.11 KLF

79^K

25,000^{FT-K}

STRESSES AT BASE
OF TOWER

300 PSI

71 PSI

-71 PSI

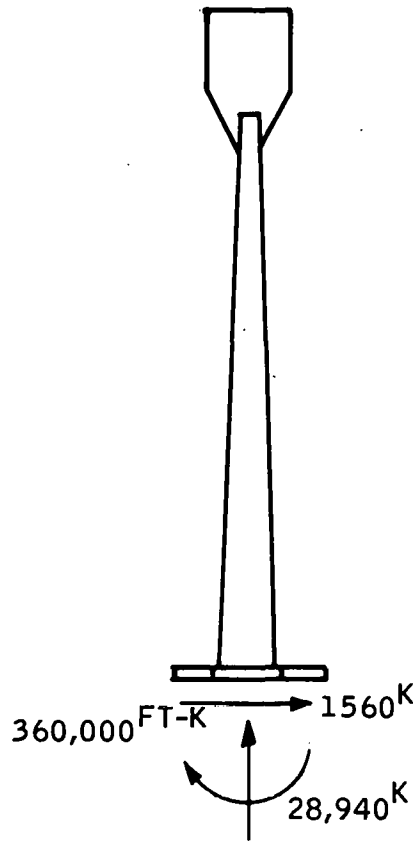SOIL PRESSURES

0.96 TSF

-0.05 TSF

0.05 TSF

Figure A-5. Seismic and Wind Loads

73
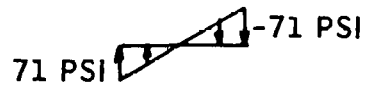
SEISMIC

GRAVITY AND SEISMIC

480 FT

1560^K

1560^K

360,000^{FT-K}

360,000^{FT-K}

1560^K

28,940^K

STRESSES AT BASE
OF TOWER

-1020 PSI

1020 PSI

-710 PSI

1330 PSI

SOIL PRESSURES

-0.67 TSF

-0:67 TSF

0.29 TSF

1.63 TSF
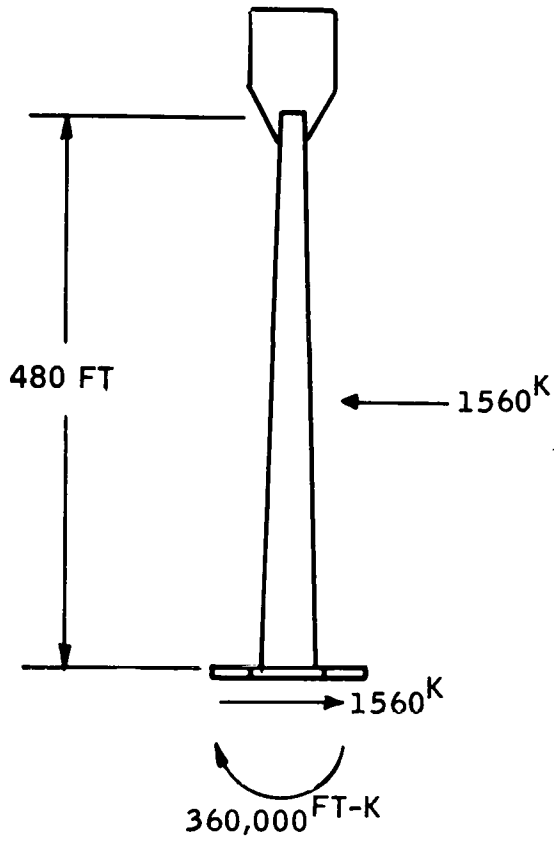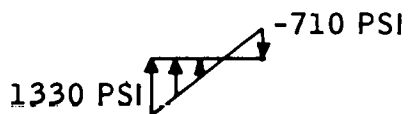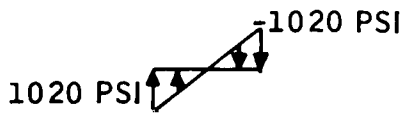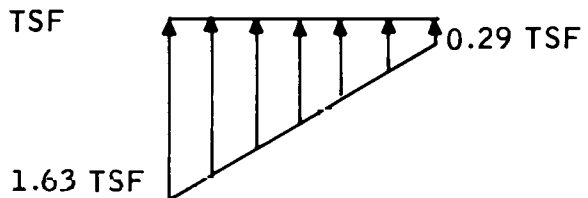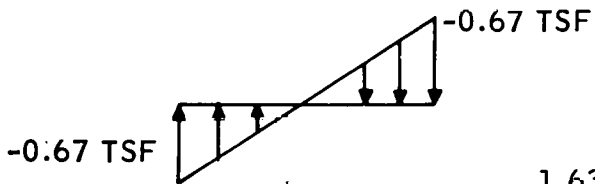
Figure A-5. Seismic and Wind Loads (Concluded)

SEISMIC ANALYSIS

Design Basis Earthquake

The basic philosophy adopted is that the tower should sustain only minor structural damage and should remain standing under the design basis earthquake (DBE). Damage to nonstructural components may be somewhat greater. As a minimum, the tower was designed to meet the standards of the ACI 307-69 Chimney Code, Seismic Zone 3.

Analysis and Design Procedures

Three different seismic analyses were performed and are described below. Results are summarized in Table A-1.

Table A-1. Seismic Forces at Base of Tower

Analysis	Tower Height (ft)	Base Shear, V (kips)	Overturning Moment, M (ft-kips)
M. W. Kellogg	410	894	141,782
ACI 307-69	480	1560	264,000
RSM	480	1440	275,000
TIIM	480	1520	360,000
Design Values	---	1560	360,000

ACI 307-69 Method -- The ACI 307-69 method was used by M. W. Kellogg for their computer analysis of the 410-foot tower. However, they unconservatively neglected the effect of the steam generator housing on the seismic forces which results in an unconservative design. The analysis was redone by hand to account for the correct 480-foot height and to include the effect of the steam generator housing above the tower. The effect of the steam generator was approximated by adding an equivalent height and mass of tower. Results are summarized as follows:

● Base Shear, $V = ZUCW_1$, where

Z = Zone Factor = 1.0 for Seismic Zone 3

U = Use Factor. Varies from 1.3 to 2.0 (assume the maximum value of 2.0)

C = Factor that depends on the fundamental period of the tower ≃ 0.072

W_1 = Total weight of tower including the steam generator housing and any other attached equipment, but excluding the weight of the foundation mat = 10,840 kips

V = (1.0) (2.0) (0.072) (10,840 kips) = 1560 kips

- Overturning Moment, $M = J_x H_x V$, where

J_x = Numerical coefficient for moment = 0.45

H_x = Height to center of seismic shear force $\simeq 2/3$ H (conservative approximation used instead of lengthy ACI 307-69 formula)

H = Equivalent height of tower and steam generator housing = 562.9 ft

V = Base shear, calculated as above

M = (0.45) (2/3) (562.9 ft) (1560 kips) = 264,000 ft-kips

Response Spectrum Method (RSM) -- The response spectrum method is a method by which individual modal responses are calculated for each natural frequency of the tower from a design input response spectrum. Since the peak modal responses all occur at different times, the maximum total response will be less than the sum of the individual peak responses for each mode. It has been shown that taking the square root of the sum of the squares (SRSS) of the individual modal responses gives a good approximation to the actual maximum total response. Frequencies higher than 20 Hz have been shown to contribute little to the total response and have been neglected. The input response spectrum used in the computer analysis was the NRC Regulatory Guide 1.60 horizontal acceleration spectra normalized to a zero-period acceleration of 0.3 g. Structural damping was taken to be 4 percent of critical damping. The reinforced concrete tower, steam generator, steam generator housing, and steam generator housing support legs were modeled by 37 beam elements as shown in Figure A-6. Results of the SAP-IV computer analysis are shown below:

Mode No.	Tower Frequencies (Hz)	Base Shear, V (kips)	Overturning Moment, M (ft-kips)
1	0.3386	865	345,900
2	1.332	1498	241,400
3	3.198	1250	114,800
4	5.819	701	42,700
5	9.136	421	18,300
6	10.49	5	200
7	12.96	205	6,600
8	16.91	105	2,700
Total by SRSS		2297	439,700

0 FT

STEAM GENERATOR

RECEIVER HOUSING

65 FT

29.0 FT

17.9 FT

SUPPORT LEGS

17.6 FT

562.9 FT

CHIMNEY TOWER

480 FT

NODE POINT (TYP)

BEAM ELEMENT
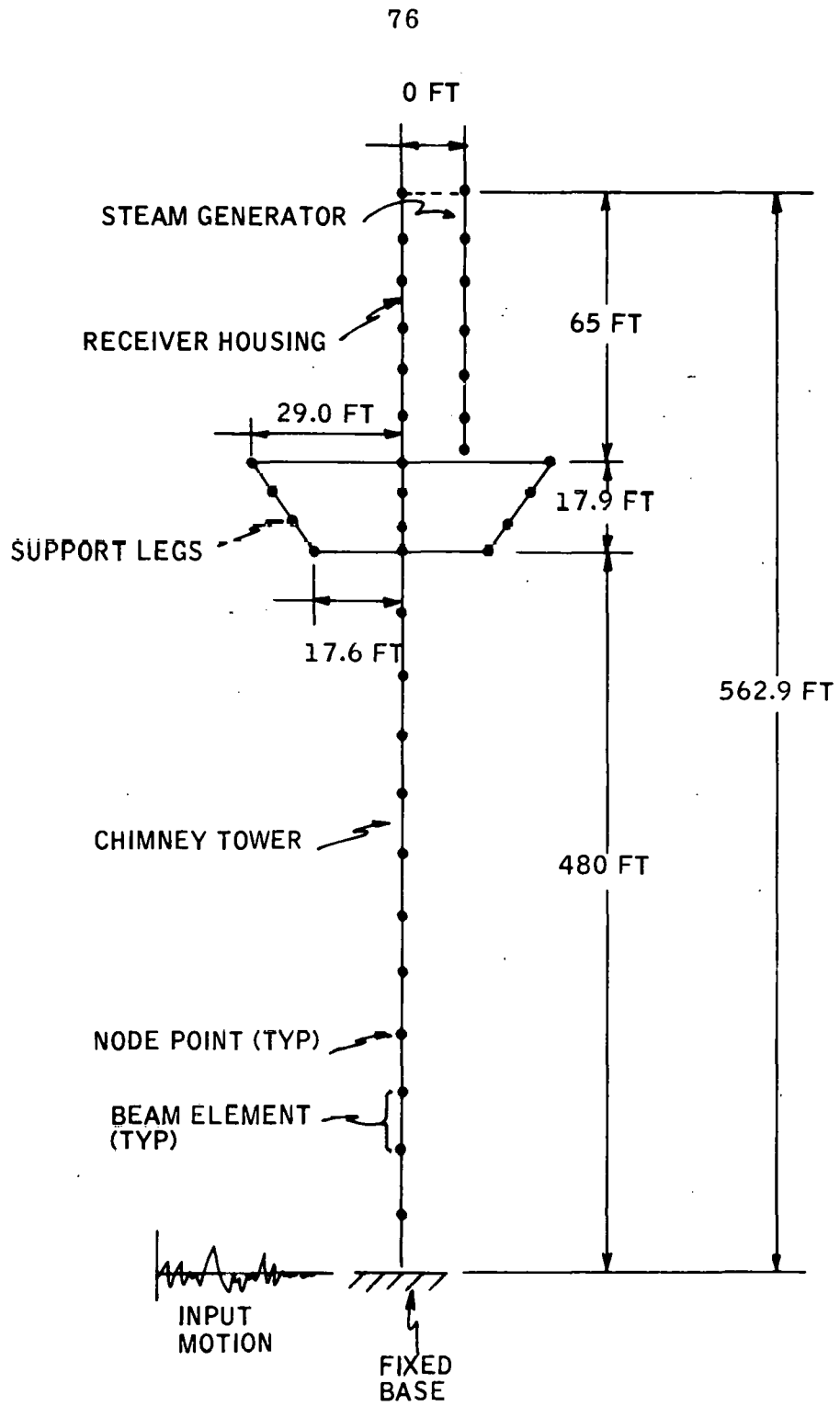(TYP)

INPUT
MOTION

FIXED
BASE

Figure A-6. Beam Element Model of Solar Tower

.To correct for ductility of the concrete tower, the final computer results were divided by a factor of 1.6. The factor of 1.6 was selected from an accompa-.nying study to provide a design which is compatible with that given by the ACI 307-69 method. The ductility factor selected obviously affects the design forces significantly:

$$\text{Base shear, } V = \frac{2297 \text{ kips}}{1.6} = 1440 \text{ kips}$$

$$\text{Overturning moment, } M = \frac{439,700 \text{ ft-kips}}{1.6} = 275,000 \text{ ft-kips}$$

Time History Method (THM) -- The time history method is a method by which the maximum response is calculated directly by solving the equations of motion for each structural frequency and adding the results on a time basis. The calculation of the tower frequencies is identical to the RSM analysis. As was done in the RSM analysis, frequencies higher than 20 Hz were neglected. An artificial horizontal ground input acceleration time history was generated based on the acceleration spectra used in the RSM analysis. The acceleration time history used had a duration of 15 seconds and was digitized at constant time intervals of 0.01 second. Structural damping was taken to be 4 percent. The reinforced tower, steam generator, steam generator housing, and steam generator support legs were modeled by 37 beam elements as was done in the RSM analysis (see Figure A-6). Results of the SAP-IV computer analysis are shown below:

	Base Shear, V	Overturning Moment, M
Maximum Response	2435 kips	574,970 ft-kips
Time of Occurrence	12.46 sec	14.42 sec

As was done in the RSM analysis, the final computer results were divided by a factor of 1.6 to correct for the ductility of the tower:

$$\text{Base shear, } V = \frac{2435 \text{ kips}}{1.6} = 1520 \text{ kips}$$

$$\text{Overturning moment, } M = \frac{574,970 \text{ ft-kips}}{1.6} = 360,000 \text{ ft-kips}$$

Stresses at Base of Tower

The assumption was made that if the stresses at the base of the tower are reasonable, then the design will be workable although perhaps not the most efficient. Results of the preliminary seismic analysis (see Figure A-5) show that service load stresses due to combined seismic and gravity loads are reasonable, as given below:

Compression, $f_c = \dfrac{Mc}{I} + \dfrac{W_1}{A} = 1330$ psi

Tension, $f_t = \dfrac{Mc}{I} - \dfrac{W_1}{A} = 710$ psi

Shear, $f_v = \dfrac{V}{0.5A} = 89$ psi

The concrete compressive stress of 1330 psi is reasonable when compared with the allowable of 1800 psi for 4000-psi concrete. The tension stress (high enough that unreinforced concrete would crack) will be taken up entirely by the vertical reinforcement. The required reinforcement ratio, p, for the vertical steel (f_a is the allowable tension for Grade 60 steel) may be conservatively calculated as follows:

$$p = \dfrac{f_t}{f_a} = \dfrac{710 \text{ psi}}{36,000 \text{ psi}} = 0.02$$

That is, the cross-sectional area of the vertical reinforcement should be about 2 percent of the gross cross-sectional area of the tower. Two-percent vertical steel is well within the maximum allowable value of 8 percent and would require about 700 square inches of steel area at the base of the tower. The maximum shear stress that can be carried by the concrete alone is 70 psi for 4000-psi concrete. A nominal amount of diagonal shear reinforcement will be required to resist the excess seismic shear.

Equipment Response Spectra

Equipment response spectra based on preliminary results of the time history method (THM) analysis show a maximum equipment acceleration of about 8 g in the steam generator housing and about 5 g in the reinforced concrete tower. Equipment damping was assumed to be 2 percent of critical. Equipment (such as piping in the steam generator, etc.) must be designed to withstand these accelerations if no damage is to occur during the design basis earthquake (DBE). In order to reduce construction costs, an alternative design procedure would be to design nonstructural components for a much lower acceleration level and replace any damaged components after a major earthquake.

CONCLUSIONS

Results of the seismic study on the preliminary baseline design of the receiver support tower show that all aspects of the conceptual design which were checked are adequate, although perhaps not the most efficient design. The 410-foot M.W. Kellogg tower was increased to 480 feet and was checked for combined seismic and gravity loadings. Wind deflections were also checked for an operational wind speed of 30 mph. Preliminary results show the tower to be adequate in all cases. Stresses in the steam generator housing support legs were checked and were shown to be below the maximum allowable values. The foundation mat was redesigned and was increased considerably in size over the M.W. Kellogg design.

THIS PAGE

WAS INTENTIONALLY

LEFT BLANK

APPENDIX B

MATERIALS EVALUATION STUDIES ON NaNO$_3$ - NaOH AND NaNO$_3$ - NaCl - Na$_2$SO$_4$ MIXTURES

It is known that sodium nitrate melts without decomposition to a liquid which is stable in air at least to 500°C and begins to decompose slowly at 600°C.[1] The decomposition reaction is:

$$NaNO_3 \rightarrow NaNO_2 + \frac{1}{2} O_2$$
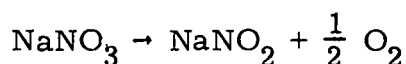
It has also been shown by differential scanning calorimetry (DSC) that even under drastic conditions, namely, NaNO$_3$ containing 30 mole % of NaOH, the mixture is stable up to 400°C (Figure B-1). The same mixture when subjected to thermal cycling between 150°C and 350°C for 140 times and analyzed by DSC showed good thermal stability (Figure B-2). Therefore, it is reasonable to assume that the stability of NaNO$_3$ containing 1% of NaOH (by weight) will approach the stability of pure NaNO$_3$. The corrosion studies carried out using a more-corrosive mixture of NaNO$_3$ - NaOH (70-30 mole %) on mild steel and stainless steel by thermogravimetry, electrochemical current potential curves, and Auger electron spectroscopy show that the above mixture is not highly corrosive. The corrosion rate on mild steel is high initially and levels off with time (Figure B-3), whereas in the case of stainless steel, the initial rate, though not very high, levels off with time (Figure B-4). The corrosion rate is about 1.5 mils/year for mild steel and is about 0.28 mil/year for stainless steel. It is also known from literature that pure NaNO$_3$ is not very corrosive because it forms a passive layer on metals and alloys.[2] Therefore, the mixture with 99% NaNO$_3$ and 1% (by weight) of NaOH should have corrosivity approaching that of pure NaNO$_3$.

The DSC studies on NaNO$_3$ containing NaOH (0.5% by weight) show that the thermal spectrum (Figure B-5) has one major endothermic peak around 305°C, a small peak around 273°C, and another small peak around 260°C after correction has been made for the high scanning rate. The major peak around 305°C is attributed to the heat of fusion of NaNO$_3$, the one at 273°C is attributed to the solid-solid transition of NaNO$_3$[3] and the small peak around 260°C is attributed to the congruently melting solid solution of NaNO$_3$ and NaOH. The thermal spectrum of NaNO$_3$ containing 1% of NaOH (by weight)

[1] K.H. Stern, J. Phys. Chem. Ref. data, Vol. I, No. 3, 747 (1972).

[2] A.J. Arvia, R.C.V. Piatti and J.J. Podesta. Electrochimica Acta 17, 901 (1972).

[3] C.N.R. Rao, B. Prakash and M. Natarajan, NSRDS-NBS53, Nat. Stand. Ref. Data Ser. Nat. Bur. Stand. 53 (1975).

shows four endothermic peaks: a major peak around 303°C; two small peaks --
one around 273°C and the other around 260°C; and a very small peak around
240°C (Figure B-6). The major peak around 303°C can be attributed to the
heat of fusion of $NaNO_3$. The peak around 273°C is due to the solid-solid
transition of $NaNO_3$, the peak around 260°C is due to the congruently melting
solid solution of $NaNO_3$ and NaOH, and the peak around 240°C is due to the
fusion of the eutectic mixture of $NaNO_3$ and NaOH. The endothermic peaks,
particularly those around 240°C and 260°C, become more pronounced in the
thermal spectrum of $NaNO_3$ containing 2% of NaOH (by weight) (Figure B-7).

The DSC curves obtained for the ternary mixture of $NaNO_3$ - NaCl - Na_2SO_4
(99.06 - 0.57 - 0.37 mole %) show two endothermic peaks, one around 287°C
due to the ternary eutectic, accounting for about 6 percent of the total mix-
ture, and the major peak around 305°C due to the pure $NaNO_3$ (Figure B-8).
The above mixture was contained in closed, mild-steel tubes and cycled
thermally 190 times between 100°C and 350°C, with arrangement to hold the
mixture around 350°C for about 1 hour. The material from one container
tube was subjected to DSC scan and it was found that there were two peaks,
a small one around 287°C due to the ternary eutectic, accounting for about
6 percent of the total mixture, and the major peak around 305°C due to pure
$NaNO_3$ (Figure B-9). The second cycled tube was sectioned into four parts
and the mixture from each part was subjected to DSC scan. It was found, as
expected, that in all four parts there were two endothermic peaks, the small
one corresponding to the eutectic mixture around 287°C, accounting for about
6 percent of the total mixture, and the major peak corresponding to pure
$NaNO_3$ melting around 305°C (Figures B-10 and B-11). It appears from these
results and those of chemical analyses that there is no phase separation of the
mixture during thermal cycling. The cooling curves obtained for 99% $NaNO_3$
with 0.5, 1.0, and 2.0% NaOH (by weight) show that, in all these cases, there
is no significant supercooling and that the cooling behavior of the mixture is
similar to that of a pure material (Figures B-12 through B-15).
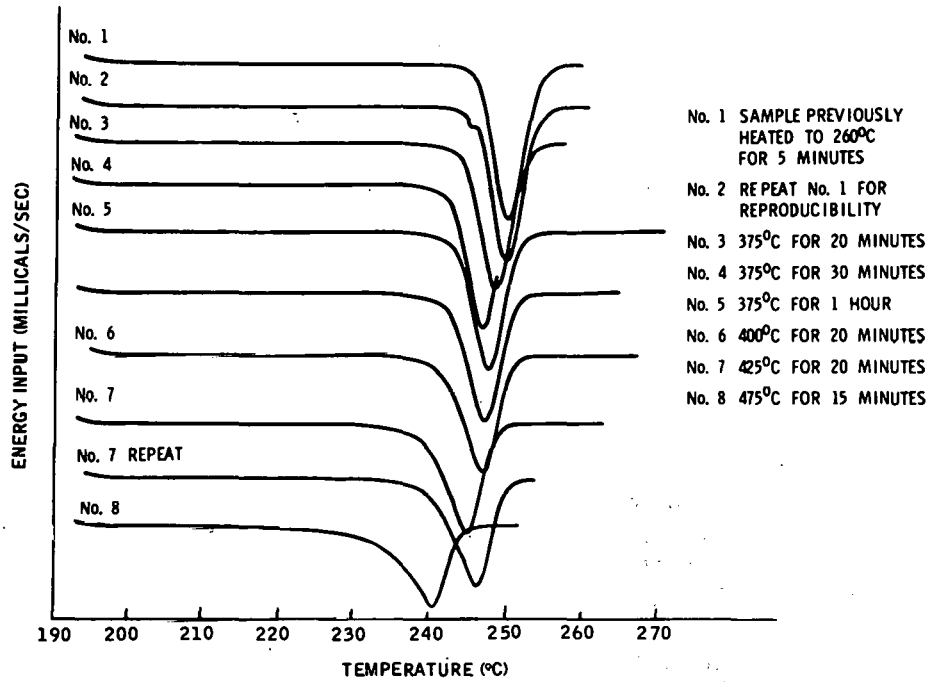
Figure B-1. Thermal-Stability Characteristics for
NaNO$_3$ + NaOH (70-30 Mole %)
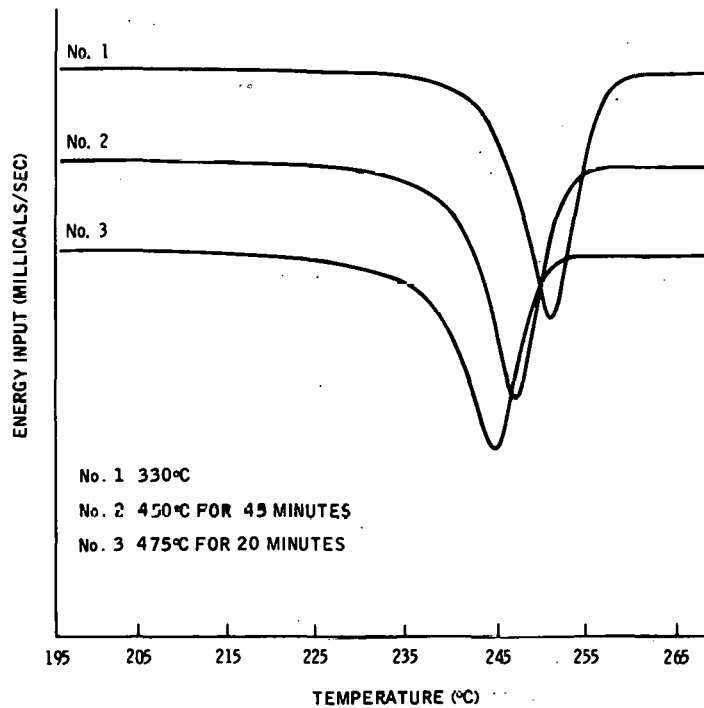

Figure B-2. Cycled Thermal-Stability Characteristics
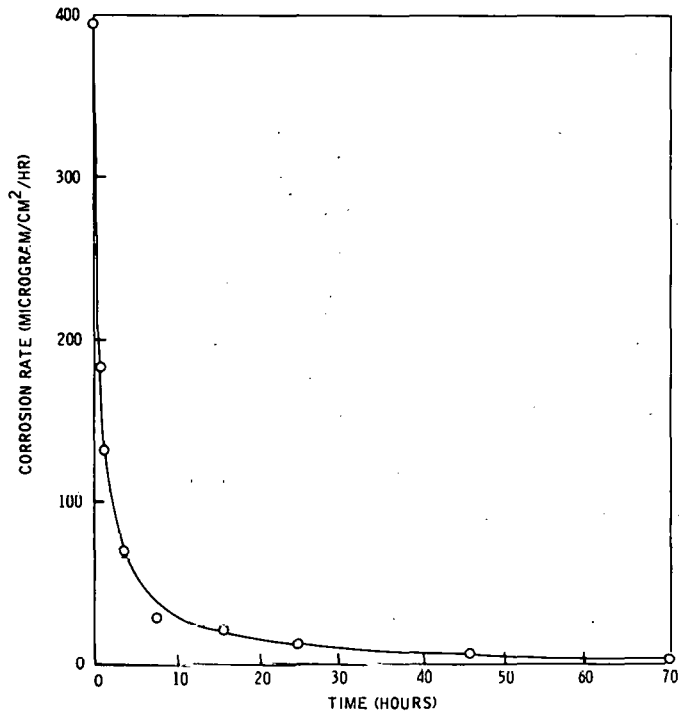for NaNO$_3$ + NaOH (140 Cycles)

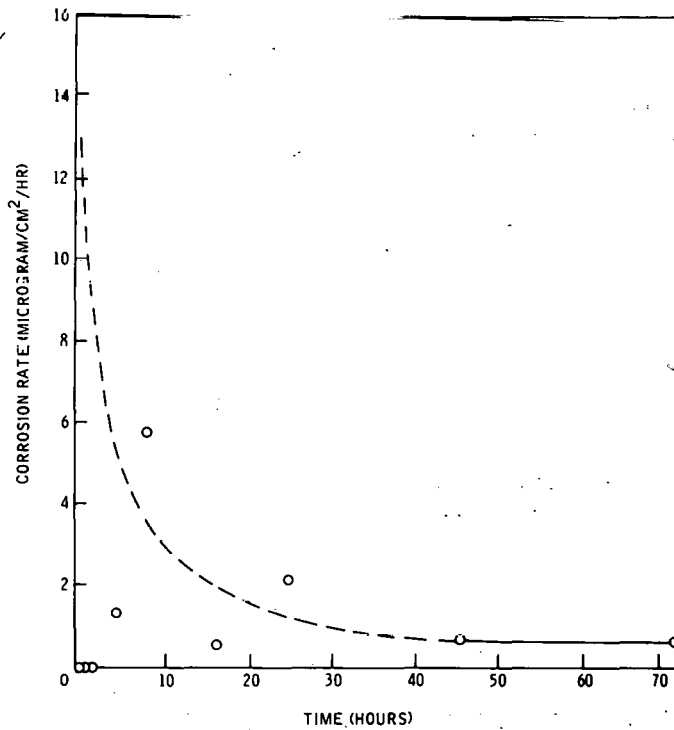Figure B-3. NaNO₃ + NaOH at 250°C --
Mild-Steel Corrosion

Figure B-4. NaNO₃ + NaOH at 250°C --
Stainless Steel Corrosion

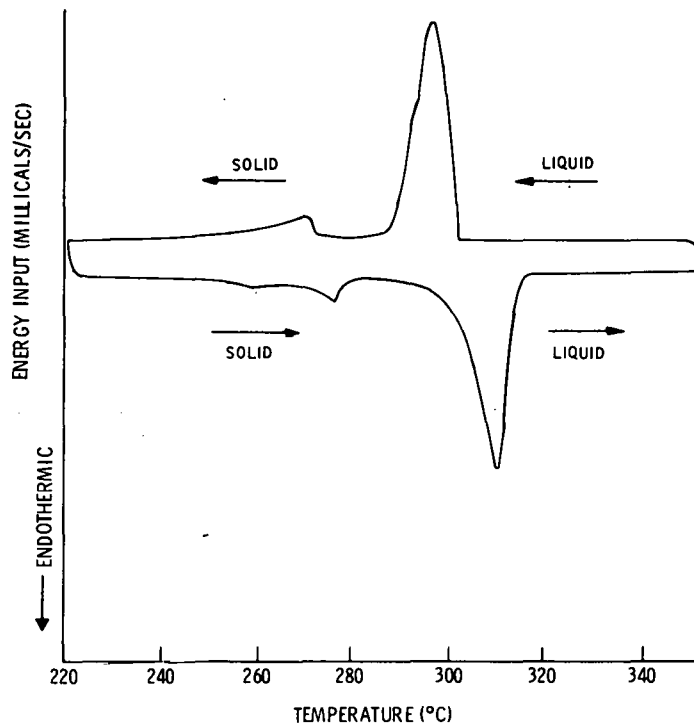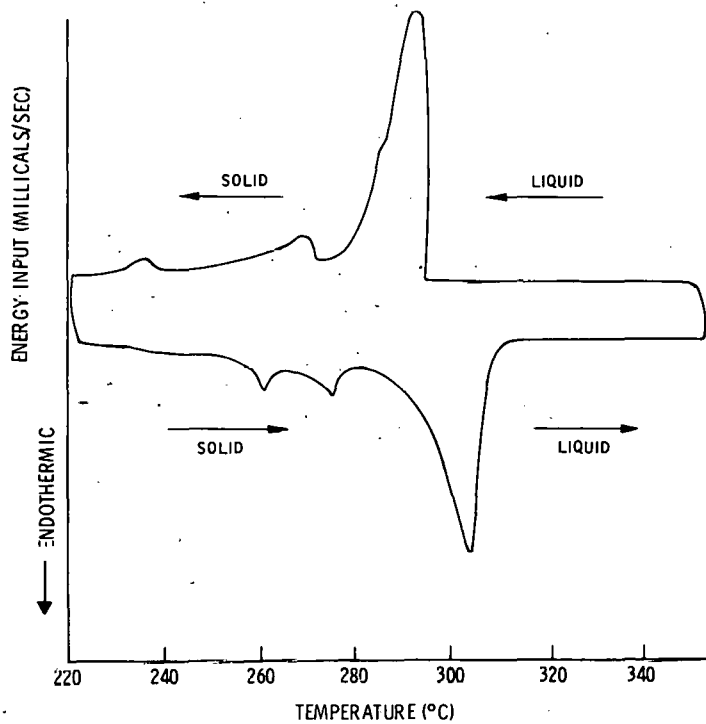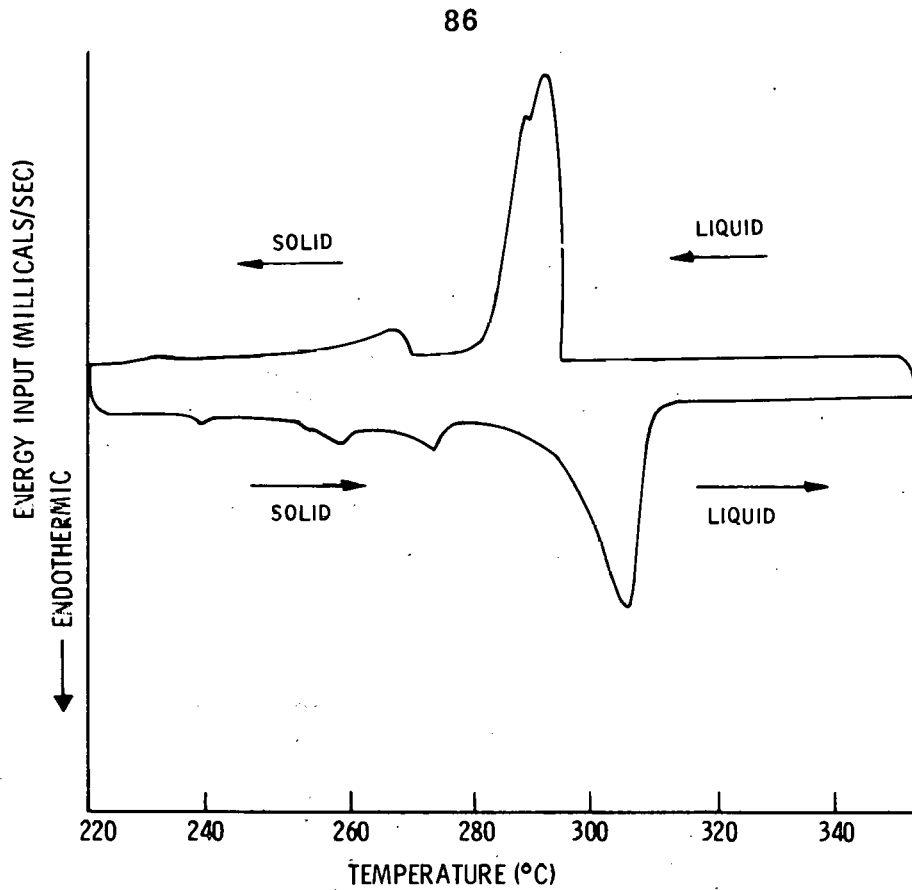Figure B-5. Liquifaction-Solidifaction DSC Curves for NaNO$_3$ + NaOH (0.5% By Weight)

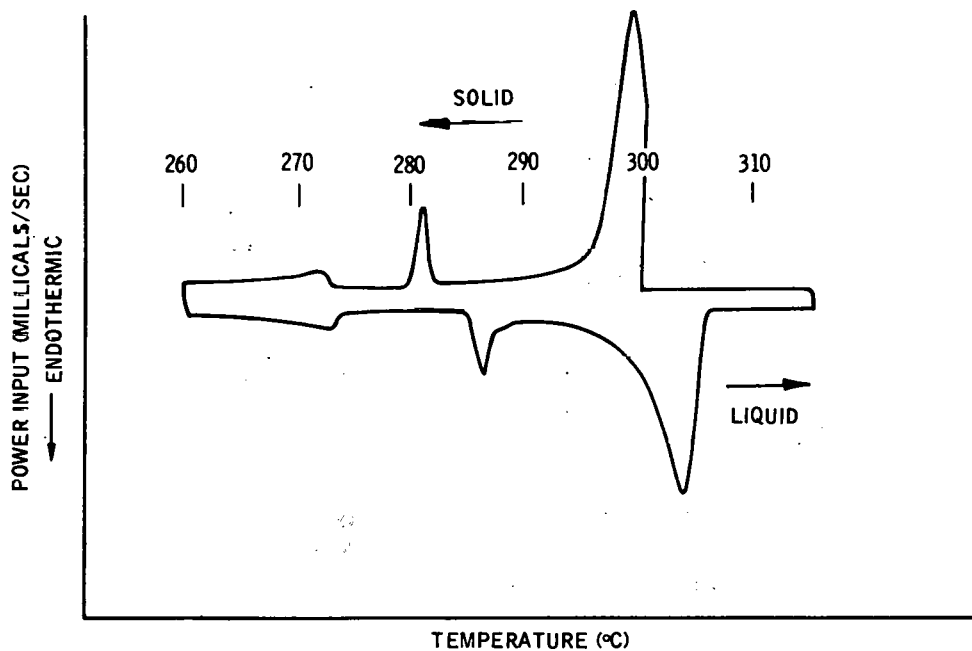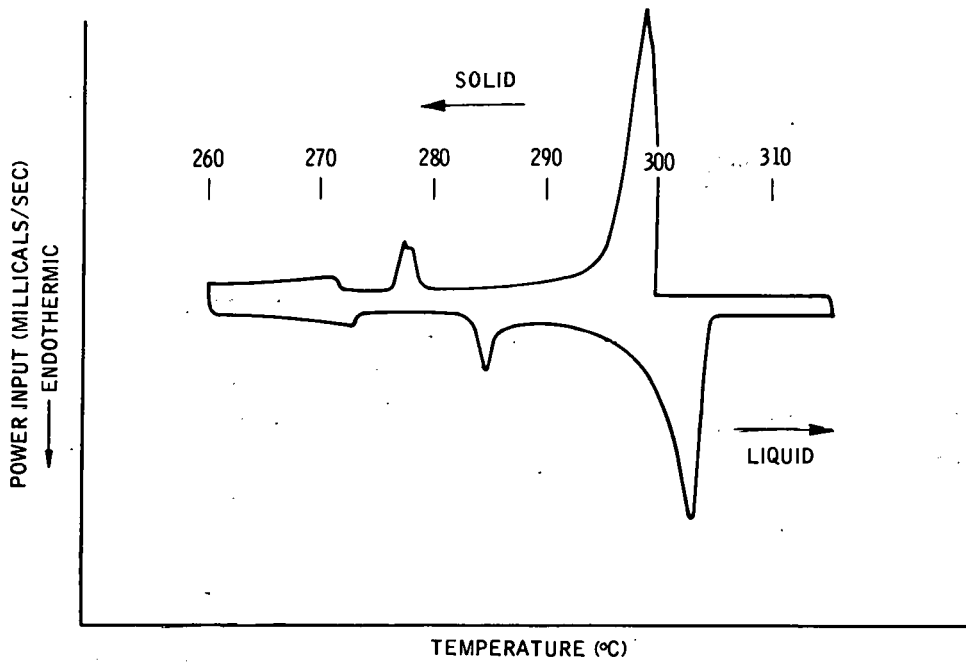Figure B-6. Liquifaction-Solifaction DSC Curves for NaNO$_3$ + NaOH (1% By Weight)

Figure B-7. Liquifaction-Solidifaction DSC Curves for NaNO₃ + NaOH (2% By Weight)

Figure B-8. Liquifaction-Solidifaction DSC Curves for NaNO₃ (99%) Not Cycled

Figure B-9. Liquifaction - Solidification DSC Curves
for NaNO$_3$ (99%) Not Cycled
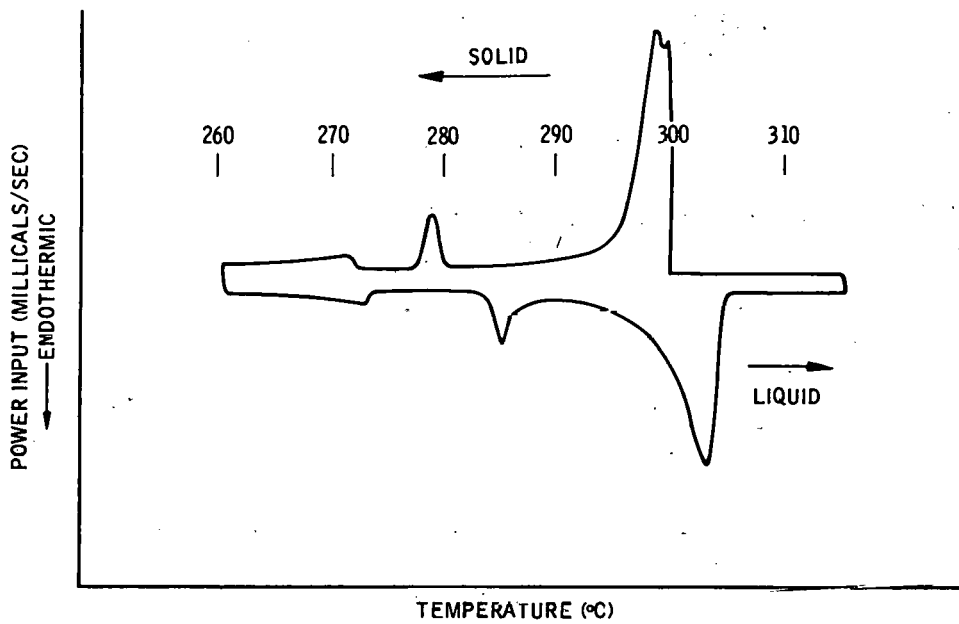
Figure B-10. Liquifaction - Solidification DSC Curves
for NaNO$_3$ (99%) -- Top Portion
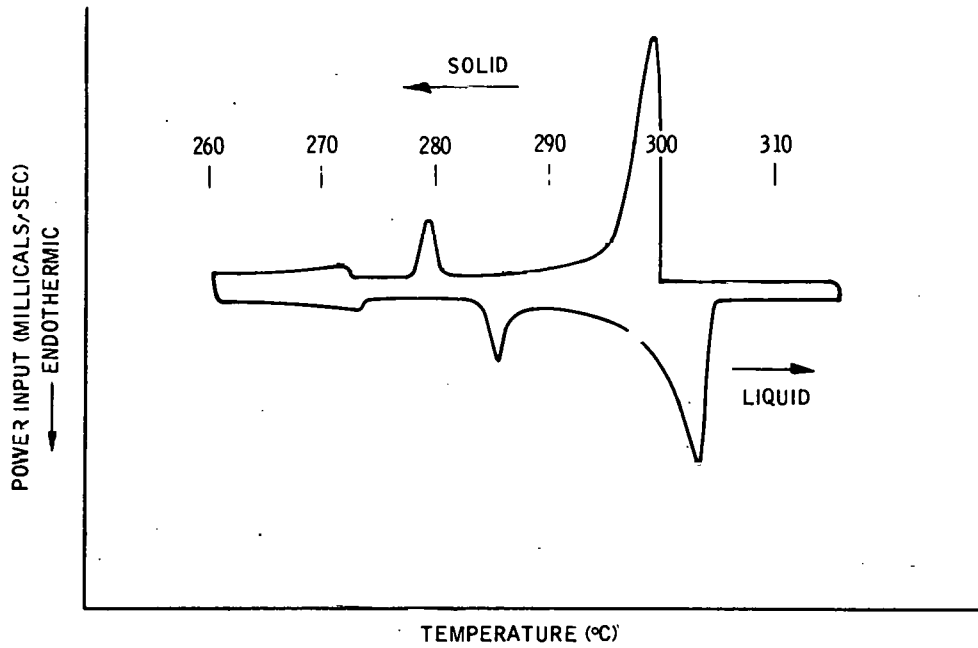
Figure B-11. Liquifaction - Solidifaction DSC Curves for
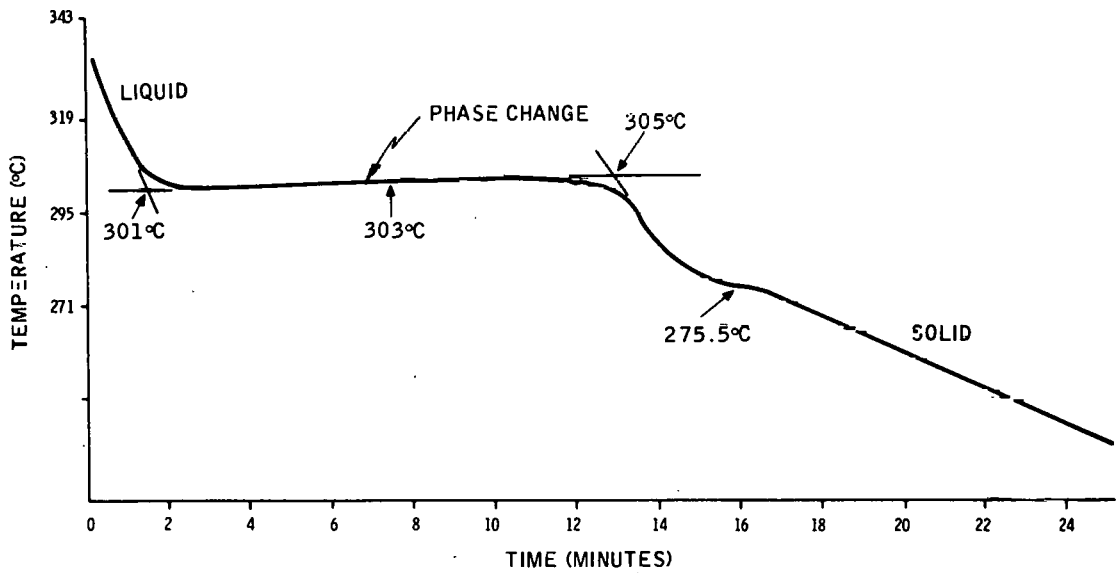NaNO$_3$ (99%) Cycled -- Bottom Portion

Figure B-12. Cooling Curve for 99.5% NaNO$_3$ + 0.5%
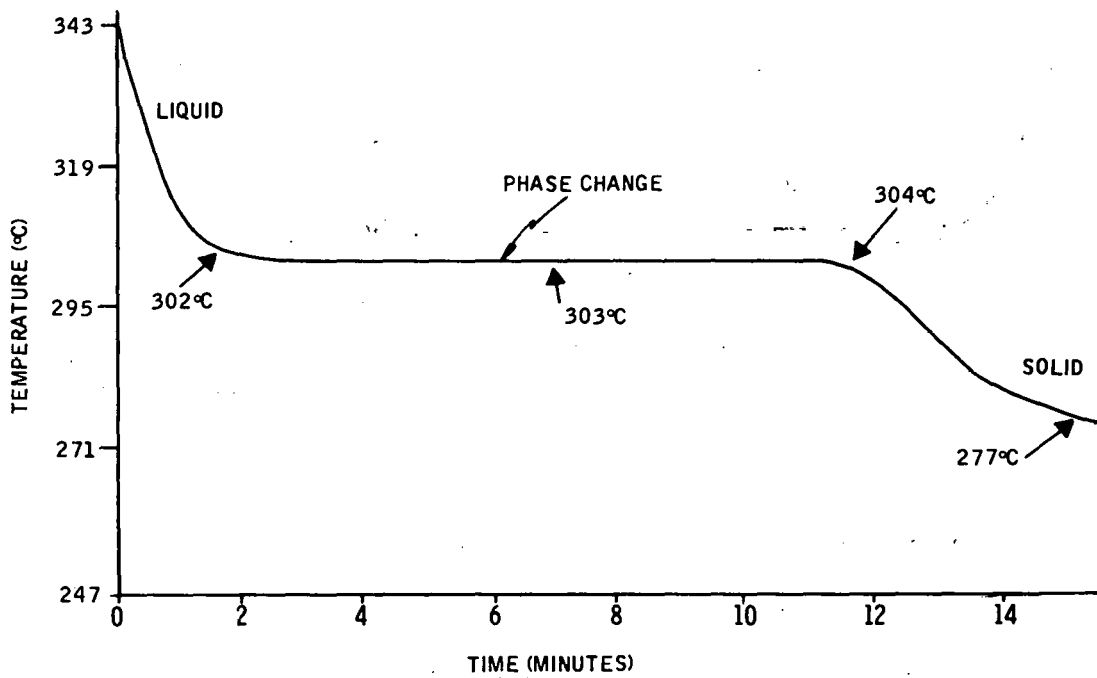NaOH (By Weight)

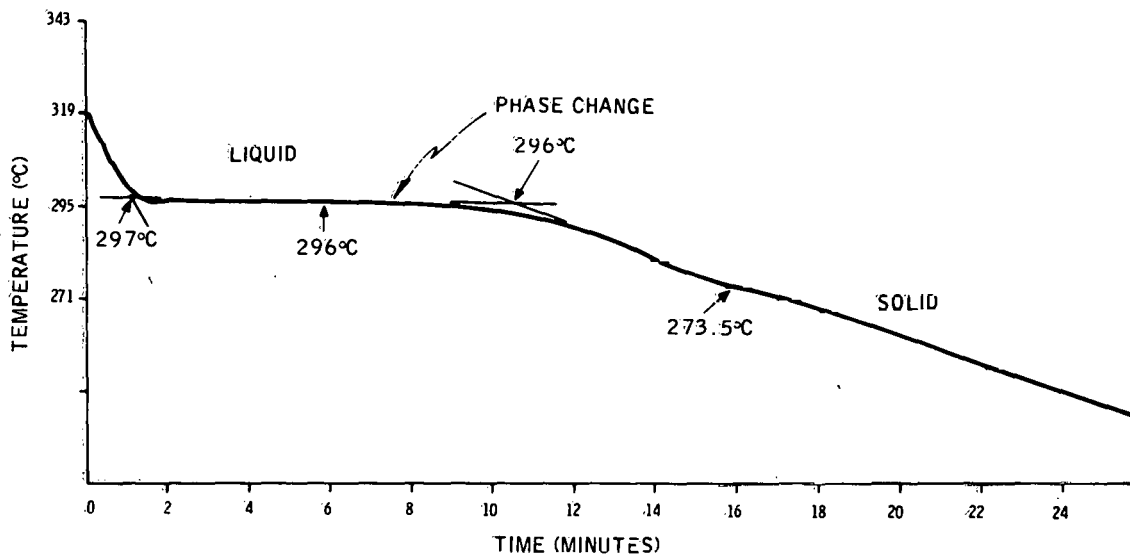Figure B-13. Cooling Curve for 99% NaNO$_3$ + 1% NaOH (By Weight)

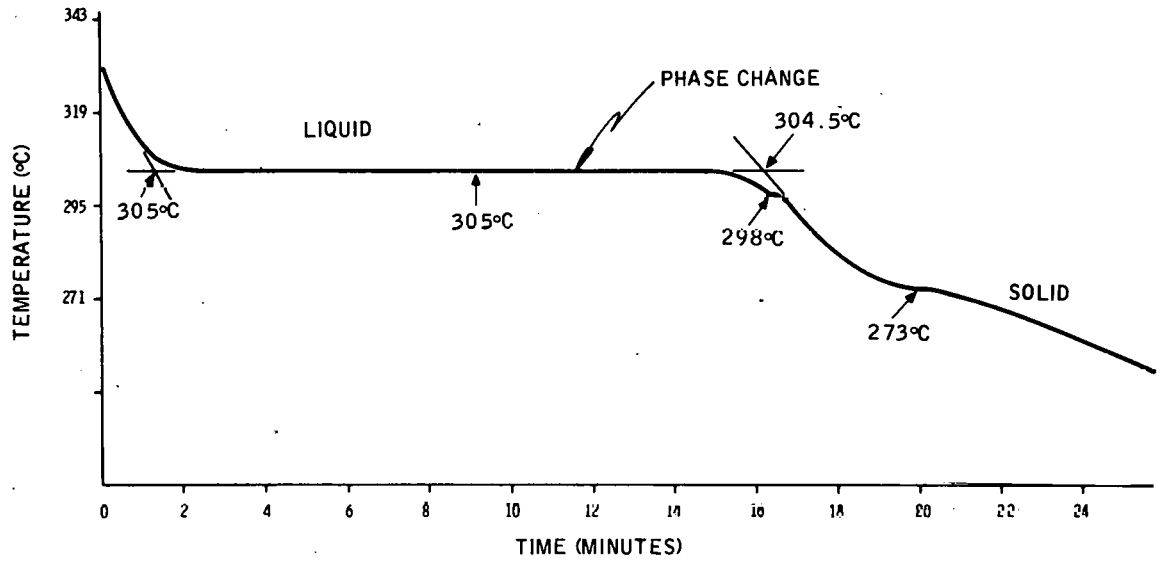Figure B-14. Cooling Curve for 98% NaNO$_3$ + 2% NaOH (By Weight)

Figure B-15. Cooling Curve for NaNO$_3$ (Ind. Grade)